

Inaugural-Dissertation zur Erlangung der Doktorwürde der Tierärztlichen Fakultät der Ludwig-Maximilians-Universität München

Advancing Therapeutic Gene Editing Strategies for Inherited Retinal Diseases: From *in vitro* Development to Preclinical Evaluation in a USH1C Pig Model

von Lucie Elisa Casalta aus Marseille, Frankreich

München 2025

Aus dem Zentrum für Klinische Tiermedizin der Tierärztlichen Fakultät der Ludwig-Maximilians-Universität München

Lehrstuhl	fiir	Mol	ekul	lare	Tierzno	cht und	l Bioteo	chnol	logie
Lemstum	Iui	IVIOI	CKU	laic	TICIZU	m unc	1 DIOIC		IUZIC

Arbeit angefertigt unter der Leitung von: Univ.-Prof. Dr. Eckhard Wolf

Mentor: Univ.-Prof. Dr. Nikolai Klymiuk

Gedruckt mit Genehmigung der Tierärztlichen Fakultät der Ludwig-Maximilians-Universität München

Dekan: Univ.-Prof. Dr. Reinhard K. Straubinger, Ph.D.

Berichterstatter: Univ.-Prof. Dr. Eckhard Wolf

Korreferent: Univ.-Prof. Dr. Cornelia A. Deeg

Tag der Promotion: 26 Juli 2025

Table of contents VIII

TABLE OF CONTENTS

I. INTRO	ODUCTION	1
II. REVI	EW OF THE LITERATURE	3
1.	Inherited Retinal Diseases	3
1.1.	Standard of Care for IRDs	4
1.2.	The Rise of Gene Therapy: Gene Supplementation	4
2.	Prospect of Gene Editing as an Efficient Treatment for IRDs	6
2.1.	Principle of GE	6
2.1.1.	CRISPR-Cas9	6
2.1.2.	Advanced GE Tools	7
2.1.2.1.	Base-Editing (BE)	7
2.1.2.2.	Prime-Editing (PE)	8
2.2.	Therapeutic GE strategies for IRDs	10
2.2.1.	Disruptive Gene Editing	10
2.2.2.	Gene Repair	10
3.	Delivery Vectors for the Eye	11
3.1.	Adeno-associated virus (AAV)	11
3.2.	Adenoviral vector (AdV)	13
3.3.	Future of gene therapy: Non-Viral vectors?	14
4.	From bench to bedside: preclinical development pipeline of	
therapeut	ic GE for IRDs	15
4.1.	Disease Modeling	15
4.1.1.	Anatomy of the Retina	15
4.1.2.	Animal Models to Recapitulate Human IRDs	17
4.1.2.1.	Small Animal Models	17
4.1.2.1.1.	Murine Models (Mice and Rats)	17
4.1.2.1.2.	Zebrafish Models	18
4.1.2.2.	Large Animal Models	18
4.1.2.2.1.	Canine Models	18
4.1.2.2.2.	Non-Human Primate (NHP) Models	19
4.1.2.2.3.	Porcine Models	19
4.1.3.	Alternative test-systems for IRDs	20

4.1.3.1.	Retina Explants (REs)	20
4.1.3.2.	Retinal Organoids (ROs)	21
5.	Research Focus: Patient Specific Therapeutic GE in Usher S 22	yndrome
III.	ANIMALS, MATERIAL AND METHODS	23
1.	Animals	23
2.	Cells	23
3.	Material	23
3.1.	Devices	23
3.2.	Consumables	24
3.3.	Buffers, Chemicals, Media and Solutions	25
3.4.	Enzymes	26
3.5.	Plasmids	27
3.6.	Oligonucleotides	27
3.7.	Primers	28
3.8.	Kits	29
3.9.	Antibodies	29
3.10.	Software	30
4.	Methods	31
4.1.	Cell Culture	31
4.1.1.	Standard PKC Culture	31
4.1.2.	Plate Coating	31
4.1.3.	Isolation of USH1C PKC	31
4.1.4.	Thawing of Cells	32
4.1.5.	Harvesting and Seeding of Cells (example for 10cm plate)	32
4.1.6.	Electroporation for Gene Editing Experiments	32
4.1.7.	Freezing of Cell Pellet for Molecular Analysis	33
4.1.8.	Delivery Vector Testing in PKC	33
4.1.9.	Flow Cytometry	33
4.2.	Molecular Biology	34
4.2.1.	DNA Isolation from Cells and Tissue	34
4.2.2.	End-point PCR for Gene Editing efficiency analysis	34
4.2.3.	Sequencing	34

Table of contents X

4.2.4.	Assessment of Gene Editing Efficiency	35
4.2.5.	RNA Isolation from Retina, Retinal Explant and RPE	35
4.2.6.	DNA Digestion and cDNA Synthesis:	35
4.2.7.	qPCR Analysis	35
4.3.	Animal Experiments	36
4.3.1.	DPOAE, ABR and ASSR Measurements	36
4.3.2.	ERG/OCT measurements	37
4.3.3.	Gene Editing Pilot in vivo Experiment	37
4.4.	Retina Explant (RE) Culture	37
4.4.1.	Culture Conditions	37
4.4.2.	Application of Delivery Vectors	39
4.5.	Immunofluorescence of Retina and Retina Explants	39
4.6.	Retina Dissociation	39
4.7.	3D Quantification of Retina Explants	40
IV.RES	ULTS	41
1.	Development of GE Strategies in Proliferative Cells	41
1.1.	Double Strand Break Mediated Homology Directed Repair (DSB	-HDR) 41
1.2.	Adenine Base Editing (ABE)	43
1.3.	Prime Editing.	45
1.4.	Innovative Delivery Vectors for GE	49
1.4.1.	Virus Like Particles (VLPs)	49
1.4.2.	Delivery Vector X	51
2.	The USH1C Pig Model for Translational Studies	54
2.1.	Breeding and Critical Postnatal Management	54
2.2.	Use of Animals for Collaborative Studies	56
2.3.	Functional Assessment of Retina in USH1C pigs	57
2.4.	Auditory Function Assessment	58
3.	Pre-clinical Assessment of Promising Therapeutic GE and Ve	ctor
Candida	ates	61
3.1.	AdV5 -mediated Delivery of TwinPE	62
3.2.	DVX-mediated Delivery of GFP Reporter	67
3.3.	Alternative Test Systems	68
3.3.1.	Establishing an in vitro Postmitotic Mimicking Cell Model	69

Table of contents XI

3.3.2.	Development and Use of Retina Explants (RE)	.73
3.3.2.1.	Testing AdV-mediated Transduction in REs	.77
3.3.2.2.	Non-Viral Delivery Vectors	.80
v. discu	JSSION	.83
1.	Considerations for Gene Therapy Preclinical Studies in Inherited	
Retinal Di	seases	.83
1.1.	Positioning the Pig as a Valuable Species for Translational Research in	
IRDs	84	
1.2.	Pilot Preclinical Testing of Gene Editing to Treat IRDs Using the USH1	C
Pig Model	86	
1.3.	Considerations in Functional Assessments of the USH1C Pig Model	.88
2.	3R Principle Considerations in Porcine Retinal Research	.90
2.1.	Maximization of research outcome from each animal	.90
2.2.	Improvement of Postnatal Management	.91
2.3.	Further functional assessment options	.91
2.4.	Development of Intermediate Test Systems	.92
3.	Therapeutic GE: Critical Barriers in Achieving Efficient Genetic	
	Therapeutic GE: Critical Barriers in Achieving Efficient Genetic	.93
Modificati	ion	.93
Modificati 3.1.	Access to the Target Cell	.93 .94
Modification 3.1. 3.2.	Access to the Target Cell Assembly of GE Components in the target cell	.93 .94 .95
Modificati 3.1. 3.2. 3.3.	Access to the Target Cell Assembly of GE Components in the target cell Access of CRISPR-Cas9 to the DNA in the nucleus of the target cell	.93 .94 .95
Modificati 3.1. 3.2. 3.3.	Access to the Target Cell Assembly of GE Components in the target cell Access of CRISPR-Cas9 to the DNA in the nucleus of the target cell Intermediate Test Systems to Model Clinical Application	.93 .94 .95 .97
Modificati 3.1. 3.2. 3.3. 4. 4.1. 4.2.	Access to the Target Cell	.93 .94 .95 . 97 .97
Modificati 3.1. 3.2. 3.3. 4. 4.1. 4.2.	Access to the Target Cell	.93 .94 .95 .97 .98
Modificati 3.1. 3.2. 3.3. 4. 4.1. 4.2. VI.SUMM	Access to the Target Cell	.93 .94 .95 .97 .97 .98
Modificati 3.1. 3.2. 3.3. 4. 4.1. 4.2. VI.SUMM VII. VIII.	Access to the Target Cell Assembly of GE Components in the target cell Access of CRISPR-Cas9 to the DNA in the nucleus of the target cell Intermediate Test Systems to Model Clinical Application Cell Cycle Shift in Proliferative PKC RE Culture as a Superior Intermediate System IARY ZUSAMMENFASSUNG	.93 .94 .95 .97 .97 .98 103
Modificati 3.1. 3.2. 3.3. 4. 4.1. 4.2. VI.SUMM VII. VIII. IX.INDEX	Access to the Target Cell Assembly of GE Components in the target cell Access of CRISPR-Cas9 to the DNA in the nucleus of the target cell Intermediate Test Systems to Model Clinical Application Cell Cycle Shift in Proliferative PKC RE Culture as a Superior Intermediate System IARY ZUSAMMENFASSUNG REFERENCES	.93 .94 .95 .97 .97 .98 103 105

Abbreviations XII

ABBREVIATIONS

AVV	Adeno-associated virus
ABE	Adenine Base Editing
ABR	Auditory Brainstem Response
AD	Autosomal dominant
AdV	Adenoviral vector
BW	Bodyweight
ASSR	Auditory Steady-State Response
B2M	Beta-2 Microglobulin
bp	Base pair
BW	Bodyweight
CBE	Cytosine Base Editing
cDNA	Complementary DNA
CiMM	Center of Innovative Medical Models
CO ₂	Carbon dioxide
CRISPR	Clustered Regularly Interspaced Short Palindromic Repeats
ddH ₂ O	Double-distilled water
DMEM	Dulbecco's Modified Eagle Medium
DMSO	Dimethylsulfoxide
DNA	Deoxyribonucleic acid
dNTP	Deoxynucleotide triphosphate
DPOAE	Distortion Product Otoacoustic Emission
DSB	Double-strand break
dsDNA	Double-stranded DNA
DTT	Dithiothreitol
DVX	Delivery vector X
EEG	Electroencephalogram
EDTA	Ethylenediaminetetraacetic acid
EMA	European Medicines Agency
ERG	Electroretinography
EtOH	Ethanol

EU	Endotoxin units
FACS	Fluorescence-activated cell sorting
FC	Flow Cytometry
FCS	Fetal Calf Serum
FDA	Food and Drug Administration
FSC	Forward scatter
GCL	Ganglion Cell Layer
GE	Gene editing
GFP	Green fluorescent protein
GT	Gene therapy
h	Hour(s)
HDR	Homology-directed repair
HEPES	4-(2-hydroxyethyl)-1- piperazineethanesulfonic acid
HEK293	Human Embryonic Kidney 293 cells
HD	High dose
Hz	Hertz
IF	Immunofluorescence
ILM	Inner limiting membrane
INL	Inner nuclear layer
iPSC	Induced pluripotent stem cells
IRD	Inherited retinal disease
IS	Inner segment
JLU	Justus-Liebig-Universität (Gießen)
kb	Kilobase
KO	Knockout
LCA	Leber congenital amaurosis
LD	Low-dose
LNP	Lipid nanoparticles
μg	Microgram
μL	Microliter
μm	Micrometer
M	Molar
MEM	Minimum Essential Medium

Abbreviations XIII

MFI	Mean Fluorescence Intensity
mGL	mGreen Lantern
min	Minute(s)
mL	Milliliter
mM	Millimolar
MMR	Mismatch repair
mRNA	Messenger RNA
NEAA	Non-Essential Amino Acids
NDS	Normal Donkey Serum
NHEJ	Non-homologous end joining
NHP	Non-human primate
NIC	Non-injected control
NLS	Nuclear localization signal
nm	Nanometer
OCT	Optical coherence
	tomography
OLM	Outer limiting membrane
ONL	Outer nuclear layer
OS	Outer segment
PAM	Protospacer adjacent motif
PBS	Phosphate-buffered saline
PCA	Principal Component
	Analysis
PCR	Polymerase chain reaction
PE	Prime editing
pegRNA	Prime editing guide RNA
PFA	Paraformaldehyde
PI	Propidium Iodide
PKC	Porcine kidney cells
PNA	Peanut agglutinin
PRC	Photoreceptor cell
qPCR	Quantitative polymerase
1	chain reaction
RCVRN	Recoverin
RE	Retina explant
RNP	Ribonucleoprotein
RO	Retinal organoid
rpm	Revolutions per minute
RPMI	Roswell Park Memorial

	Institute (medium)
RPE	Retinal pigment epithelium
RT	Reverse transcriptase
RTT	Reverse transcriptase template
S	Second(s)
SD	Standard deviation
SSB	Single-strand break
ssDNA	Single-stranded DNA
ssODN	Single-stranded oligodeoxynucleotide
TALENs	Transcription activator-like effector nucleases
TUM	Technical University of Munich
TwinPE	Twin prime editing
USH1C	Usher syndrome type 1C
UV	Ultraviolet
VLP	Virus-like particle
WT	Wild type
ZFN	Zinc-finger nuclease

I. Introduction 1

I. Introduction

Vision is one of our most precious senses, allowing us to navigate the world and connect with others. For approximately 1 in 2000 individuals worldwide, this ability is threatened by inherited retinal diseases (IRD) – genetic conditions that lead to progressive vision loss and in the most severe cases to complete blindness (SCHNEIDER et al., 2021). Despite significant advances in understanding the molecular basis of these diseases, no effective cure was conceivable until recently.

The approval of voretigene neparvovec (Luxturna) in 2017 as the first gene therapy (GT) for an IRD marked a watershed moment in the field, demonstrating that genetic interventions could restore visual function in patients with specific mutations (RUSSELL et al., 2017). The approach is simple in theory, it consists of delivering a functional copy of the diseased gene in the affected cells, an approach also known as gene supplementation.

However, conventional gene supplementation approaches have significant limitations. They cannot address all types of mutations, particularly dominant negative ones, and are constrained by the packaging capacity of viral vectors to deliver the functional copy (MCCLEMENTS et al., 2024). These limitations have spurred interest in gene editing (GE) – a revolutionary approach that allows for precise modification of the genome itself (JINEK et al., 2012; KOMOR et al., 2016; GAUDELLI et al., 2017; ANZALONE et al., 2019). Rather than simply adding functional genes, GE technologies like CRISPR-Cas9 and its derivatives can correct mutations at their source, potentially offering more durable and comprehensive solutions (SUH et al., 2022).

Translating the promise of GE from laboratory to clinical application requires addressing multiple challenges: developing efficient editing techniques, creating suitable delivery systems, and validating safety and efficacy in appropriate models (JAIN and DAIGAVANE, 2024; SZABÓ et al., 2025).

To achieve these goals, this thesis focuses on Usher syndrome type 1C (USH1C), caused by mutations in the gene encoding harmonin, a protein crucial for both hearing and vision (CASTIGLIONE and MÖLLER, 2022). The USH1C c.C9T/p.R31X point mutation creates a premature stop codon, making it an ideal candidate for precision editing techniques that would restore the production of a

I. Introduction 2

healthy protein.

Using a humanized pig model of USH1C (GROTZ et al., 2022), this research explores GE strategies, from traditional CRISPR-Cas9 approaches to more sophisticated prime editing (PE) techniques. It investigates the challenges of delivering these editing tools to retinal cells and explores intermediate test systems that bridge the gap between simplified cell culture and complex animal models.

The journey from genetic understanding to therapeutic intervention represents one of the most exciting frontiers in modern medicine. For patients with IRDs, this journey offers hope that genetic science might one day restore what genetics has taken away – the gift of sight.

II. REVIEW OF THE LITERATURE

1. Inherited Retinal Diseases

Inherited retinal diseases (IRD) are a leading cause of vision loss, affecting approximately 1 in 2000 individuals worldwide. They stem from mutations across a wide range of genes, impacting the function of different retinal cells and eventually leading to their degeneration. As of today, roughly 50 diseases subtypes are known, involving at least 277 identified genes as reviewed in (SCHNEIDER et al., 2021) (Table 1). The diverse pathogenic mechanisms underlying IRDs pose significant challenges in developing unified therapeutic approaches. To this day, there is no drug or molecular agent capable of tackling the retinal degeneration inherent to IRDs. This complexity has accelerated the shift of healthcare toward personalized medicine, with gene therapy (GT) as a hope for affected patients.

Table 1: Most Common IRDs

Disease	Global prevalence*	Age of Onset	Key Characteristics
Retinitis Pigmentosa (RP)	1 in 3,000 – 1 in 4,000	Childhood to early adulthood	Night blindness, peripheral vision loss progressing to tunnel vision.
Stargardt Disease (STGD)	1 in 6,500	Late childhood to early adulthood	Central vision loss, color vision impairment, light sensitivity.
Usher Syndrome (USH)	1 in 25.000	Birth to adolescence	Combined hearing loss and progressive vision loss; three types with varying severity.
Cone-Rod Dystrophy (CRD)	Up to 1 in 30,000	Childhood	Decreased visual acuity, photophobia, color vision loss, peripheral vision loss.
Achromatopsia (ACHM)	Up to 1 in 30,000	Birth or early infancy	Total or partial absence of color vision, light sensitivity, reduced visual acuity.
Leber's Hereditary Optic Neuropathy (LHON)	1 in 30,000 – 1 in 50,000	Young adulthood	Acute or subacute loss of central vision, predominantly affects males.
Leber Congenital Amaurosis (LCA)	Up to 1 in 33,000	Infancy	Severe visual impairment, light sensitivity, nystagmus, eyepoking behavior.
Choroideremia (CHM)	Up to 1 in 50,000	Early childhood	Night blindness, progressive peripheral vision loss leading to blindness in late adulthood.
Ocular Albinism Type 1	1 in 50,000	Birth	Reduced visual acuity, nystagmus, light sensitivity, lack of pigment in the retina.
Bardet-Biedl Syndrome (BBS)	Up to 1 in 140,000	First decade of life	Night blindness, tunnel vision, obesity, extra fingers or toes, kidney abnormalities, developmental delays.

^{*}Estimated global prevalence. Adapted from <u>Inherited Retinal Diseases (IRD) | Eyes on Genes HCP</u> (https://www.eyesongenes.com/hcp/inherited-retinal-diseases)

1.1. Standard of Care for IRDs

The management of IRDs has historically centered on supportive approaches aimed at maximizing patients' remaining visual function while monitoring disease progression. Traditional clinical care involves regular comprehensive ophthalmological examinations with specialized imaging and functional testing to document the rate of retinal degeneration, such as electroretinography (ERG) or tomography (OCT) (LORENZ optical coherence al., 2021; PARAMESWARAPPA et al., 2024; FEO et al., 2025). These assessments provide crucial information for both prognostic counselling and therapeutic planning, allowing clinicians to tailor interventions to individual disease trajectories. Visual rehabilitation constitutes a cornerstone of standard care, encompassing a range of interventions from optical devices such as magnifiers and specialized filters to advanced electronic assistive technologies (COLOMBO et al., 2025). Virtual reality-based technologies are becoming increasingly important in diagnosis, specifically in pediatric ophthalmology (NIKOLAIDOU et al., 2024). These tools, combined with strategic behavioral adaptations, help patients maintain independence and quality of life despite progressive vision loss. The psychological impact of vision loss receives increasing attention within comprehensive care models, with many centers incorporating psychosocial support to address the emotional challenges associated with progressive visual impairment (D'AMANDA et al., 2020; SIMONELLI et al., 2022; MURRO et al., 2023).

1.2. The Rise of Gene Therapy: Gene Supplementation

The concept of GT emerged in the 1970s, when scientists first proposed the idea of introducing genetic material into cells to treat inherited diseases at their source rather than focus on treating the symptoms (FRIEDMANN and ROBLIN, 1972). In 1990, the first approved GT clinical trial in a human patient for the treatment of immunodeficiency took place, with a successful outcome (BLAESE et al., 1995). The field was then opened to other diseases, with a growing interest in IRDs. The eye presents a unique opportunity for GT therapies due to several favorable attributes as reviewed in (CHIU et al., 2021; CHOI et al., 2023; BANOU et al., 2024; MURPHY and MARTIN, 2025). Firstly, the eye's immunity advantages, characterized by the presence of the blood-retinal barrier, tight junctions between retinal cells, and diminished lymphatic drainage, reduce the risk of systemic immune response. Secondly, its accessibility allows for localized delivery of

therapeutic agents, minimizing systemic exposure and potential side effects. Moreover, the ability to treat one eye while using the other as a control provides a robust framework for evaluating treatment efficacy and safety. Finally, the relatively small amount of tissue requiring treatment makes the eye an ideal candidate for precision medicine approaches.

To date, most clinical applications of GT in the eye have focused on gene supplementation to address autosomal recessive loss-of-function IRDs as reviewed in (MCCLEMENTS et al., 2024; SZABÓ et al., 2025). These methods introduce a functional copy of the defective gene into a patient's cell to restore normal function. The approval of voretigene neparvovec-rzyl (Luxturna) in 2017 (RUSSELL et al., 2017) marked a historic milestone in the treatment of IRDs as the first Food and Drug Administration (FDA) approved GT for an IRD. Developed for patients with biallelic RPE65 mutations causing Leber congenital amaurosis (LCA), this therapy demonstrated meaningful improvements in functional vision and light sensitivity in clinical trials. The intervention involves subretinal delivery of an adeno-associated viral vector (AAV) carrying functional copies of the RPE65 gene, enabling treated RPE cells to produce the essential isomerohydrolase protein involved in the visual cycle. Long-term follow-up studies have shown sustained improvements in multiple measures of visual function for at least four years post-treatment, establishing proof-of-concept for ocular gene replacement therapy (TESTA et al., 2024; JALIL et al., 2025). In the wake of the Luxturna flagship, a total of 159 clinical trials dedicated to gene therapy for eye diseases were launched by 2022 (reviewed in AMERI et al., 2023).

During long-term follow-up of first Luxturna patients, however, treatment related adverse events became prominent in a significant number of patients (approximately 1/4 - 1/3 of treated patients), mostly due to inflammation-related chorioretinal atrophies. Further, secondary applications, either as a booster treatment of a declining GT function over time or the complementary treatment of a former contralateral control eye caused atrophic events (KU et al., 2024), presumably due to pre-sensitization during previous interventions.

Finally, the gene size that can be packaged into established GT vectors is limited, preventing the treatment of many IRD mutations affecting large genes.

2. Prospect of Gene Editing as an Efficient Treatment for IRDs

So far, therapeutic Gene Editing (GE) - and its aim to repair genetic defects at the genomic level - mostly focused on cancer, blood disorders, inflammatory, metabolic and infectious diseases, with numerous ongoing clinical trials as reviewed in (BAIRQDAR et al., 2024; SONG et al., 2024; WIJEYESINGHE and CHINEN, 2025). In 2023, the FDA of the United States and the European Medicines Agency (EMA) approved the first CRISPR/Cas9 therapy for the treatment of Sickle-cell disease and beta-thalassemia, a turning-point for the field (PARUMS, 2024).

Looking ahead, the potential of GE holds promises for addressing a broader spectrum of retinal diseases, including autosomal dominant inherited disorders, offering the prospect of a single, durable treatment as reviewed in (J. PULMAN, 2022; CARVALHO et al., 2023; LING et al., 2023). The BRILLIANCE clinical trial for the treatment of CPE290-related LCA has been launched in 2019 (NCT03872479), showing improved vision and no significant adverse effects in its patients in first reports (PIERCE et al., 2024).

2.1. Principle of GE

2.1.1. CRISPR-Cas9

Initially, the development of GE relied on engineered proteins such as meganucleases, transcription activator-like effector nucleases (TALENs) and zinc-finger nucleases (ZFNs). Their widespread adoption was limited by complex design requirements and inflexible targeting capacities (BAIRQDAR et al., 2024). The field was revolutionized in 2012 with the development of CRISPR-Cas9 which gained popularity due to its unprecedented flexibility and straightforward design process (JINEK et al., 2012). This breakthrough later earned its developers, Jennifer Doudna and Emmanuelle Charpentier, the 2020 Nobel Prize in Chemistry.

Biologically, CRISPR-Cas9 represents a bacterial immune defense mechanism, with a consistent Cas protein, acting as molecular scissors that is directed to a target site by a pathogen-specific guide RNA (gRNA) (HOCHSTRASSER and DOUDNA, 2015; HILLE et al., 2018). In biotechnological transformation, the same Cas protein can be directed to almost any desired site in prokaryotic and eukaryotic cells by tailoring synthetic gRNAs. After binding to its target site, the Cas protein

induces a double-strand break (DSB), which has to be fixed by the cell's own DNA repair mechanisms (SAMPSON and WEISS, 2014; KNOTT and DOUDNA, 2018; VAN DER OOST and PATINIOS, 2023). Among these repair mechanisms, the most prominent are the blunt mending of the linear ends by non-homologous end joining (NHEJ) and the recombination-based repair by homology-directed repair (HDR) in case a repair template is available (Fig.1, A).

NHEJ is more frequent and faster, but it is prone to errors by inserting or deleting nucleotides into the DNA strand. In protein coding regions this causes a shift of the reading frame of amino acid encoding trinucleotides, amino acid deletion or insertions, which eventually disrupt the protein function. Thus, CRISPR-Cas based NHEJ approaches are mostly used to induce a loss-of-function in a gene of interest. In contrast, the repair template principle in HDR allows to embed almost any kind of modification between homologous arms that bind to a target site up- and downstream of a DSB. After sealing the DSB, the modification becomes an integral part of the genome. Depending on the repair template, larger or smaller modifications can be precisely introduced into the target site.

Over time, the CRISPR-Cas9 system has evolved into various Cas9 derivatives as reviewed in (PICKAR-OLIVER and GERSBACH, 2019; WANG and DOUDNA, 2023). First, different nickases were developed by mutating the Cas protein to only allow the cutting of one DNA strand – either the gRNA binding or the opposite strand – thus inducing single strand breaks (SSB). Further advancements resulted in a "dead" Cas, a protein that is directed to its binding site, but does not interfere with DNA strand integrity. In other attempts, Cas proteins were physically linked to protein domains that add alternative functions. By these advancements, innovative GE such as base editing (BE), and prime editing (PE) have expanded the toolkit, enabling more specific and versatile approaches.

2.1.2. Advanced GE Tools

2.1.2.1. Base-Editing (BE)

BE, developed by David Liu's group in 2016, combines a modified Cas9 with a deaminase enzyme, which modifies the biochemical constitution of nucleotide bases. A H840A mutation transforms the Cas9 into a nickase, opening one DNA strand but keeping the other strand and therefore overall genome integrity intact. CBE convert C•G pairs into T•A (KOMOR et al., 2016) while ABE facilitate A•T

to G•C conversions (GAUDELLI et al., 2017) (Fig.1, B). By avoiding DSB, BE significantly reduces the risk of unwanted insertions and deletions and minimizes off-target effects. There are, however, 2 major drawbacks with BE. First, the existing BE portfolio is limited to CBE and ABE, only allowing defined nucleotide transitions. Second, even optimized deaminases lack precision in the localization of their action (GEHRKE et al., 2018). Consequently, in addition to the desired target site, other C or A within a window of several nucleotides can be modified as well, which normally compromises the intended effect.

2.1.2.2. Prime-Editing (PE)

PE, also introduced by David Liu's group, offers unprecedented versatility to GE. Like BE, PE utilizes Cas9 H840A. This nickase is fused to a reverse transcriptase (RT) domain which utilizes an extension of the gRNA to generate a DNA repair template by reverse transcription (ANZALONE et al., 2019). Thus, the PE gRNA component (pegRNA) is serving two purposes: First, it directs the Cas9-RT complex to its target site and second it precisely defines the genetic alteration that should be introduced into the genome (Fig.1, C). Both aspects provide high flexibility for tailored GE approaches. Unlike BE, PE can mediate all possible base-to-base transitions and transversions, as well as small insertions and deletions. The superior flexibility and precision of PE is notably counterbalanced by a typically lower editing efficiency, compared to other CRISPR-Cas9 systems.

Importantly, the ease of tailoring gRNA and repair templates promoted the popularity of GE and made it a fast-paced field, bearing regular optimization and adaptations of the systems for high efficacy, precision and safety. In the past decade, GE and its advancements dramatically changed high-throughput *in vitro* screenings, genomic modification of animal models and precision medicine.

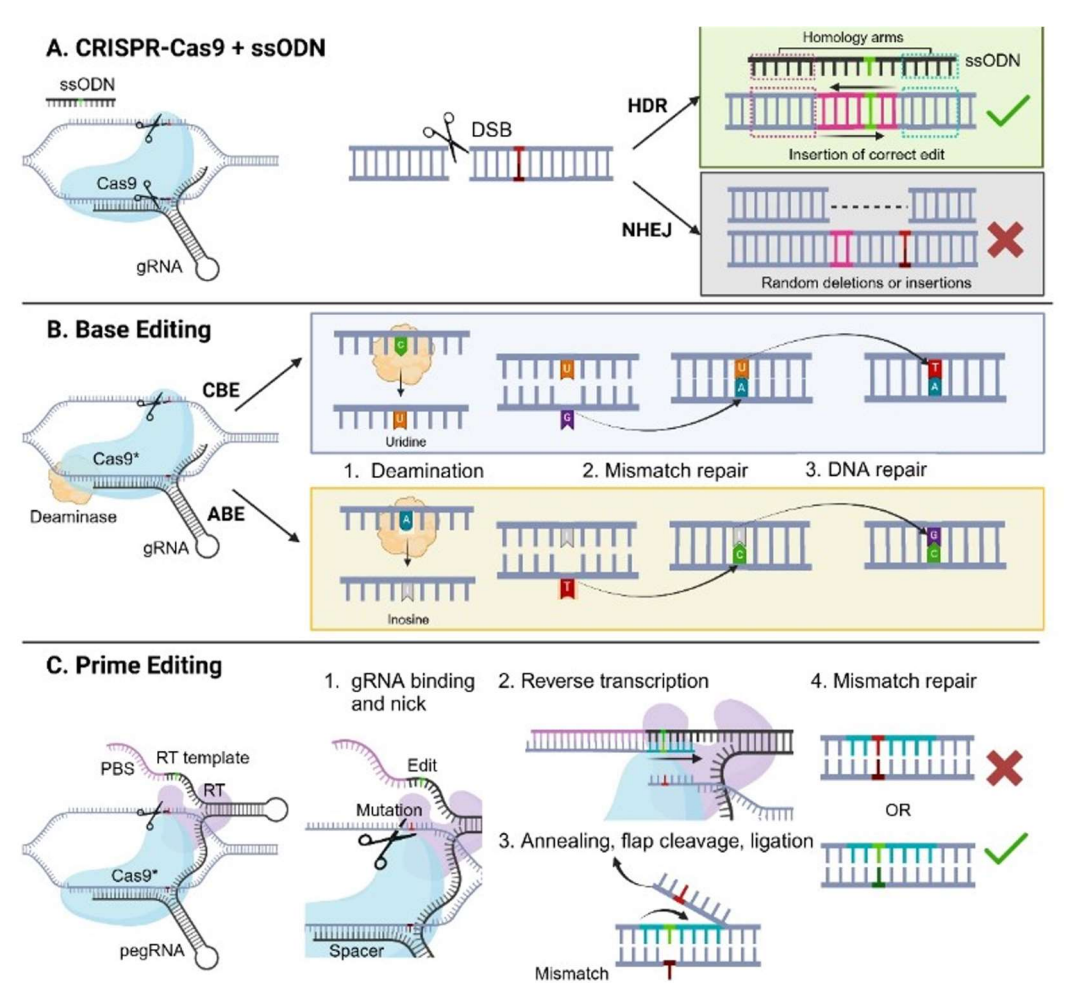


Figure 1: CRISPR-Cas variants for GE. Adapted from (UDDIN et al., 2020). Created with BioRender. (A) In its initial form, the gRNA-Cas ribonucleoprotein binds to the target site, unwinds the DNA double helix and induces a DSB. In most cases, the DSB is mended by NHEJ which may leave traces in the form of random nucleotide exchange, deletions or insertions. The HDR alternative is less frequent and depends on cell cycle status and the availability of a repair template which is invading the genome on both sides of the DSB via recombination-based mechanisms. Biologically, the repair template would be sister chromatid. In biotechnology, a single-stranded oligo-deoxynucleotide (ssODN) of up to 200 bp length is often used for this purpose. (B) BE uses a Cas9 $^{
m H840A}$ -deaminase fusion protein. The mutated Cas acts as a nickase, inducing a single-strand break (SSB). The deaminase removes an -NH2 amino group from a defined base. In the case of CBE, the deaminase transforms a C into an Uracil (U), the following DNA mismatch repair results in a U•A pairing. After eventually replacing the U by the corresponding T, the initial C•G has been converted into a T•A. In the case of ABE, the target A is deaminated into the intermediary Inosine, which binds C and is eventually replaced by a G. Thus, ABE is transforming an A•T into G•C. (C) PE also induces a SSB, created by a mutated Cas9 H840A nickase. The resulting free end of genomic DNA then becomes a binding partner for the other end of pegRNA, the Primer Binding site (PBS). This RNA-DNA dimer serves as initiator of the Reverse Transcriptase (RT) domain, which elongates the genomic strand according to the repair template, containing the desired edit. This new strand competes with the original DNA sequence and is eventually integrated into the genome. As a mismatch occurs, a final mismatch repair takes place to edit the opposing strand.

2.2. Therapeutic GE strategies for IRDs

The availability of GE has transformed almost any field in life science in multiple ways. This is specifically true for novel therapeutic approaches, allowing for interference at the immediate causative level, the genome. Given the complexity of IRDs, involving multiple distinct genes and disease mechanisms, GE is exceptionally suitable to treat genetic defects in the eye. Furthermore, retinal cell types are post-mitotic, transforming a successfully treated gene into a life-long therapeutic effect. The choice for therapeutic GE must refer to the specific disease mechanisms and the exact kind of mutation. Basically, therapeutic GE aims to address IRDs by either silencing dominant mutations, i.e. disease variants that induce pathological alterations from one affected allele (disruptive GE) or by restoring recessive mutation, in case a gene has been inactivated (gene repair).

2.2.1. Disruptive Gene Editing

Autosomal dominant (AD) mutations create a constellation where a mutant allele affects or dominates the function of a remaining intact WT allele. Selectively eradicating the mutant variant by disruptive editing can be used to retain the function of the healthy allele (ARBABI et al., 2019; J. PULMAN, 2022). Disruptive GE may be achieved by several technical approaches. Inducing a frameshift in the coding sequence, removing the harmful allele in parts or completely is all valuable if it alleviates its detrimental effects. This approach is technically easier to apply as it does not require precise restoration of gene function (ATHANASIOU et al., 2018). Instead, the therapeutic outcome can be achieved by NHEJ via classical CRISPR-Cas9 approaches, which is mostly easy to achieve and often highly effective. A major challenge in disruptive GE is the efficient discrimination between the diseased and the healthy allele as the latter is required for gene function after therapeutic intervention.

2.2.2. Gene Repair

In the case of loss-of-function mutations, therapeutic GE must restore the intact gene function, requiring precise gene repair. Importantly, most loss-of-function mutations affect autosomal genes, making heterozygous carriers transmitters of the disease but not patients themselves. Consequently, repair of the intact coding region on one allele is mostly sufficient to restore gene function. From a technical point of view, gene repair can be initiated by CRISPR-Cas9 paired with a donor template,

BE or PE, depending on the causative mutation. Discrimination between alleles is not necessary in case of gene repair, but the GE needs to be precise to lead to a therapeutic effect (ANZALONE et al., 2020; RAGURAM et al., 2022). In case of accompanying mutations, caused by NHEJ processes or any other bystanding effect, the repair of the causative mutation might be fruitless. In addition to recessive diseases, few mono-allelic disease variants may require gene repair. This is specifically true in cases of haplo-insufficiency which produces intact proteins, but an insufficient amount of it. Evidently, gene repair is also applicable to any AD variants, providing a better controlled and safer GE compared to the disruptive approach. However, it must be considered that so far, the efficacy of gene repair attempts stays far behind disruptive GE.

3. Delivery Vectors for the Eye

Eventually, the success of therapeutic GE requires efficient delivery of GE components into target cells. Based on previous achievements, GE components are mostly packaged into vectors that have been established for gene supplementation as those provide validated transduction efficacy, tolerability and safety. Since recently, a fundamentally distinct attitude in gene supplementation and therapeutic GE was neglected: while GT aims at an "as long as possible" durability, GE success would be sufficient if the components remained in the target cell "as long as necessary" and, for safety reasons, fade out after sufficient modification of the genome.

In general, delivery vectors are broadly categorized into viral and non-viral types, introducing GE components as DNA, RNA, or RNPs into the target cells. Vectors are selected for key requirements, such as the specificity to enter target cells, expression capacities, cargo, and low immunogenicity. For GT into the eye, several vector variants have entered distinct stages of development.

3.1. Adeno-associated virus (AAV)

AAVs are currently the most widely used vectors for ocular delivery as reviewed in (HU et al., 2021; FORD et al., 2024; WANG et al., 2024). Discovered as incidental agents in adenovirus infections, without noticeable pathogenic potential by themselves, AAVs have been tailored to become autonomous, non-pathogenic,

and low immunogenic delivery vectors for therapeutic applications. They can package up to 4.7 kilobases (kb) of exogenous single stranded DNA (ssDNA), which is sufficient for delivering transgenes for many gene supplementation approaches (SCHÖN et al., 2015). The synthesis of a complementary strand by the host cell machinery results in a delayed but more sustained gene expression. The long-term persistence of AAV genome as stable episomal DNA in host cells presents a major advantage in gene supplementation.

Extensive testing in clinical trials has proven their safety and efficacy in treating IRDs with LCA1-treating Luxturna serving as a landmark example of success (RUSSELL et al., 2017). In addition to naturally occurring AAV variants, engineering advancements have resulted in the development of chimeric or synthetic serotypes with enhanced or more specific tropism for neuroretinal tissue, particularly photoreceptors and retinal pigment epithelium (RPE) cells (PAVLOU et al., 2021).

The limited cargo capacity of AAVs remains a significant challenge for the delivery of larger genetic constructs, affecting the supply of transgenes for many IRDassociated large genes as well as the delivery of GE components, with the coding region of the most widely used Cas9 from Streptococcus pyogenes being alone 4000bp. To extend the cargo capacity potential of AAVs, strategies have been developed that allow the division of genetic material across two or even more AAVs, their independent delivery into a target cell and the constitution of a functional protein or RNP after recombination of transcripts or proteins (TRUONG et al., 2015; FERREIRA et al., 2023; RIEDMAYR et al., 2023). However, a generally reduced efficiency of complementary AAV approaches remains an area of ongoing optimization as reviewed in (CARVALHO et al., 2017; MCCLEMENTS and MACLAREN, 2017). For GE applications, the long-term appearance of AAV genome in host cells is detrimental as well. Accordingly, approaches for reduced temporary abundance of the GE components have been developed to eventually minimize off-target effects and reduce the risk of immune responses as reviewed in (QUINN et al., 2021).

3.2. Adenoviral vector (AdV)

Adenoviruses (Ads) were among the first viruses harnessed as vectors for delivering GT (WOLD and TOTH, 2013; WATANABE et al., 2021). They can efficiently transduce a large proportion of dividing and non-dividing cells, including retinal cells, and their large cargo capacity allows them to package up to 35 kb of double-stranded DNA (dsDNA). This feature makes adenoviral vectors (AdVs) well-suited for delivering larger genetic payloads, including GE components like the full CRISPR-Cas9 machinery (EHRKE-SCHULZ et al., 2017). The constituent dsDNA genome of AdVs is rapidly transcribed and translated by the host cell, compared to the ssDNA delivered by AAVs. Moreover, AdV production in large scale is well established, which simplifies their clinical use (SAKURAI et al., 2008). They are used in several approved therapeutics, including COVID-19 vaccines (Johnson and Johnson, Astrazeneca) as well as in oncolytic agents, such as Adstiladrin, a treatment for bladder cancer.

In their early development as therapeutic agents, AdVs have been linked to fatal outcomes after systemic high dose application in immune compromised patients (RAPER et al., 2003). As a result, AdVs have long been labelled as highly immunogenic and their popularity in GT waned for AAVs. Meanwhile, ongoing advancements have resulted in third-generation AdVs with reduced immune activation and expanded therapeutic potential (LAM et al., 2014; DAWSON et al., 2024; MCDONALD et al., 2024). In figures, AdVs are used in 15.5% of over 4,000 clinical trials, particularly in the field of oncology, making them the most used vectors.

Interestingly, the immune response that raised concerns about AdVs safety, may be favorable in therapeutic GE, contributing to the degradation of the vectors and transient gene expression (LIU and MURUVE, 2003). The fast onset, high packaging capacity and temporary abundance make AdVs interesting candidates for GE.

3.3. Future of gene therapy: Non-Viral vectors?

The evolutionary optimized transduction capacity of viral vectors provides excellent delivery properties for GT. However, safety concerns and the partially limited packaging capacity stimulated the development of alternative non-viral delivery vectors with tailored cargo load, immunogenicity and cell-type specificity. Among them, lipid nanoparticles (LNP) and virus-like particles (VLP) have gained attraction. LNPs aim at encapsulating nucleic acids in small cationic lipids that penetrate plasma membranes (HALD ALBERTSEN et al., 2022; CULLIS and FELGNER, 2024). LNPs are widely used in trials on GT, especially on cancer treatment, and as vaccines. The latter is best illustrated by the fundamental success in Moderna and BioNtech COVID vaccination approaches. Similarly, VLPs played a major role in the overcoming of the COVID pandemic (NOORAEI et al., 2021; YADAV et al., 2023). In contrast to fully synthetic LNPs, VLPs closely reflect the structure of viruses, but completely lack genetic virus information. Their virusrelated surface thus allows for similar tailoring for cell-type specificity as in viral vectors and the highly flexible incorporation of genetic information (LECLERC et al., 2024). This last feature allows a quick translation of the GE components and reduces the expression time of the delivered components inherently enabling safer GE action (SAINZ-RAMOS et al., 2021). First evidence that VLPs can target the RPE in ocular therapy have been presented (BANSKOTA et al., 2022).

Together, attempts on therapeutic GE are a radically new approach to achieve lifelong therapy in IRDs and vectors have been developed to deliver them efficiently into target cells of the retina. However, progress towards efficient treatment of IRDs by GE so far lacked consistent success. Very often, the pre-clinical findings were later not recapitulated in clinical trials, putting the pipelines of pre-clinical models into question (CUKRAS et al., 2018).

4. From bench to bedside: preclinical development pipeline of therapeutic GE for IRDs

Like other therapeutic approaches, GE is founded on comprehensive pre-clinical testing. Initially, extensive validation and optimization is done in cell culture assays. The enormous flexibility of CRISPR-Cas based GE tools has produced myriads of test systems and design tools. Among them are scientific publications on protocols for high throughput arrayed mutagenesis (SHALEM et al., 2015; KWEON and KIM, 2018; RAVI et al., 2023), standard cell lines that allow rapid screening of gRNA or pegRNA (DOENCH et al., 2016; FELDMAN et al., 2019; SIMON et al., 2022), prediction tools to design appropriate gRNAs and evaluating their efficiency and specificity (ALIPANAHI et al., 2023) as well as numerous commercial solutions for the same purposes.

Conventional cell culture provides a controlled environment and allows the assessment of various parameters, including the effectiveness of different gRNAs, Cas variants, and editing approaches. While they are invaluable for basic assessments, they have limitations: They do not replicate the complex *in vivo* environment of human tissue such as the eye, which poses challenges for assessing toxicity and immunogenicity and the approachability of to the target cell type within tissue. This is of specific importance in the case of degenerating tissue, as in many IRDs. Similar for alternative therapies, GE development must thus prove concept in relevant disease models to evaluate safety and efficacy comprehensively.

4.1. Disease Modeling

4.1.1. Anatomy of the Retina

The eye is a highly specialized organ, with the retina serving as the primary sensory tissue for vision (HOON et al., 2014; BADEN et al., 2020). The retina consists of two major components: the neuroretina, responsible for phototransduction, and the retinal pigment epithelium (RPE), which provides critical support. Photoreceptors (PRC), located in the outermost layer of the neuroretina, are crucial for capturing light and initiating the visual process through rod-mediated dim light vision and cone-mediated color and daylight vision. Müller glia cells play a supportive role by maintaining the retinal structure, regulating ion and water homeostasis, and recycling neurotransmitters. The RPE, a monolayer of pigmented cells adjacent to the photoreceptors, is essential for maintaining retinal homeostasis, recycling

photopigments, and phagocytosing shed photoreceptor outer segments. Together, these structures form a tightly coordinated system critical for visual function.

From a therapeutic standpoint, the RPE is more amenable to targeted GT: it forms a single, easily accessible layer and exhibits low cellular turnover (CAMPBELL et al., 2016; BUCHER et al., 2021; HU et al., 2021). Notably, the phagocytic properties of RPE provide a high endocytic capacity, facilitating the uptake of GT vectors, specifically those of non-viral origin. Therefore, it is not surprising that the first approved eye GT, Luxturna, aims at RPE65-related Leber congenital amaurosis (LCA). Other prevalent IRDs, such as Stargardt disease, affect the RPE. However, approximately 60–70% of IRDs involve PRC dysfunction (HANANY et al., 2020; SCHNEIDER et al., 2021; LIN et al., 2024). PRC are embedded within the outer retina, with high density and tightly packed outer and inner segments. Reaching the PRC central inner nuclear layer (INL, Fig. 2) that is responsible for transcription and translation, therefore necessitates deeper delivery of vectors. Recapitulating this specific anatomy, the overall complexity of retinal cell types and their interaction is key for pre-clinical assessment of GT. Conventional in vitro test systems are only valuable in early steps of development. Later, evaluation in more comprehensive animal models or advanced in vitro and ex vivo test systems is required.

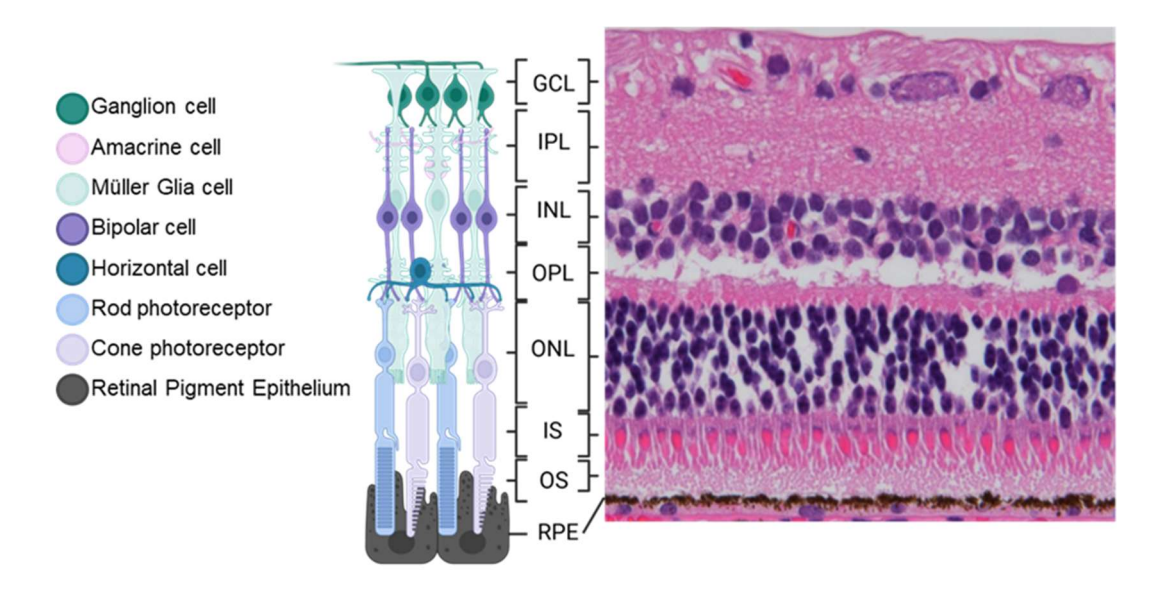


Figure 2: Anatomy of the Retina

Created with BioRender. The retina is comprised of two main elements, the neuroretina and the RPE. In the neuroretina, 7 cell types can be found. They lay very close to each other and build areas recognizable histologically. Among them, the Ganglion Cell Layer (GCL), the Inner Plexiform Layer (IPL), the Inner Nuclear Layer (INL), the Outer Plexiform Layer (OPL) and the Outer Nuclear Layer (ONL). The ONL is formed by the nuclei of the photoreceptor cells (PRCs). The PRCs are divided into rods and cones. Both share a similar organization, comprised of their Inner and Outer Segments (IS and OS). The latter are in close interaction with the RPE. On the right side, a hematoxylin and eosin staining of a pig retina can be seen.

4.1.2. Animal Models to Recapitulate Human IRDs

IRD animal models are standard tools for exploring disease mechanisms and therapies *in vivo*. IRD models have been established in various species, each representing specific advantages and limitations (CHADER, 2002; KOSTIC and ARSENIJEVIC, 2016).

4.1.2.1. Small Animal Models

4.1.2.1.1. Murine Models (Mice and Rats)

As for many other diseases, mice are extensively utilized in IRD research due to their genetic manipulability, short reproductive cycles, and well-characterized genomic backgrounds (COLLIN et al., 2020). The availability of numerous transgenic and knockout strains facilitates the study of specific gene functions and disease mechanisms, specifically for general aspect of eye diseases (MCDOWELL et al., 2022). The long-term experience with laboratory rodent strains also facilitates

the development of highly standardized tests, including multimodal ocular imaging and functional testing, as well as behavioral tests (KREMERS and TANIMOTO, 2018; LEINONEN and TANILA, 2018). However, murine models have notable limitations: their retinal structure differs significantly from humans, among other reasons due to the preferred nocturnal activity of the species. Therefore, the macula, a region with high cone density responsible for high-acuity vision in humans, is lacking in and the few cones are di-chromatic, i.e. they comprise two of the 3 types of cone-opsins present in human - S-cones and M-cones – but no L-cones. They also possess UVS-cones that are missing in the human retina. Additionally, their smaller eye size poses challenges for surgical interventions and *in vivo* imaging.

4.1.2.1.2. Zebrafish Models

Zebrafish have emerged as valuable species to model retinal development and disease due to their rapid embryonic development, optical transparency, and the ease of genetic manipulation (CHHETRI et al., 2014; ZANG and NEUHAUSS, 2021). Their retinas share structural similarities with humans, including the presence of all major retinal cell types and a cone-dominated retina, with an additional presence of UVS-cones, making them suitable for high-throughput genetic and pharmacological screenings. However, significant anatomical and physiological differences exist between zebrafish and human eyes, such as the absence of macula and differences in eye size and organization. Further, the capacity of zebrafish retina to regenerate provides an excellent tool to study the development of the retina but may mislead studies on the pathogenesis of degenerative IRDs.

4.1.2.2. Large Animal Models

4.1.2.2.1. Canine Models

Dogs have proven value in IRD research (PETERSEN-JONES and KOMÁROMY, 2015; BYOSIERE et al., 2018). The canine eye is similar in size to the human eye, facilitating surgical interventions and *in vivo* imaging. Additionally, dogs possess a region analogous to the human macula, known as the area centralis, which is rich in cone photoreceptors and crucial for high-acuity vision. These features make canine models particularly valuable for studying diseases affecting central vision. Specifically, the extraordinary genetic selection according to human breeder's preferences created a very distinct evolutionary pressure, causing substantial

inbreeding and the enforcement of unattended genetic disease variants (LEEB et al., 2023). This specifically includes dog models for IRDs (PETERSEN-JONES and KOMÁROMY, 2015; PALANOVA, 2016; BUNEL et al., 2019), involving disease-causing genes that are also involved in human IRDs such as RPGR, RHO, RPE65, CNGB3, GUCY2D etc. However, the generation of tailored genetic modifications in dogs is not well established. Moreover, maintaining dog colonies for biomedical research purposes is associated with high costs and ethical considerations alone that must be acknowledged.

4.1.2.2.2. Non-Human Primate (NHP) Models

NHPs, such as macaques, share close genetic, anatomical, and physiological similarities with humans, including the presence of a macula in their eye (SEAH et al., 2022). Most often NHPs are being used in pre-clinical studies aiming at safety and biodistribution of GT products (MATET et al., 2017; RAMACHANDRAN et al., 2017; KELLISH et al., 2023; LUO et al., 2024). Notably, the disruptive therapeutic GE approach EDIT-101 on CEP290 (MAEDER et al., 2019) as well as a BE-based repair of ABCA4 (MULLER et al., 2025) were successfully validated in NHP models. Generally, however, the use of NHPs is accompanied by significant ethical considerations, high maintenance costs, and limited availability. Establishing genomic modifications relevant in IRDs in NHPs may raise further regulatory concerns. Additionally, longer lifespans of NHPs and their delayed and limited reproductive capacity necessitate extended study durations to observe disease progression and therapeutic outcomes.

4.1.2.2.3. Porcine Models

Pigs have recently emerged as promising models for monogenic disease research due to the physiological characteristics closely resembling those of humans, the high reproductive capacity and the meanwhile well-established procedures for genomic manipulation (WOLF et al., 2014; HOLM et al., 2016; STIRM et al., 2022; MEYERHOLZ et al., 2024). In the case of IRDs, the comparable eye size, and retinal structure and photoreceptor characteristics raised interest in pig models (MCCALL, 2024). A pig model with transgenic overexpression of an AD variant of rhodopsin (RHO^{P23H}) was the first genetically engineered pig model for biomedical research (PETTERS et al., 1997). Since then, numerous other models for RHO, ELOVL4, GUCY2D have been developed (SOMMER et al., 2011; ROSS

et al., 2012; KOSTIC et al., 2013). In addition to studying IRDs variants in a large animal model, pigs are more generally used to investigate novel therapy options such as intravitreal application routes (CHENG et al., 2024), intein-mediated CRISPR trans-splicing (TORNABENE et al., 2019) or CRISPR-mediated transcriptional regulation (BURNIGHT et al., 2023). Evidently, pig maintenance for biomedical research requires specialized housing and handling facilities (EGERER et al., 2018), often raising economic concerns about extended use of genetically modified model herds.

4.1.3. Alternative test-systems for IRDs

Costs, and species-specific differences in the retina are major drawbacks of animal models in IRD research. In addition, ethical concerns require to keep animal experiments to a minimum to ensure animal welfare in line with the 3R principle – Replace, Reduce, Refine - and explore alternative test systems (POH and STANSLAS, 2024; RINWA et al., 2024).

4.1.3.1. Retina Explants (REs)

The composition of diverse cell types, their strict assembly and the tight packaging render retina a small, but complex tissue structure. To recapitulate retinal structure for systematic ex vivo assessment, REs represent a precious resource (MURALI et al., 2019; SCHNICHELS et al., 2021). REs can be gained from human organ donors, experimental animals, or even be collected at slaughterhouses from WT animals (XU et al., 2022; AHMED, 2023; WELLER et al., 2024; VATS et al., 2025). After enucleation of the eyeball, small pieces of the retina can be dissected and kept in culture separately, maximizing the use of one eye to test distinct culture or treatment conditions. Compared to other in vitro test systems, REs reconstitute neuroretinal tissue architecture and maintain cellular interactions. REs are suitable to explore transduction efficacy of GT or GE as well as cellular responses to the treatment e.g. cytotoxicity. However, REs are affected by declining integrity and function during culture, a challenge that previous optimization attempts have addressed, but not yet sufficiently resolved (CAFFÉ et al., 2001; THANGARAJ et al., 2011; ALARAUTALAHTI et al., 2019; WELLER et al., 2024). Importantly, common RE protocols lack the critical interaction of PRC with RPE (BELHADJ et al., 2020).

4.1.3.2. Retinal Organoids (ROs)

ROs represent a groundbreaking approach minimizing animal experimentation by enabling the reconstitution of retinal tissue in its entire complexity from progenitor cells (CLEVERS, 2016; AFANASYEVA et al., 2021; ELDRED and REH, 2021). Mostly derived from human (and even patients) induced pluripotent stem cells (iPSC) (KELLEY and WU, 2023; MANDAI, 2023; MCDONALD and WIJNHOLDS, 2024), ROs are claimed to mimic the human retina as close as possible. However, ROs face significant challenges, including imbalanced cell type compositions, incomplete cellular maturation of the respective cell types in the organoid. In addition, establishing ROs that include functional and interacting nonretinal components such as microvasculature (HUANG et al., 2023; INAGAKI et al., 2025) or microglia like constituents (CHICHAGOVA et al., 2023; USUI-OUCHI et al., 2023; GAO et al., 2024) are difficult to achieve. Further, reproducibility between different organoid preparations is generally low and diversity between different iPSC lines are significant, requiring tightly controlled and long-term culture protocols (QUADRATO et al., 2017) with a minimum maturation time of 85-100 days, making them costly and time consuming.

5. Research Focus: Patient Specific Therapeutic GE in Usher Syndrome

My thesis aims at advancing the therapeutic GE options for IRDs. My work is following previous work by Dr. med. Vet. Hannah Auch (AUCH, 2023) and focuses on the systematic comparison of distinct GE approaches and translating promising candidates from simple cell culture test assays to more valid test systems such as *in vivo* or *ex vivo* experiments. Specifically, my work deals with a patient relevant mutation in Usher Syndrome, USH1C^{R31X} for which a pig model with partially humanized USH1C gene has been created (GROTZ et al., 2022), allowing for the exploration of primary cells, REs and *in vivo* experiments from the same source.

Hallmarks of my work were the variations of cell culture conditions of primary cells to mimic the post-mitotic status of retinal cells, the conduction of first *in vivo* experiments on therapeutic GE and the development of porcine REs to establish a robust ex vivo test system for therapeutic GE. This work thus involves advanced molecular, histological and cell culture techniques, combined with maintenance and reproduction work on the highly sensitive USH1C pig model.

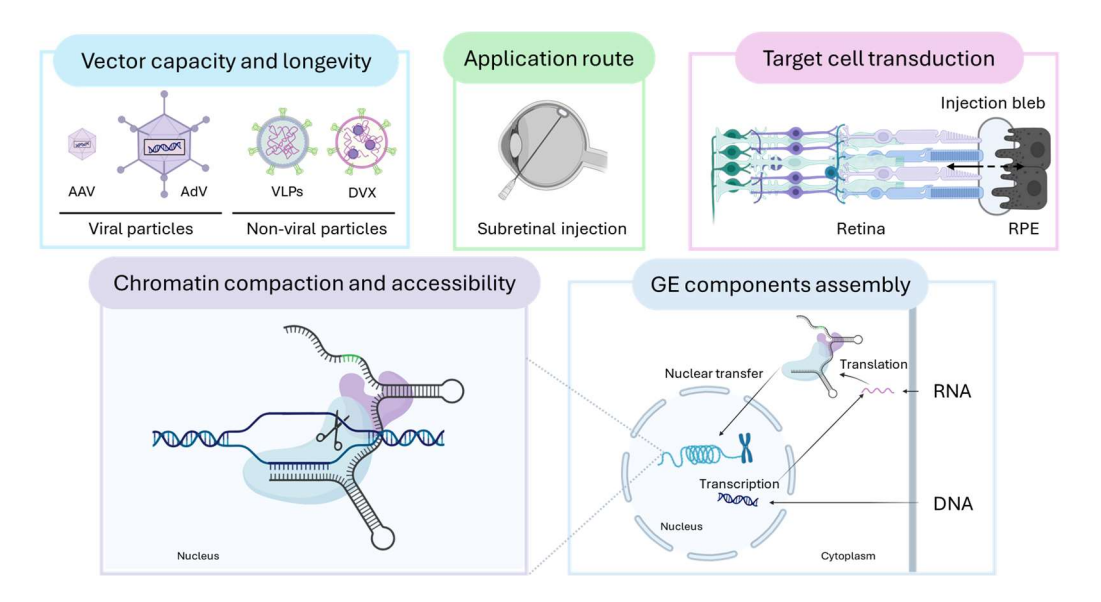


Figure 3: Key Aspects of Gene Editing for the Treatment of IRDs

Created with BioRender

III. ANIMALS, MATERIAL AND METHODS

1. Animals

The USH1C animals were produced according to (KUROME et al., 2015) and characterized in (GROTZ et al., 2022).

The animal experiments were conducted according to German Animal Protection Law and authorized by the Regierung von Oberbayern. (AZ 55.2-1-54-2532-70-12 and AZ 02-17-136).

The 3 USH1C animals used in the therapeutic gene editing *in vivo* pilot experiment originated from the Pigmod, Liblice (CZ), where a sister herd of USH1C pigs is housed. The experiments were authorized by the Ministry of Agriculture of Czech Republic under the project numbers 75/2019 and AV CR 4188/2023 SOV II.

2. Cells

Primary fibroblasts of porcine kidneys derived from the cell lines 5613 (USH1C^{R31X}/USH1C^{Del}) and 13824 (USH1C^{R31X}/USH1C^{Del}).

3. Material

3.1. Devices

Accu-jet® pro Brand GmbH, Wertheim

Analytik Jena US UVP GelStudio Plus Thermofisher Scientific, USA

Axiovert 200M Fluorescence Microscope Zeiss, Oberkochen

BD LSR Fortessa Flow Cytometer Becton Dickinson, USA

Cellavista® automated cell culture microscope Synentec, Elmshorn

Corning® CoolCell™ Sigma Aldrich, USA

Cryostar NX50 Cryotome Epredia, Switzerland

Eppendorf Centrifuge 5417 R Eppendorf, Hamburg

Eppendorf Centrifuge 5424 Eppendorf, Hamburg

Eppendorf Centrifuge 5804 Eppendorf, Hamburg

Eppendorf Centrifuge 5910 R Eppendorf, Hamburg

Grant JB Nova 5 water bath Grant Instruments Ltd, UK

Heraeus Biofuge pico Heraeus, Hanau

HeraSafe workbench Heraeus, Hanau

Light Cycler 96® qPCR Roche, Switzerland

LSR FortessaTM Flow Cytometer Becton. Dickinson, USA

Millicell® Standing Cell Culture Milipore, USA

Nucleofector® 2b Device Lonza, Switzerland

Nyone ® Image cytometer Synentec, Elmshorn

Pipettes Gilson Inc., USA

Pipettes Research Plus Eppendorf, Hamburg

Select vortexer Select BioProducts, USA

Sentiero Advanced PathMedical GmbH,

Germering

Shaking Incubator GFL 3031 with orbital motion Lauda-GFL, Burgwedel

SimpliNano™ spectrophotometer Biochrom GmbH, Berlin

Thermoblock HTM HTA-BioTec, Bovenden

Thunder Imager Tissue Leica microsystems, Wetzlar

RETImap System Roland Consult, Brandenburg

an der Havel

VHC Pro vacuum pump Vacuubrand GmbH, Wertheim

3.2. Consumables

Cell culture plates:

(10cm, 6 well, 48 well, 96well full area) Sigma-Aldrich, USA

Cryovials 1.5 mL Thermofisher Scientific, USA

Corning® cell strainer 40 µm, 70 µm, 100 µm Sigma-Aldrich, USA

Falcon® 5 mL tube, Cell Strainer cap Fisher Scientific, USA

PCR reaction tubes (0.2 mL)

Brand GmbH, Wertheim

Pipet tips with filter Eppendorf, Hamburg

qPCR plates 96 wells Eppendorf, Hamburg

Safe-Lock reaction tubes 1.5 mL, 5 mL Eppendorf, Hamburg

3.3. Buffers, Chemicals, Media and Solutions

2-Mercaptoethanol Sigma Aldrich, USA

Bromophenol blue Carl Roth, Karlsruhe

Cell culture grade water Biowest, France

Collagen 2% Serva, Heidelberg

DMSO (Dimethylsulfoxide) Sigma Aldrich, USA

dNTP mix (100mM) Agilent Technologies, USA

Double-distilled water by BarnsteadTM EasypureTM II

DTT (Dithiothreitol) Thermofisher Scientific, USA

EDTA (Ethylenediaminetetraacetic acid) Carl Roth, Karlsruhe

EtOH (Ethanol 99.8%) Carl Roth, Karlsruhe

Fetal Calf Serum (FCS)

Thermofisher Scientific, USA

GelRed® Nucleic Acid Gel Stain Biotium, USA

Gene RulerTM 1 kb DNA ladder Thermofisher Scientific, USA

GibcoTM Amphotericin B Thermofisher Scientific, USA

GibcoTM Antibiotic-Antimycotic (100X) Thermofisher Scientific, USA

GibcoTM B-27TM Plus Supplement (50X) Thermofisher Scientific, USA

GibcoTM DMEM GlutaMAXTM Thermofisher Scientific, USA

Superscript III

Gibco™ Hepes Buffer Solution	Thermofisher Scientific, USA
Gibco™ MEM NEAA	Thermofisher Scientific, USA
Gibco™ N-2 Supplement (100X)	Thermofisher Scientific, USA
Gibco™ Neurobasal™-A Medium	Thermofisher Scientific, USA
Gibco™ Neurobasal™-A Medium,	Thermofisher Scientific, USA
no D-glucose, no sodium pyruvate	
Gibco TM Penicillin-Streptomycin (Pen/Strep) Glucose	Thermofisher Scientific, USA Carl Roth, Karlsruhe
Herculase II Reaction Buffer	Agilent Technologies, USA
L-Glutamine	Anprotec, Bruckberg
oligo(dT)	Thermofisher Scientific, USA
PFA (Paraformaldehyde)	Sigma Aldrich, USA
PBS (Phosphat buffered saline)	Sigma Aldrich, USA
RPMI 1640 w/o L-Glutamine	Anprotec, Bruckberg
Saccharose	Carl Roth, Karlsruhe
Staining Buffer	Becton-Dickinson, USA
Tris (Tris-hydroxymethyl-aminomethane)	Carl Roth, Karlsruhe
Trypsin	Thermofisher Scientific, USA
Universal Agarose	Bio&SELL, Nuremberg
3.4. Enzymes	
DNAse	Thermofisher Scientific, USA
Fast Start SYBR® Green Master	Roche, Switzerland
Herculase II Fusion DNA Polymerase	Agilent Technologies, USA
Proteinase K	Agilent Technologies, USA
RNAse A	Thermofisher Scientific, USA

Thermofisher Scientific, USA

Uracil-DNA Glycosylase

Thermofisher Scientific, USA

3.5. Plasmids

Table 2: Plasmids

Name	Description	Provider
Cas9	WT-Cas9 protein coding plasmid	Asst. Prof. MD. Julian
		Grünewald (TUM)
PE2	Prime editor (Cas9 H840A + RT)	Asst. Prof. MD. Julian
		Grünewald (TUM)
PE2Max	Prime editor (Cas9 H840A + RT) with Max	Addgene, USA
	architecture	Cat. Number: 174820
PE4Max	Prime editor (Cas9 H840A + RT) codon optimized	Addgene, USA
	with Max architecture	Cat. Number: 214102
PE2Max-	Coding for PE2Max and additional GFP reporter	Addgene, USA
GFP		Cat. Number: 180020
ABE8e-	All in one plasmid coding for ABE8e and	Dr. Dong-Jiun Jeffery Truong
USH1C	urg1/gRNA2	(HZM Munich)
ABE9-	All in one plasmid coding for ABE9 and urg1/gRNA2	Dr. Dong-Jiun Jeffery Truong
USH1C		(HZM Munich)

3.6. Oligonucleotides

gRNAs were designed by Dr. med. vet. Hannah Auch (AUCH, 2023) with the exception of the TwinPE pegRNAs, who were designed using an AI based tool (MATHIS et al., 2023) and ordered as plasmids by Dr. Christoph Gruber. Two consecutive capital letters indicate the cutting site of the gRNA, additional capital letters in the pegRNAs indicate the desired edits in the RTT part of the pegRNA, one corresponds to the causative mutation site, the other to a blocking mutation.

Table 3: Summary of gRNAs sequences

Name	Sequence 5'-3'
urg1	ggacccagcacacttaCTgg
asgRNA1	tcctccctgaggtctgCTat
asgRNA2	ctttgtcttcagggagCCct
asgRNA3	gatgggttgttctgagACag
asgRNA4	ctgaggtctgctatggGTgg
pegRNA1	ggacccagcacacttaCTgg- gtttaagagctatgctggaaacagcatagcaagtttaaataaggctagtccgttatcaacttgaaaaagtggcaccgagtcggtgc ttgCgaatgtaTcaccagtaagtgtgc
pegRNA2	ggacccagcacacttaCTgg- gtttaagagctatgctggaaacagcatagcaagtttaaataaggctagtccgttatcaacttgaaaaagtggcaccgagtcggtgc ttgCgaatgtaTcaccagtaagtgtgctg
pegRNA3	ggacccagcacacttaCTgg- gtttaagagctatgctggaaacagcatagcaagtttaaataaggctagtccgttatcaacttgaaaaagtggcaccgagtcggtgc ttgCgaatgtaTcaccagtaagtgtgctgggt
pegRNA4	ggacccagcacacttaCTgg- gtttaagagctatgctggaaacagcatagcaagtttaaataaggctagtccgttatcaacttgaaaaagtggcaccgagtcggtgc tatgtgctgCgaatgtaTcaccagtaagtgtgc
pegRNA5	ggacccagcacacttaCTgg- gtttaagagctatgctggaaacagcatagcaagtttaaataaggctagtccgttatcaacttgaaaaagtggcaccgagtcggtgc tatgtgctgCgaatgtaTcaccagtaagtgtgctg

peg	gRNA6	ggacccagcacacttaCTgg- gtttaagagctatgctggaaacagcatagcaagtttaaataaggctagtccgttatcaacttgaaaaagtggcaccgagtcggtgc tatgtgctgCgaatgtaTcaccagtaagtgtgctgggt
	USH1C	gattgaaaatgatgcaGAga-acacttactggtgAtacattcGcagcacatcatagagatagtctttctctgcatc
Twin-pegRNA1	fwdI	
n-pe	USH1C	ggacccagcacacttaCTgg-
Twi	revI	ttgaaaatgatgcagaaggactatctctatgatgtgctgCgaatgtaTcaccagtaagtgtgctggg
	USH1C	gattgaaaatgatgcaGAga-tggtgAtacattcGcagcacatcatagagatagtctttctctgcatc
Twin-pegRNA2	fwdII	
in-pe	USH1C	ggacccagcacacttaCTggagaaggactatctctatgatgtgctgCgaatgtaTcaccagtaagtgtgctggg
Twi	revII	

Several ssODNs were designed and tested by Dr. Hannah Auch (AUCH, 2023). The best one was used for this thesis. The capital letters indicate the desired edits at the causative site and for the integration of a blocking mutation.

Table 4: ssODN Sequence

Name	Sequence 5'-3'
urt1.3	tctgattgaaaatgatgcagagaaggactatctctatgatgtgctgCgaatgtaTcaccagtaagtgtgctgggtccagctcttgtgggccac
	ttgggttcctttgtcttcagggagecctgggatggttgttctgagacagaggagctcagagggtggatgctcacggctcctggaaa

3.7. Primers

Table 5: Summary of Primer Sequences

Name	Forward 5'-3'	Reverse 5'-3'
huUSH2	ccttgctctgttacccgttc	gttctgtccaacaatcatgc
huUSH4	tgagcctggagctgtgattc	tgagcctggagctgtgattc
ush1s	gtgcctggccacatctgga	
eGFP	gagegeaceatettettea	gttcaccttgatgccgttct
CAS9	cagcacaagcactacctgga	cccagattggtcagggtaa
pegRNA	cagagagtttaagagctatgctgga	tgtgctgcgaatgtatcacc
GAPDH	cagaacatcatccctgcttc	getteaceacettettgatg
IL1Bf	ggcacactcaccccaaagaa	gtcctctgtccttggcacc
CCL2	ttctccagtcacctgctgcta	ccacttctgcttgggttctg
IL8	tacgcattccacacctttcc	ggtccaggcagacctctttt
IFNg	tcaaaggagcatggatgtga	tetgaettetetteegetttet
TNFa	cgttgtagccaatgtcaaagc	tggtgtgagtgaggaaaacg
TGFbeta	cctgggctggaagtggattc	ccgggttgtgctggttgta
CYBB	aggcagactcaaggcattcaa	gegeagacceaagaagtttt
NLRP3	agcatgagctccttgccatt	ttgcatcttggctgaggtcc
ACTA2	agtgegacattgacateagg	ggagtatttgcgctcagga
cd45	ctgatgaacgtggagcctatc	accetgeateteegtttatate
CD68	ctccaagcccagattcagatt	cagccatgtagttcaggtagac
CD172a	caggtccggaggaagtgaac	acceteactettgagteeca
RHO	ccatcaacttcctcacgctcta	agacaaagtatccatgcagagagg
PDE6A	ggctaccgcaggatcaccta	ggtcaatgtcgtggcagaag
ARR3	tecaceaacaaggteateaa	agccaggagtggggttactt
RLBP1	ttcaagggctttaccatgc	aagaagggtttgaccacgtt
GAD1	gaccgtgcagttcctactgg	gggtggtcagagagttccaa
ONECUT1	tcagggcaaatggaagagat	atteteegaaaggteteaeg
RPE65	cgtgagaactgggaagaggt	agecagatggtetegteact
GFAP	agatecatgaegaggaggtg	gttaggtccgcaaacttgga
MYO7A	ctcacaatccctccaagagc	gtgtcccattgacgaaggtc
USH1C	getetteateteeeacetea	tgcctcactttgatggacac

SANS	ctgcataccacggcaatct	tgtccaggcaccagatgtt
PCD15	ccagaccaggaagcaagtatc	gggtctgcatcttcagcataa
CDH23 U	ctatgtgctgtccctctgg	egetggeteatteteataea
CDH23_D	cacccacatttcacaaccag	cactgtcgatggcaaagaac
WHR	ggcagtgtgtccgtggag	gtccaggtcttgcggagag
USH2A	tgtaatcagtgtctcccaggttt	caaggetgacatettecagte
ADGRV1	gtgcctccacctctgaacat	tectecagecacettgatta
SOD1	ggatcaagagggcacgttg	ctgcccaagtcatctggttt
CAT	cacagegaataccetettatee	acggaagggacagttcacag
GFX4	agaacggctgtgtggtgaag	ctagaggtagcacggcaggt
TXN	cagtgcaggagagaaactcg	cacactetgaageaacateet

3.8. Kits

AmaxaTM Basic NucleofectorTM Kit Lonza, Switzerland

DNeasy® Blood & Tissue Kit Qiagen, Hilden

Endofree Plasmid Maxi Kit Qiagen, Hilden

FIX & PERMTM Cell Permeabilization Kit Thermo Fisher Scientific, USA

NucleoSpin Gel and PCR Clean-up Macherey-Nagel, Düren

Neural tissue dissociation kit (P) Miltenyi Biotec, Bergisch-

Gladbach

RNeasy Plus Micro Kit Qiagen, Hilden

3.9. Antibodies

Table 6: Primary antibodies

Name	Target	Host	Clonality (Clone)	Isotype	Supplier	Catalogue Number
RCVR	PRC	Rabbit	Monoclonal (clone 1K10 ZooMAb®)	IgG	Merk	ZRB1448- 4X25UL
RBPMS	Ganglion cells	Rabbit	Polyclonal	IgG	Abcam	ab152101
CRALBP	Müller glial cells	Mouse	Monoclonal (Clone # B2)	IgG ₁	Bio-Techne	NB100- 74392
CHX10/ VSX2	Bipolar cells	Mouse	Monoclonal (N/A)	IgG2a κ	Santa Cruz Biotechnology	sc-365519
IBA1/AIF1	Microglial cells	Chicken	Monoclonal (Ch311H9)	IgY	Synaptic Systems	234 009

Table 7: Secondary antibodies

Name	Target	Host	Clonality	Isotype	Supplier	Catalogue
						Number
Donkey anti-Rabbit IgG AF555	Rabbit IgG	Donkey	Polyclonal	IgG	ThermoFisher	A-31572
Donkey anti-Rabbit IgG PE	Rabbit IgG	Donkey	Polyclonal	Ig	ThermoFisher	12-4739-81
Donkey anti-Rabbit IgG AFPlus594	Rabbit IgG	Donkey	Polyclonal	IgG	ThermoFisher	A32754
Donkey anti-Mouse IgG AFPlus488	Mouse IgG	Donkey	Polyclonal	IgG	ThermoFisher	A32766
Donkey anti-Mouse IgG AFPlus647	Mouse IgG	Donkey	Polyclonal	IgG	ThermoFisher	A32787
Donkey anti-Mouse IgG AF790	Mouse IgG	Donkey	Polyclonal	IgG	ThermoFisher	A11371
Donkey anti-Chicken IgY AF594	Chicken IgY	Donkey	Polyclonal	IgG	ThermoFisher	A78951
Donkey anti-Goat IgG AF647	Goat IgG	Donkey	Polyclonal	IgG	ThermoFisher	A-21447

3.10. Software

BD FACSDivaTM Becton-Dickinson, USA

BioEdit Sequence Alignment Editor 7.0.5.3 Informer Technologies Inc.,

USA

Claude (used for grammar and syntax check)

Anthropic, USA

Endnote20 Clarivate Analytics, UK

FinchTV 1.4.0 Geospiza Inc., USA

FlowJo v10.10 Becton-Dickinson, USA

ImageJ/Fiji

Light Cycler 96® Software 1.1.0.1320 Roche Diagnostics,

Switzerland

LAS X Office Leica, Wetzlar, Germany

Microsoft Office 2016 Microsoft Corporation, USA

Mira Revision Pathmedical GmbH, Germering
SnapGene Viewer 6.0 Graph Pad Software, USA
Ugene 52.0 Unipro, Russia

4. Methods

4.1. Cell Culture

4.1.1. Standard PKC Culture

All the protocols bellow were adapted from the work of (RICHTER et al., 2012). Standard culture conditions: Incubator at 37°C, CO2 5%. Work under sterile conditions in HeraSafe (Heraeus) workbench.

Table 8: Standard medium composition (15% FCS)

Total volume	500 mL
DMEM GlutaMAX	410 mL
MEM NEAA	5 mL
HEPES-Buffer	5 mL
Mercaptoethanol + PBS (3,5 μL in 5 mL)	5 mL
FCS	75 mL

4.1.2. Plate Coating

All plates used for the culture of PKC were coated with a 1:10 dilution of Collagen 2% (Serva) in cell culture grade ddH2O. After coating, the plates were incubated for 1h in an incubator at 37°C. The surplus of collagen was aspirated, and the plates were placed in the fridge at 4°C upon use.

4.1.3. Isolation of USH1C PKC

After kidney collection from USH1C pigs, a 1x1x1 cm piece from the cortex was cut out and washed in PBS containing 2% of Amphotericin B and 2% Pen/Strep. The tissue was disrupted manually using 2 scalpel blades and washed with medium. After being transferred to a centrifugation tube and centrifuged for 5 minutes at 170 g, the supernatant was removed. The disrupted tissue was placed in an Erlenmeyer flask and supplemented with 10 mL of Collagenase-II. A digestion took place for

ca. 1h30 at 37°C under shaking conditions. The digested tissue was washed with medium and passed twice through a 100 µm cell strainer. The obtained cell suspension was resuspended in medium supplemented with 1% of Amphotericin B and 1% of Pen/Strep, then seeded on 10cm plates using different seeding densities. Confluency should be reached within 48h-72h after which the cells can be frozen or further passaged.

4.1.4. Thawing of Cells

Cells were cryopreserved in aliquots of 1.10⁶ cells in a 1:10 dilution of DMSO in FCS and stored in liquid nitrogen. Upon thawing, the content of the cell aliquots was resuspended in 5 mL of culture medium and centrifuged at 170 g for 5 minutes. The supernatant was aspirated, and the cell pellet resuspended in 10 mL of medium, then seeded on a 10 cm plate.

4.1.5. Harvesting and Seeding of Cells (example for 10cm plate)

After visual assertation of the confluency under a light microscope, the cells were either passaged or harvested for further processing (electroporation, freezing of cell pellet). The medium was aspirated, and the plates were washed twice with 10 mL of PBS. After aspiration, 1,5 mL of Trypsin 0,4% were applied on the cells. After 5 minutes of incubation in an incubator, a minimum of 5,5mL of medium was used to wash the plate and transfer the cell suspension to a centrifugation tube. The cells were counted using a counting chamber and centrifuged for 5 minutes at 170 g. The supernatant was aspirated, and the cell pellet resuspended in a volume of medium according to the desired concentration. In general, 1.10⁶ were seeded on a 10 cm plate and harvested each 24h at 70% confluency.

4.1.6. Electroporation for Gene Editing Experiments

Construct preparation: Endotoxin-free prepared plasmids were electroporated. All were prepared prior to each experiment in 1,5 mL centrifugation tubes. The general rule applied was to use all components in a similar ratio except if mentioned differently. For each reaction, 1,5 μ g of each necessary plasmid were used in a total volume of 5 μ L (dilution in endotoxin free H2O).

The cells were harvested according to the protocol above. The cell pellet was resuspended to a 0,5.10⁶ cells/mL of medium concentration and transferred to 1,5

mL centrifugation tubes, one per electroporation reaction. After centrifugation of the tubes for 5 minutes at 2000 rpm, one tube at a time, the supernatant was aspirated, the cell pellet resuspended in 100 μL of Amaxa-Solution, transferred to the tube containing the construct and finally to an electroporation cuvette. The program U-12 of the Nucleofector 2b was used. After successful electroporation, the content of the cuvette was resuspended in medium and seeded on a 6-well plate. The cells were harvested 24-72h after electroporation.

4.1.7. Freezing of Cell Pellet for Molecular Analysis

The cells were harvested according to the standard culture protocol. The final centrifugation was executed in 1,5mL centrifugation tubes for 5 minutes at 5000 rpm. After aspiration of the supernatant, the cell pellet was washed once in PBS and frozen at -80°C upon further analysis.

4.1.8. Delivery Vector Testing in PKC

For the testing of different gene vectors in PKC, the cells were seeded on either 48-well or 96-well plates according to the standard protocol. The seeding densities were 20.000 cells for a 48-well and 10.000 for a 96-well. Once the cells attached to the plate, the vectors were applied directly in the medium in different concentrations. After 72h, the cells were either harvested and frozen and stored at -80°C as a cell pellet upon further analysis or harvested for flow cytometry analysis and assessment of transfection efficiency. All vectors were provided by collaborators and diluted in PBS.

4.1.9. Flow Cytometry

The cells were harvested and after a PBS wash, the cell suspension was fixed with $500~\mu L$ of 4% PFA for 20 minutes at room temperature, washed again with PBS and stored at $4^{\circ}C$ upon further analysis.

The flow cytometry analysis was performed using the BD LSR Fortessa (Beckon-Dickinson) of the Gene Center Flow Cytometry Facility (LMU). All analyses were recorded with the FACS Diva Software and further analyzed with the FlowJo v10.10 software. After gating the cell singlets using forward and side scatter, GFP signal was measured and gated based on the signal in negative samples from the same experience.

4.2. Molecular Biology

4.2.1. DNA Isolation from Cells and Tissue

For DNA isolation, the DNeasy® Blood & Tissue Kit of Qiagen was used according to the manufacturer's protocol.

4.2.2. End-point PCR for Gene Editing efficiency analysis

Table 9: PCR protocol upon sanger sequencing

PCR protocol		Cycler program			
H ₂ O	17.45 μL	Denaturation	95°C	5 min	
dNTP (100mM)	0.25 μL	Denaturation	95°C	30 s	
Q-Solution	0 μL	Annealing	59°C	30 s	2.5
Herculase II Reaction Buffer	5 μL	Elongation	72°C	1 min	35x
huUSH2f (10μM)	0.4 μL	Final	72°C	10 min	
huUSH2r (10μM)	0.4 μL	Termination	4°C	10 min	
Herculase II	0.5 μL				
DNA sample	1 μL				

Table 10: PCR protocol upon NGS sequencing

PCR protocol		Cycler program			
H ₂ O	17.45 μL	Denaturation	95°C	5 min	
dNTP (100 mM)	0.25 μL	Denaturation	95°C	30 s	
Herculase II Reaction Buffer	5 μL	Annealing	59°C	30 s	
huUSH4f (10 μM)	0.4 μL	Elongation	72°C	15 s	35x
huUSH4r (10 μM)	0.4 μL	Final	72°C	10 min	
Herculase II	0.5 μL	Termination	4°C	10 min	
DNA sample	1 μL				•

4.2.3. Sequencing

All PCR products were prepared for subsequent experiments using the NucleoSpin Gel and PCR Clean-up kit (Macherey-Nagel) according to the manufacturer's instructions.

Sanger sequencing was performed at the sequencing service of the LMU. Both forward and reverse electropherograms were obtained for one sample and the mean was documented for each experiment. NGS sequencing was performed through the Genewiz (Azenta) platform using the amplicon EZ protocol.

4.2.4. Assessment of Gene Editing Efficiency

After sanger sequencing, result files were uploaded to the Synthego ICE webtool (https://ice.editco.bio). The software assesses the height of the modified peaks of the electropherograms compared to a control sample and calculates accordingly the percentage of edited cells. The results were plotted as the mean value of the editing efficiency in the forward and reverse sequences of one sample.

NGS sequences were analyzed by collaboration partners using the software Geneious prime. The percentage of GE efficiency corresponds to the proportion of reads containing the desired mutations.

4.2.5. RNA Isolation from Retina, Retinal Explant and RPE

For RNA isolation, the RNeasy Plus Micro Kit (Qiagen) and according to manufacturer's protocol was used.

4.2.6. DNA Digestion and cDNA Synthesis:

To 1 μ L of isolated RNA, 1.5 μ L DNase and 1.5 μ L of DNase buffer were added and the total volume adjusted with ddH2O to 15 μ L. After 30 minutes of incubation at 37°C, 1 μ L of EDTA (50mM) were added to the mix and incubated for 10 minutes at 65°C. Immediately after, the tubes were placed on ice for 1 minute. cDNA was synthesized from the DNase-treated RNA in a reaction mixture containing 1 μ g of RNA, 1 μ L of 10 mM dNTPs, 1 μ L of cDNA synthesis primers*, 1 μ L of 0.1 M DTT, 4 μ L of reaction buffer, and 1 μ L of SuperScript III reverse transcriptase, with the final volume adjusted to 20 μ L using nuclease-free water. First, they were incubated for 60 minutes at 50°C and finally for 15 minutes at 70°C.

* oligo(dT) primers were used to detect all transcripts, while it was replaced by Random hexamers for the detection of pegRNAs, which lack a poly-A tail.

4.2.7. **qPCR** Analysis

qPCR was carried out in a 10 μL reaction mixture containing 5 μL of FastStart Essential DNA Green Master (Roche Life Science, Basel, Switzerland), 0.3 μL of specific primers (300 Nm, listed in table 1), 2 μL of cDNA (0.5 ng), 0.06 μL of Uracil-DNA glycosylase (Thermo Fisher Scientific), and 2.34 μL of ddH2O. Reactions were performed in duplicate using the LightCycler96 RT-PCR system (Roche Life Science) with the following thermal cycling conditions: 50°C for 2 min, 95°C for 10 min, followed by 45 cycles of 95°C for 10 s, 63°C for 90 s

(combined annealing and extension step). A final melt curve analysis was performed to verify PCR specificity by detecting a single, distinct peak.

GAPDH or the combination of PPIA, GAPDH and RPL19 expressions were used for data normalization. The relative expression of each gene was calculated using the $\Delta\Delta$ Ct method. Data analysis was conducted using the LightCycler96 software results were extracted and processed in Microsoft Excel.

4.3. Animal Experiments

For all *in vivo* experiments, the following anesthesia protocol was followed:

The animals were sedated with an intramuscular injection of Azaperone (2 mg/kg BW), Atropine sulfate (0.02 mg/kg BW), and Ketamine (20 mg/kg BW). An intravenous ear vein catheter was used to deepen anesthesia with Propofol (2 mg/kg BW), followed by endotracheal intubation to ensure manual or mechanical ventilation. Anesthesia was maintained via continuous Propofol infusion and Isoflurane inhalation (GROTZ et al., 2022).

4.3.1. DPOAE, ABR and ASSR Measurements

The procedure began with an otoscopic examination to assess ear cleanliness, followed by cleaning with cotton swabs as needed to insure a tight fit of the ear inserts. For measurements, the Sentiero Advanced (PathMedical) device was used.

DPOAE testing was conducted first. A single transducer with size-appropriate silicone or foam insert was placed in the ear. After device calibration and leak check, measurements were recorded at stimulus levels of 65/55 dB and 55/45/35 dB at frequencies between 1000 Hz and 8000 Hz for each ear.

For ABR and ASSR tests, the configuration was modified. Three needle electrodes were placed as follows:

- Active electrode: high forehead, midway between frontal foramina and occipital bone
- · Reference electrode: right mastoid muscle (ipsilateral for right ear, contralateral for left)
- · Ground electrode: nose

Bilateral measurements were enabled by inserting ear probes in both ears simultaneously. Tests included ABR clicks, ABR tone burst, and ASSR.

4.3.2. ERG/OCT measurements

The measurements were performed according to the methodology described in (GROTZ et al., 2022).

4.3.3. Gene Editing Pilot in vivo Experiment

The pilot experiment was performed at the Pigmod, Liblice (CZ) where a sister herd of the USH1C pig model was established several years ago. Two USH1C pigs, were used, both male and littermates, 1,5 years old. Additionally to the standard anesthesia protocol, Rocuronium (0,6 mg/kg BW) was given to prevent eye muscle movement. Pupil dilation was achieved using a topical application of Tropicamide 1% and Atropine 0.5%. The periorbital region was shaved and disinfected before vector injection, and Proxymetacaine was used as a local anesthetic.

The subretinal injection was performed by Prof. Dr. Dr. MD Dominik Fischer (Oxford Eye Hospital, Oxford University, UK). A speculum was placed in the eye, followed by three sclerotomies and a pars plana vitrectomy. A 41-gauge needle was used to apply the vectors in the subretinal space, creating so-called "injection blebs". Finally, 0.5 mL of a solution containing Dexamethasone (1 mg) and Piperacillin (25 mg) was injected subconjunctivally to prevent infection and inflammation. The animals were given an intravenous dose of Meloxicam (0.4 mg/kg BW) for pain relief.

After one week, both animals and a third non injected USH1C control animal were sedated again. An assessment of the eye's fundus and an OCT measurement of each eye were performed. After the measurement, the animals were euthanized and the eyes collected.

4.4. Retina Explant (RE) Culture

4.4.1. Culture Conditions

The protocol used was taught and provided by Maria Weller, Dr. Brigitte Müller and Prof. Knut Stieger (JLU Gießen). It can be found in the following publication (WELLER et al., 2024). In brief, pigs were sedated and euthanized, and their eyeballs were enucleated. The eyes were placed in tubes containing transport medium and kept on ice upon further processing. After a waiting time of at least 30min, the eyes were processed under sterile conditions in a cell culture laminar

flow. The wait insured the success of the further steps as we had trouble collecting the explants when the eyes were too fresh.

The intact eyeballs were placed shortly in 70% EtOH, rinsed with ddH2O and finally opened by cutting around the iris. After removal of the vitreous, the eye cups were rinsed once in PBS. The visual streak was cut out and divided in 4-6 pieces of 4x5mm. The retina of these pieces was collected using a raspartorium to detach it from the underlying RPE and placed on a cell culture insert, photoreceptors side laying down on the insert and ganglion cell layer on top. Contrarily to the original protocol, Millicell® Standing Cell Culture Inserts were used. Each insert was placed in a 6-well plate on top of 1mL of Neurobasal medium containing 5% of Anti-anti and further processed according to the planned experiment. Medium change happened every 48-72h, after one week of culture the concentration of Anti-anti in the culture medium was changed to 1%.

Table 11: Transport Medium Composition

Total volume	100 mL
DMEM GlutaMAX	40 mL
RPMI	40 mL
Anti-Anti	10 mL
HEPES 250mM	10 mL

Table 12: Neurobasal Culture Medium for RE (5% Anti-anti)

Total volume	100 mL				
Neurobasal-A + Glucose	20,2 mL				
Neurobasal-A - Glucose	70,8 mL				
B27	2 mL				
L-Glutamine	1 mL				
Anti-Anti	5 mL				
N2	1 mL				

4.4.2. Application of Delivery Vectors

The application of delivery vectors took place in different concentrations ranging from 5μ L to 45μ L. They were applied on top of the explants at d0.

4.5. Immunofluorescence of Retina and Retina Explants

The REs were washed once with PBS. The membrane of the inserts was cut around them and used to transfer them into 6-well plates using forceps. Retina and RE were fixed for 45min with 4% PFA at room temperature on an oscillator. After washing with PBS, 2mL of 30% sucrose were applied and the explants were kept in the parafilm sealed plates overnight at 4°C.

The fixed tissue was embedded in Cryomolds using O.C.T. The cryomolds were then frozen with liquid nitrogen. After completion, the cryomolds were packed in parafilm first, then aluminium foil, and stored at -20°C for short-term and -80°C for long-term storage. The Cryostar NX50 cryotome (Epredia) was used to cut $14\mu m$ cross sections of the retina. Superfrost Epredia slides were used. After 1h of drying at room temperature, the slides were stored at -20°C for short-term and -80°C for long-term storage.

The slides were thawed at room temperature for 30 minutes and afterwards washed with PBS. They were first blocked in PBS containing 5% of Normal Donkey Serum (NDS) for 1h at room temperature. After a new PBS wash, they were incubated overnight at 4°C with the primary antibodies diluted in PBS and 5% NDS. The primary antibodies were washed off with PBS and the slides incubated for 1h at room temperature and in the dark with the secondary antibodies and DAPI, again diluted in PBS and 5% NDS. After a final PBS wash, the slides were covered with fluorescence mounting medium and coverslip. After approx. 1h of drying, the slides could be analyzed with the Axiovert M200 fluorescence microscope (Zeiss) or Thunder (Leica) fluorescence microscope.

4.6. Retina Dissociation

The protocol was adapted from the publication of (MULLER et al., 2025). Shortly, the Neural tissue dissociation kit (P) kit was used to dissociate the REs. First, 40μL of Enzyme P and 950μL of Buffer X were mixed and added to an explant in a 12-well plate. After 20-30 minutes of shaking at 37°C, 5μL of Enzyme A and 10μL of Buffer Y were mixed and added. After an additional 15 minutes of incubation at 37°C while shaking and resuspension using a pipette, 1mL of Neurobasal Medium

was used to transfer the cell suspension into a 15 mL centrifugation tube. The total volume was adjusted to 5mL and the cells were centrifuged for 5 minutes at 300rcf and 4°C. After removing the supernatant, the cells were washed with Neurobasal medium again and passed through a 70μm, followed by a 40μL cell strainer. After a final centrifugation and removal of supernatant, the cell pellet was resuspended in 100μL of Staining buffer. Using the Fix and Perm kit (Thermofisher) and according to the manufacturer's protocol, 100μL of Medium A were added to fix the cells. After 15 minutes of incubation at room temperature, the cells were washed with 800μL of staining buffer and centrifuged for 5 minutes at 900rcf and 4°C. The pellet was resuspended in 300μL in staining buffer. For permeabilization and staining, the mix was supplemented with 100μL of Medium B and primary antibodies and incubated for 30min at room temperature. After washing and centrifugation according to the previous steps, the pellet was resuspended in a mix of secondary antibodies and DAPI. After a final wash and centrifugation in staining buffer, the cells were ready for flow cytometry analysis.

4.7. 3D Quantification of Retina Explants

The explants were fixed as described in paragraph 4.5. After fixation, a permeabilization of 6h using 0,2% Triton-X diluted in PBS was performed. After a PBS wash, the REs were incubated with the primary antibodies for 24h. After a wash, the secondary antibodies and DAPI were applied overnight. The analysis took place at the Institute of Physics (LMU) and was performed by Teresa Rogler based on her preprint (ROGLER et al., 2024)

IV. RESULTS

1. Development of GE Strategies in Proliferative Cells

The first part of my thesis focused on *in vitro* testing of therapeutic gene editing (GE) strategies, using proliferative porcine kidney cells (PKC) isolated from USH1C pigs. Different GE variants were tested in collaboration with partners from the Helmholtz Zentrum Munich (HZM). Initial testing of GE variants in PKC was performed by highly effective plasmid electroporation. For defined settings, I also explored delivery by innovative non-viral vectors.

1.1. Double Strand Break Mediated Homology Directed Repair (DSB-HDR)

Basic attempts at gene repair for the treatment of USH1C based on the c.91C>T/p.R31X mutation (short R31X) were conducted previously (AUCH, 2023), aiming at homology-directed repair (HDR) with a single stranded oligonucleotide donor template (ssODN) serving as repair template and CRISPR-Cas9 inducing DSB. Besides the correcting mutation, the ssODN aims at a silent nucleotide exchange in the genome, i.e. a nucleotide variant that does not alter the amino acid sequence but prevents repeated re-cutting by disrupting the target site for the gRNA ("blocking mutation") (Fig. 4, A). Relevantly, DSB-HDR competes with NHEJ repair pathways, bearing the risk of detrimental bystanding mutations. GE efficiency was consistently examined by Sanger sequencing of PCR products amplified from the modification site (Fig. 4, B and C).

When re-evaluating DSB-HDR, I observed substantial variability in editing efficiency between technical replicates. These variations correlated with altered cell culture conditions, such as confluency of the cells upon electroporation and their passage number. Aiming at stable, justifiable conditions with high editing rates, experiments were standardized for low passage numbers (P6 at the maximum) and 70% confluency at the time point of harvesting for electroporation. Using this optimized protocol, an average HDR efficiency of 16.3% and average NHEJ of 41.4% (Fig. 3, D) were obtained from 9 technical replicates.

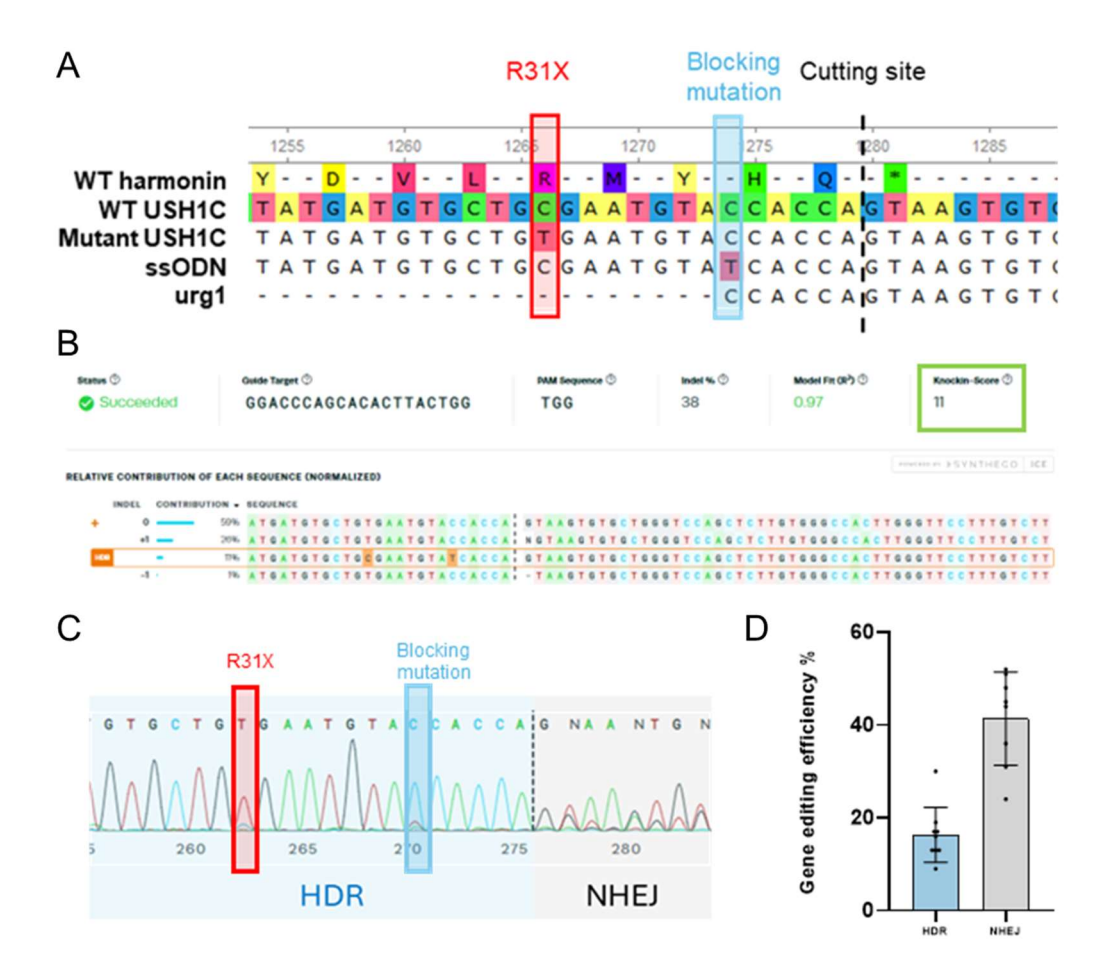


Figure 4: DSB-HDR Gene Repair Approach

(A) Modification site in the USH1C exon 2 with cutting site of urg1 gRNA (dotted line), the intended repair mutation site (red box) and blocking site (blue box). (B) Representative GE efficiency assessment using the Synthego ICE software (https://ice.editco.bio/) for a DSB-HDR approach. The tool indicates the rate of NHEJ-mediated indels as well as the percentage of HDR (Knock-in Score, Green box, upper panel). The most abundant sequence variants are given according to their frequency (lower panel), with the vertical dotted line indicating the cutting site. In case of HDR, the intended differences to the non-modified sequence (top line) are marked by orange boxes. (C) Representative electropherogram of a DSB-HDR experiment. Cutting site of urg1 gRNA (dotted line), the intended repair mutation (red box) and blocking site (blue box) indicated. The reading from left-to-right reflects the 5'-3'-direction of the Sanger sequencing orientation, demonstrating NHEJ by mixed electropherogram peaks downstream of the cutting site. (D) Summarized GE efficiency of DSB-HDR electroporated USH1C PKC using the standardized protocol and an incubation time of 24 hours post electroporation. Each dot represents a single experiment. Mean ± SD of n=9 technical replicates.

1.2. Adenine Base Editing (ABE)

The USH1C R31X mutation is a candidate for gene repair using an ABE approach through an A•T to G•C conversion. Thus, ABE variants were designed, tested in HEK293 standard assays and then examined in PKC from the USH1C pig model in collaboration with Dr. Dong-Jiun Jeffery Truong and Prof. Dr. Gil Westermeyer (HZM). Among the ongoing refinements of ABE, I tested 2 versions: ABE8e, which showed significantly increased conversion capabilities compared to previous ABE variants (RICHTER et al., 2020) and ABE9, optimized for a narrow modification window and thereby reducing bystander mutations (CHEN et al., 2023). Both ABE variants were guided by urg1, determined in the initial DSB-NHEJ experiments or an alternative gRNA.

ABE9 + urg1 resulted in 4% editing of the causative mutation and 1% editing of a neighboring adenosine base located 4 nucleotides (nt) downstream of the target site (Fig. 5, A). ABE8e + urg1 resulted in 14.5% editing of the causative mutation and 5% editing of closely located adenosines downstream (+4nt) and upstream (-5nt) of the causative mutation. Both unintended A•T to G•C conversions in flanking positions induce missense mutations (Fig. 5, B), resulting in detrimental V29A and M32T variants.

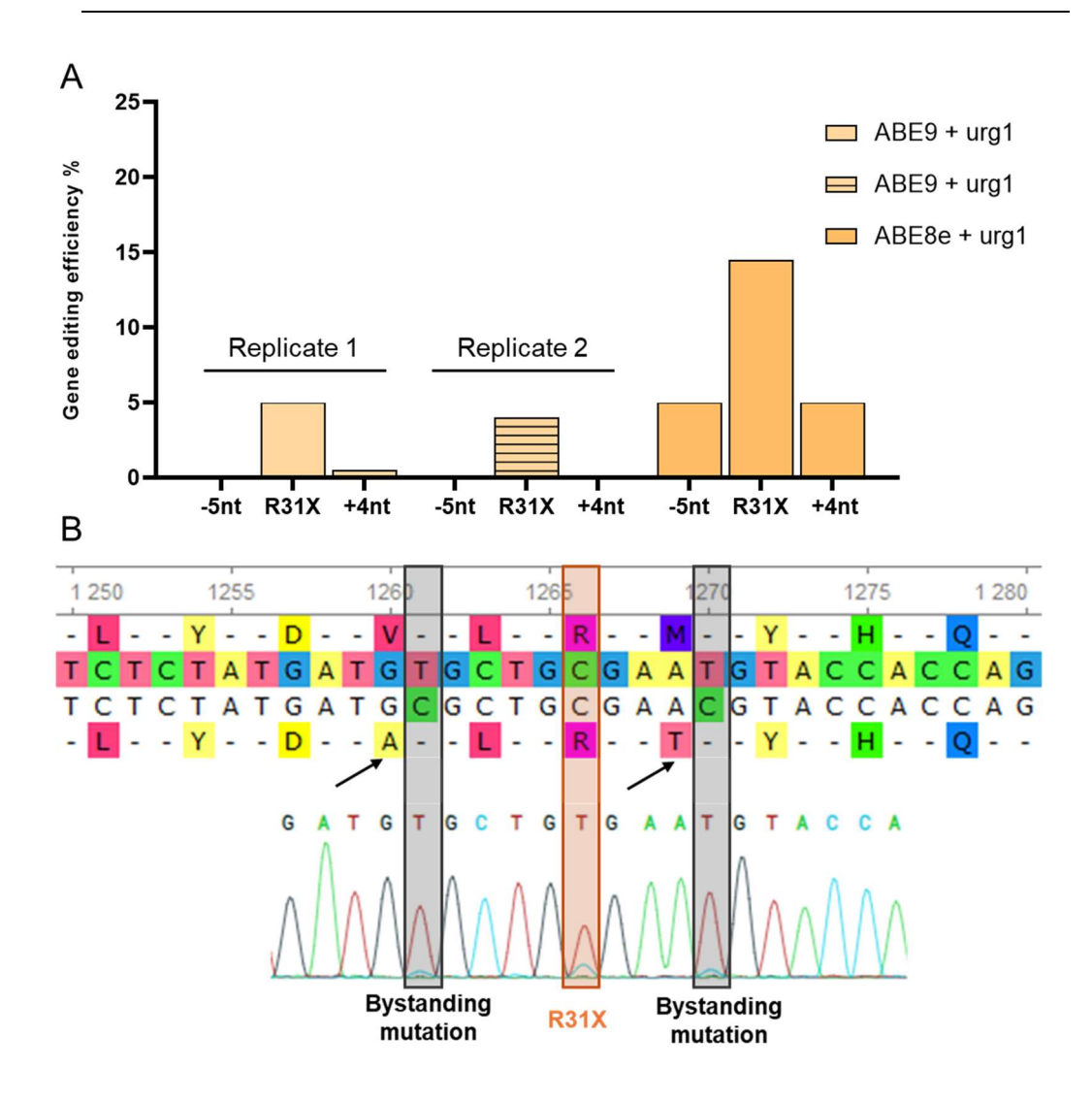


Figure 5: Adenosine Base Editing in USH1C Porcine Kidney Cells

(A) In 2 independent experiments, ABE9-urg1 combinations achieved 4% of editing of the causative mutation on average and showed some minor editing activity in neighboring bases after electroporation of a single plasmid carrying both components. ABE8e + urg1 reached 14,5% of editing at the R31X mutation and 5% edits in the +4nt and -5nt neighboring adenosine bases after cultivation for 72 hours. (B) Consequences of ABE-mediated nucleotide exchanges around the USH1C c.91C>T site. The intended correcting mutation is highlighted by the orange box. Original nucleotide sequence and corresponding amino acid codons (upper lines) are compared to the alterations resulting from unintended modifications (black boxes, arrows in lower lines). The sequences are compared to a representative electropherogram from an ABE8e + urg1 experiment.

1.3. Prime Editing

Among GE variations, prime editing (PE) is highly flexible, allowing almost any transition or transversion at a defined site. Again, several variants emerging from the literature were designed, tested in HEK293 cells and compared in PKC of the USH1C pig model, in collaboration with Dr. Christoph Gruber and Dr. Florian Giesert (HZM).

First, we tested PE3 (ANZALONE et al., 2019), an advancement to previous PE attempt by adding an assistant guide RNA (asgRNA), creating an additional single strand break (SSB) on the non-edited strand near the target site. First, different asgRNAs were evaluated for their capacity to induce DSB-mediated NHEJ (Fig. 6, A). Then the most potent asgRNA3, was combined with different pegRNA in a PE3 attempt, showing varying efficacy from 0% to 2.7% on average (Fig. 6, B).

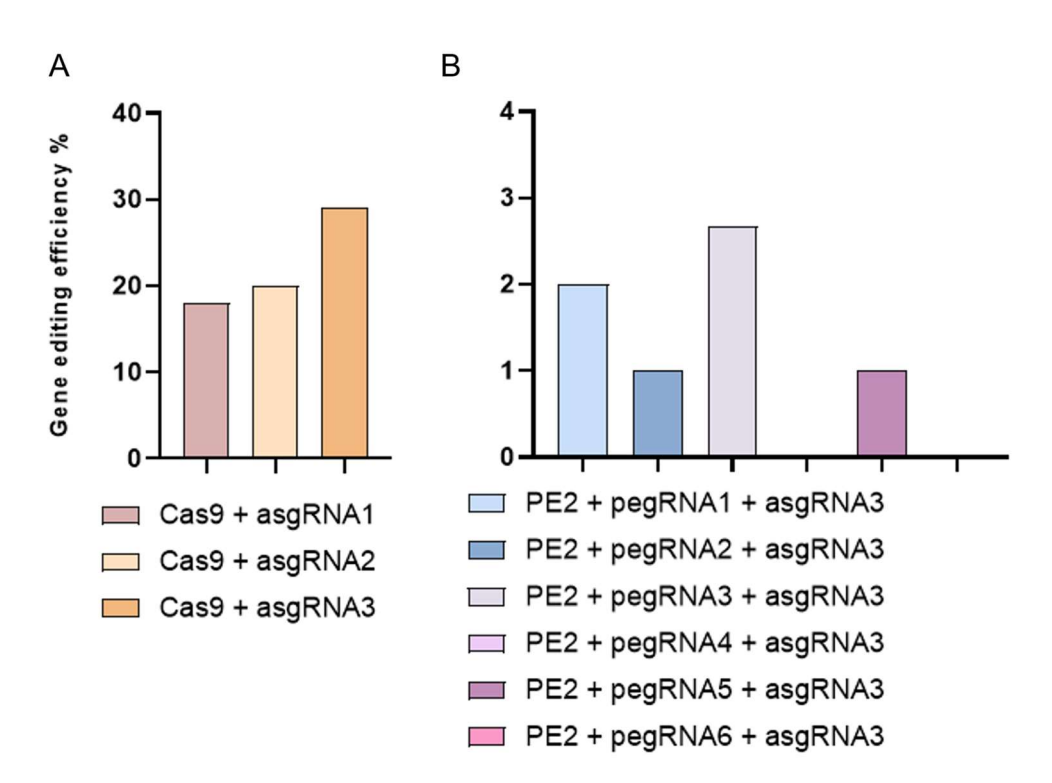


Figure 6: Prime Editing Using PE3 with Different asgRNA and pegRNA

(A) NHEJ capacity of asgRNA candidates in explorative experiments, using co-transfection of plasmids carrying asgRNA and Cas9 cassettes. (B) PE3 experiment of distinct pegRNA, combined with asgRNA3 after electroporation of single plasmids comprising all PE components. As best combination, pegRNA3 + asgRNA3 reached 2,7% of GE efficiency after an incubation time of 72h post electroporation.

In an alternative setting, PEMax was tested, comprising an alternative Cas9 coding sequence, a codon-optimized RT domain and an additional nuclear localization signal (NLS) (CHEN et al., 2021). Compared to PE3 (7.5% correction), PE3Max reached a slightly increased efficiency of 10.5% (Fig. 7).

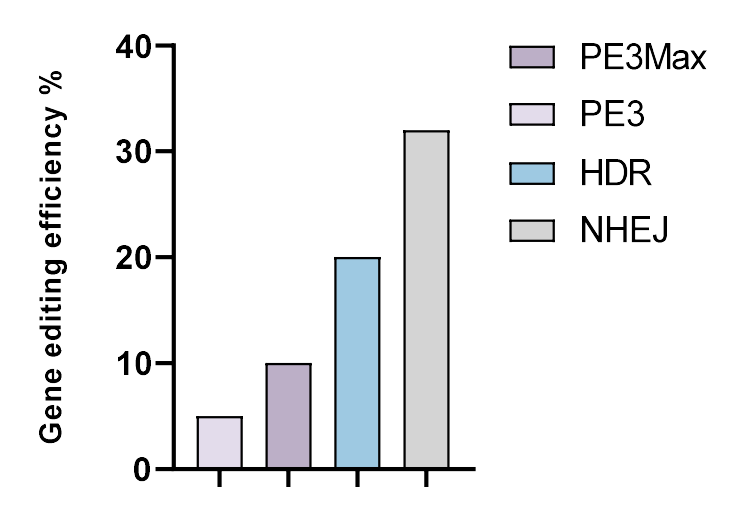


Figure 7: Prime Editing Using PEMax.

PE experiment comparing the efficacy of PE3 and PE3Max. The max architecture reached 10,5% of editing efficiency, while PE3 reached 7,5% after 72h of incubation post electroporation.

Next, twin prime editing (TwinPE) was explored. In this setting, 2 pegRNA bind on the forward and the reverse strand and induce 2 independent PE events (ANZALONE et al., 2022). Unlike single pegRNA PE, which produces only one edited DNA flap, TwinPE thus generates two complementary modified DNA flaps that can hybridize to one another, facilitating stable incorporation of the edited sequence and reducing reliance on cellular mismatch repair (MMR) mechanism. TwinPE design employed AI-assisted system integrating literature and target sequence information for optimized PBS and RTT sequences (MATHIS et al., 2023). After pre-screening candidates in HEK293T cells, I tested the two bestperforming TwinPE sets in the USH1C PKC. For optimized Cas-RT performance, PE4Max was used, representing further optimizations to the RT domain and improved nuclear localization, compared to PE2Max (CHEN et al., 2021). Both TwinPE sets achieved efficiencies of 24.5% and 25% respectively (Fig. 8, A) on a first attempt. Benchmark experiments with PE3Max revealed 1,5% and 3,5% repair efficiency. These findings were reproduced in subsequent experiments, with efficiencies at 32% and 28%, respectively (Fig. 8, B). Notably, the upstream

blocking mutation indicated lower editing than the causative and downstream mutations (Fig. 8, C).

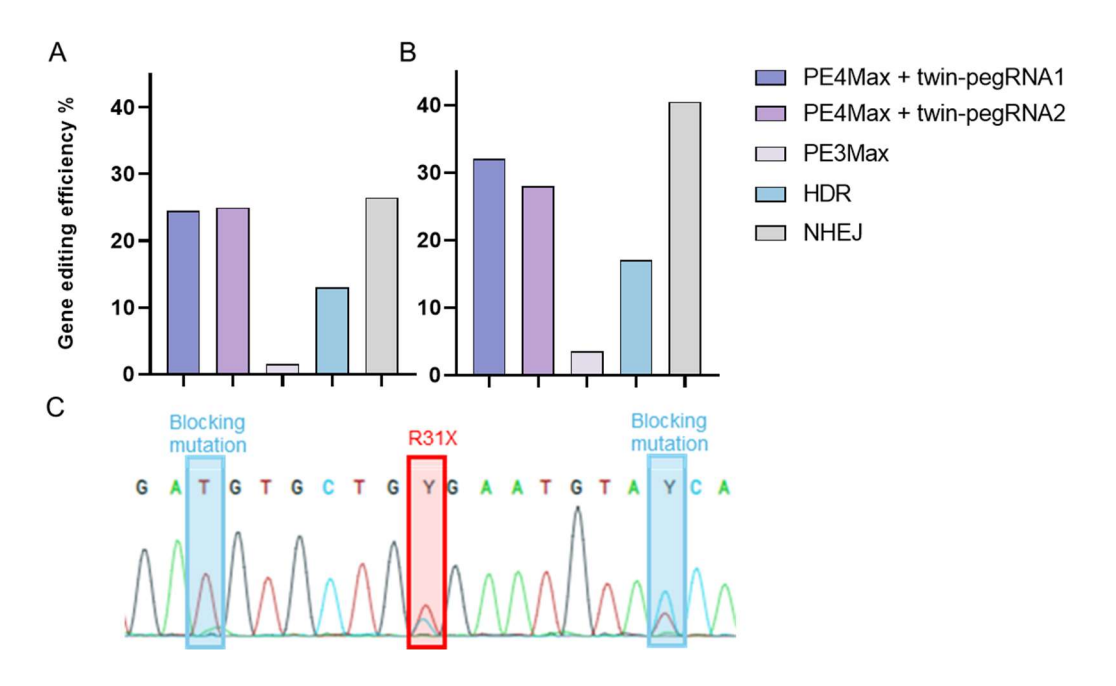


Figure 8: Prime Editing Using TwinPE.

(A) 2 TwinPE sets were compared to PE3Max and DSB-HDR experiments with NHEJ bystanding mutations in standard experimental protocols. (B) The experiment was reproduced and showed overall higher GE efficiencies (C) Representative electropherogram of PE4Max + twin-pegRNA set 2 with blocking mutation (blue box) and the target mutation (red box).

Complementary analysis of TwinPE with next-generation sequencing (NGS) confirmed accurate incorporation of the desired modifications and the editing efficiencies of 30% for approximately 50k reads (Fig. 7). In line with Sanger Sequencing, the most common variant is the correction of the causative mutation and integration of the downstream blocking mutation (17,23%). In 10,34% of the reads, all 3 mutations are integrated, hinting at a difference in efficiency between the forward and reverse pegRNA.

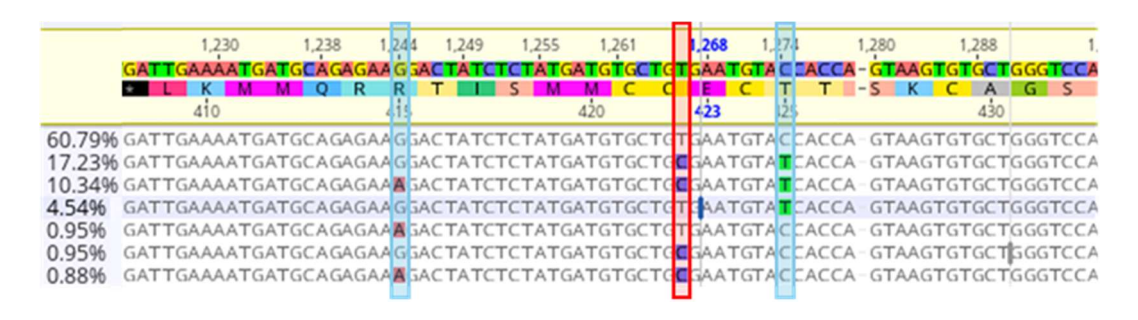


Figure 9: Next generation sequencing (NGS) analysis of TwinPE set 2

The target region with the blocking sites (blue boxes) and correcting site (red box). The read variants are ordered according to their frequency. The intended modifications are highlighted in orange, blue and green.

Overall, various GE tools showed distinct efficacies in correcting the USH1C mutation c.91C>T in proliferating PKC. Remarkably, TwinPE combinations indicated the highest and consistent repair efficacy.

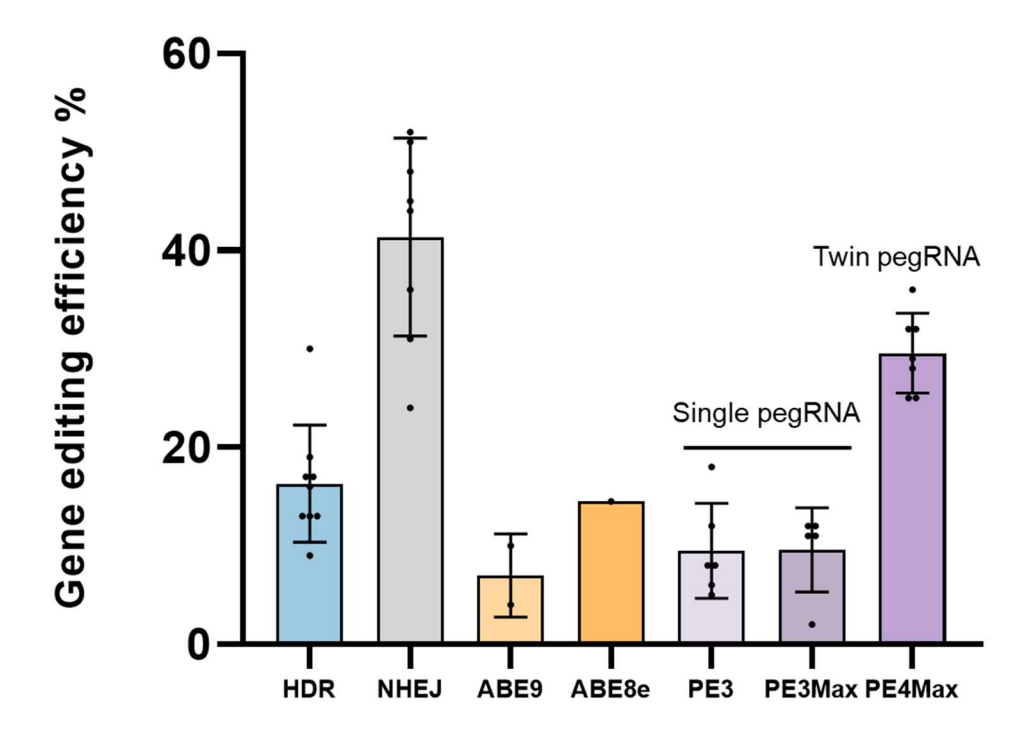


Figure 10: Summary of GE Approaches in vitro

Survey on all experiments aiming at gene correction of the USH1C c.91C>T mutation after plasmid nucleofection of the respective GE compounds in PKC from USH1C pigs. Each dot corresponds to one individual experiment. Mean \pm SD of n= 1-9 technical replicates.

1.4. Innovative Delivery Vectors for GE

While vectors for GT are designed for longevity, vectors for therapeutic GE would in ideal cases deliver functional GE tools that disappear after gene correction has been achieved. In line with this, alternative innovative vectors, capable of delivering transcripts of GE compounds were provided by collaboration partners and tested in PKC from USH1C pigs *in vitro*.

1.4.1. Virus Like Particles (VLPs)

Virus-like particles (VLP) were developed and produced by Dr. Dong-Jiun Jeffery Truong and Prof. Dr. Gil Westermeyer (HZM). First, transfection efficiency was tested in serial dilutions of VLP encoding the mGreen Lantern (mGL) reporter (CAMPBELL et al., 2020). mGL experiments showed great transfection potential of VLP, with transduction capacities >99% at 1/384 dilutions and a substantial efficacy of 66% at 1/1536 dilutions, without sign of cell toxicity (Fig 11, A). Delivery of ABE8e for the USH1C c.91C>T site (Fig. 3) with the same VLP, however, showed GE only in 6% of the cells, maximum at ¼ dilutions (Fig. 11, B).

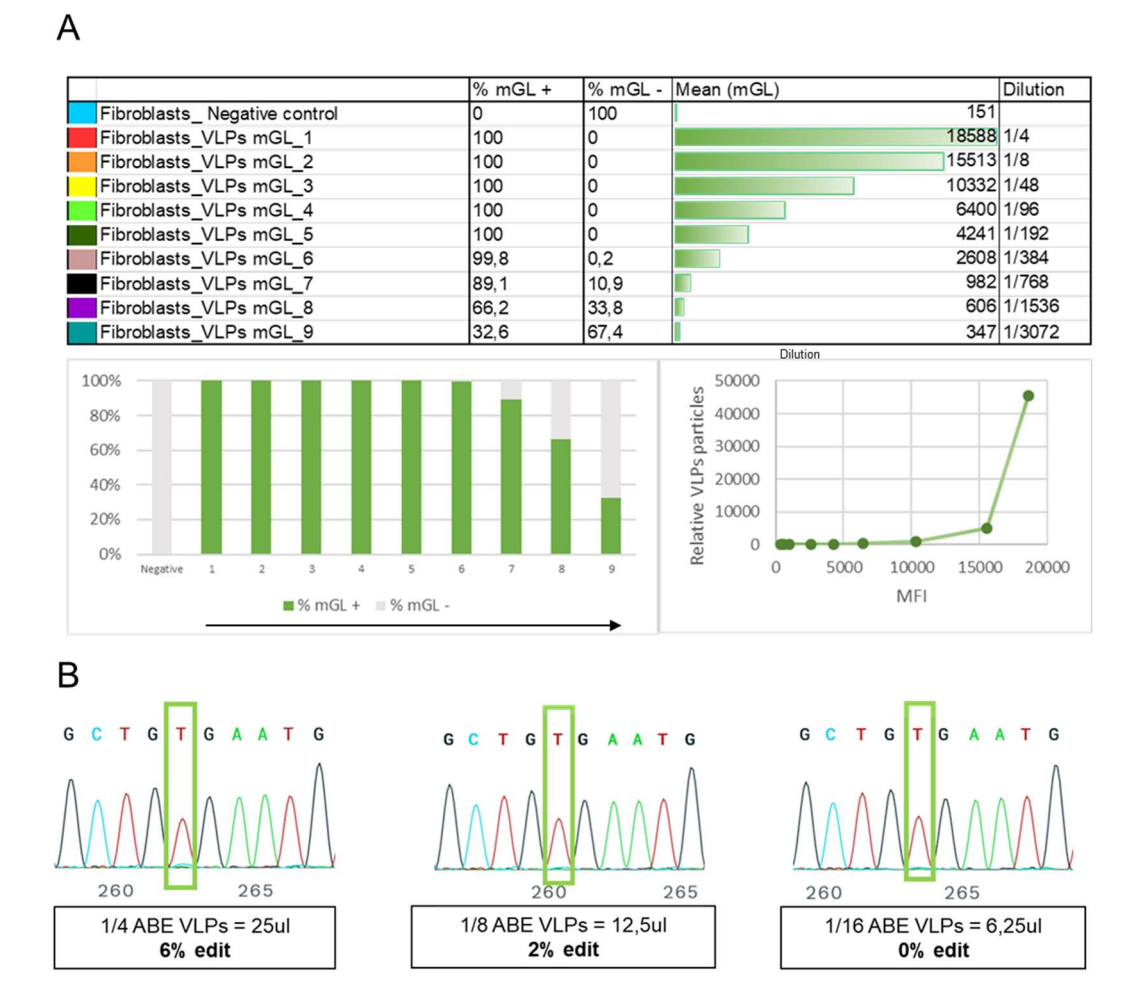
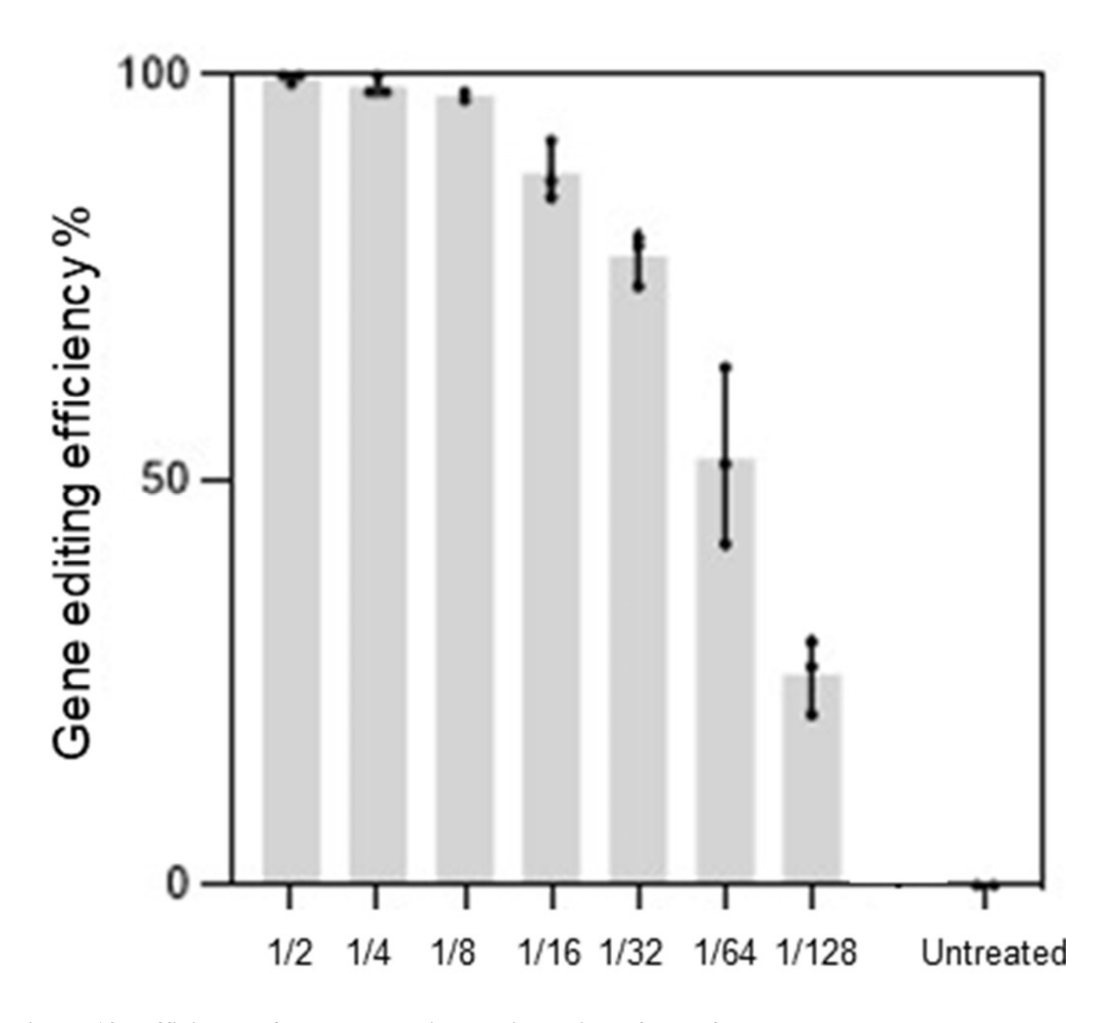


Figure 11: VLP testing in USH1C PKC

(A) Results of flow cytometry analysis reveal 99,8-100% of transfection efficiency with dilutions ranging from 1/4 to 1/384 of the original suspension. The mGL Mean Fluorescence Intensity (MFI) is proportional to the dilution. (B) Shows Sanger sequencing from the USH1C targeting with ABE after VLP delivery and shows only very low efficiency (2% and 6%), even at the highest concentrations.

In contrast, VLP-mediated delivery of GE components to disrupt the B2M locus, known to be in an open chromatin state in almost every mammalian cell, showed editing efficiencies ranging from 20-100% in serial dilutions (Fig. 12).



 $Figure\ 12:\ Efficiency\ after\ VLP-mediated\ Disruption\ of\ the\ B2M\ locus.$

Triplicates were prepared for serial VLP dilutions and analyzed by Sanger sequencing.

1.4.2. Delivery Vector X

In addition to VLPs, an alternative novel non-viral vector was provided by Dr. Christoph Gruber and Dr. Florian Giesert (HZM). For publishing and patenting issues, this vector is designated as "Delivery vector X" (DVX). For testing transduction capability and potential cell toxicity, I explored different amounts of DVX, delivering CRISPR-Cas9 components that induce NHEJ-mediated mutations. While up to 80% of the genome evaluated by Sanger Sequencing showed indels (Fig. 13), signs of cytotoxicity or increased apoptosis were lacking even at the highest dose.

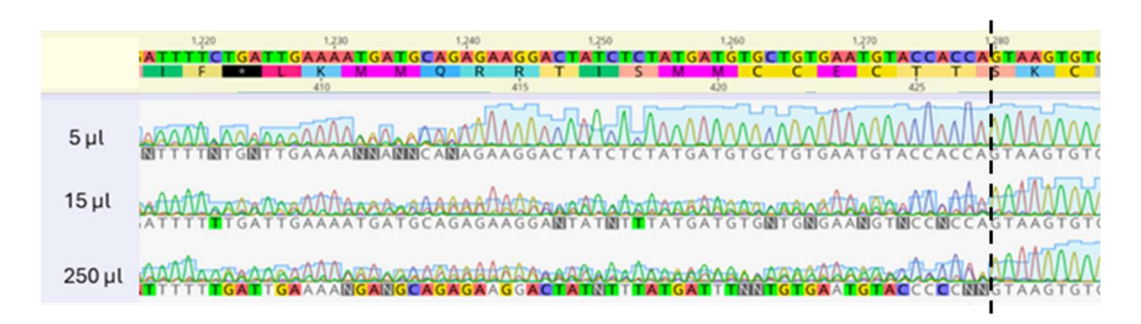


Figure 13: GE Efficiency at the USH1C Locus Using Delivery Vector X.

PKC were treated with DVX delivering CRISPR-Cas9 components inducing NHEJ. The GE efficiency ranged from 10% to 80% after Sanger sequencing, depending on the amount of DVX. The dashed line represents the cutting site of the Cas9.

Delivering the most promising TwinPE with twin-pegRNA set 2 (Fig. 8) with DVX showed contrary results. After initial attempts showed no edits with Cas9^{H840A}-nickases, I combined the pegRNAs with fully intact Cas9, inducing DSB instead of SSB at the respective target sites. As a result, a consistent and precise deletion of 40bp between the 2 cutting sites occurred. With 2μL, 12μL, and 36μL of DVX applied, deletions increased from 4% to 54% and 69% respectively (Fig. 14). Alternative indels were observed especially with the 12μL DVX.



Figure 14: DVX-mediated Delivery of pegRNA and Intact Cas9.

For increasing volumes of DVX, Sanger electropherograms (upper panels) and Synthego ICE GE analyses are combined. The most frequent edit is a deletion between the 2 cutting sites of the forward and reverse pegRNA.

Overall, therapeutic GE for the USH1C c.91C>T variant was consistent and, in particular for TwinPE, convincing *in vitro*, suggesting approval for testing in an animal model.

2. The USH1C Pig Model for Translational Studies

2.1. Breeding and Critical Postnatal Management

As previously described, the USH1C pig model was established and promoted for extended use in pre-clinical research (GROTZ et al., 2022), (GROTZ, 2021) and (AUCH, 2023). During my work for the Dr. med. vet. degree, I was responsible for the surveillance of the USH1C colony at the Center of Innovative Medical Models (CiMM, LMU). This specifically included veterinary monitoring of the herd, breeding management, post-natal treatment, supply of animals for preclinical studies and the organization of and support in these studies.

Importantly, homozygous USH1C piglets exhibit distinguishable behavior immediately after birth as a consequence of a cochlear and vestibular dysfunction. USH1C piglets struggle significantly with balance, making it difficult for them to stand without falling and reach their mother's teats for nursing. Without intervention, this impairs their ability to consume sufficient colostrum during the critical first hours of life, profoundly affecting their development and survival, and requiring excellent postnatal management.

An initial attempt at providing individual access to the mother sow so that they could consume colostrum on their own during the first 24 hours proved tedious, as some piglets needed assistance beyond 24 hours and the protocol required permanent presence in the delivery pen, presumably causing stress for the mother. Thus, I adapted that protocol in interaction with Dr. med. vet. Josep Miquel Cambra. The refined approach consisted of temporarily separated homozygous piglets from the sow during the first 24 hours after birth, housing them in a pen with deep straw or wood wool bedding (Fig. 15, A). This bedding provided crucial stability support, allowing piglets to move with greater confidence while cushioning their frequent falls, thereby preventing injuries and reducing stress. Further, colostrum administration every four hours, applied with a feeding tube was combined with ad libitum access to milk prepared from powder and supplemented with specially designed milk buckets originally developed for lambs (Fig. 15, B). The adapted protocol stimulated the piglets to practice and develop suckling behavior without support (Fig. 15, C). Consequently, supportive bedding and adapted feeding reduced the time until homozygous piglets were re-integrated into the litter to just a few hours postpartum, compared to more than 24 hours of intensive care in the

previous protocol. After re-integration, piglets quickly adapted to their environment and demonstrated nursing behavior comparable to their heterozygous and WT siblings. They moved completely autonomously albeit vestibular dysfunction persisted. For further support, the milk buckets they were trained to in the intensive care period were placed in the main pen as a permanent feeding source. This compensated for the congenital hearing deficit, that prevents response to the mother's feeding call and occasionally leads to missing feeding sessions (GROTZ et al., 2022).

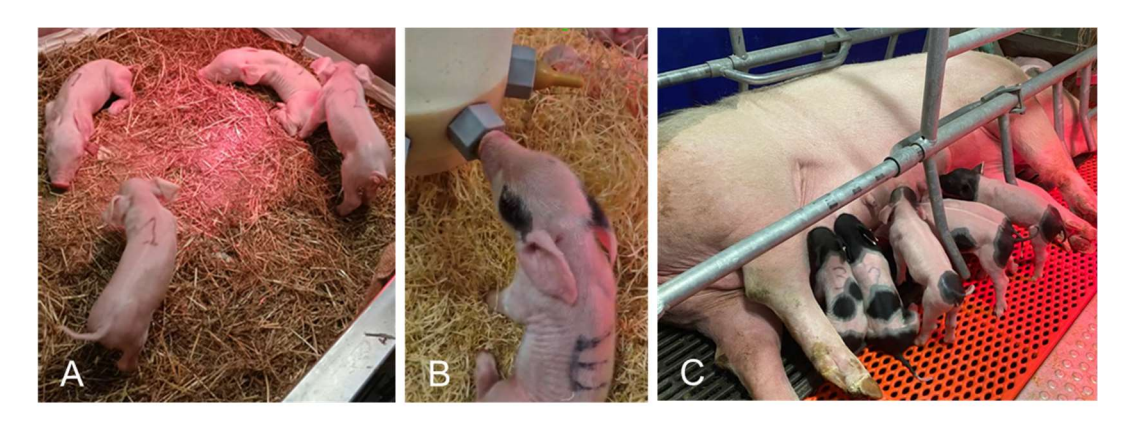


Figure 15: Postnatal Management for USH1C Piglets

(A) Pen with straw to support standing stability of piglets. (B) Milk bucket to stimulate autonomous suckling and provide an additional food source. Of note, some piglets tend to sit down for more stability during the first hours of life, without adverse side effects later. (C) Piglets nurse themselves autonomously at their mother after reintroduction to unaffected littermates.

The adapted post-natal management was developed and applied to 21 litters involving USH1C piglets during my work on this thesis between 2022 and 2025 (Table 11). From these litters, a total of 199 piglets were born, with 60 of them being of biallelic USH1C-KO genotype.

Table 13: Summary of all USH1C Litters between April 2022-March 2025

Litter	Mother	Father	Number of piglets		
			Het	Hom	WT
1	Het	Het	9	2	2
2	Het	Het	4	0	0
3	Hom	Het	2	9	0
4	Het	Het	5	2	2
5	Het	Het	7	0	5
6	Het	Het	4	3	0
7	Het	Het	8	1	8
8	Hom	Het	3	1	0
9	Het	Het	3	2	4
10	Het	Het	0	2	2
11	Het	Het	6	2	1
12	Het	WT	5	0	5
13	Het	Hom	9	4	0
14	Het	Hom	6	4	0
15	Het	Het	4	4	3
16	Het	Het	5	4	1
17	Het	Het	6	4	2
18	Het	Het	4	2	1
19	Het	Het	3	2	1
20	Hom	Het	3	8	0
21	Het	Het	6	4	0
Total	19	99	102	60	37

2.2. Use of Animals for Collaborative Studies

37 USH1C animals and 20 WT littermate control animals from the USH1C farrowings were supplied to collaborative research initiatives aiming at various research purposes such as molecular, structural and functional phenotyping as well as pre-clinical GT experiments. This work involved veterinarian, medical, biological and pharmaceutical expertise from contributors across Europe (Fig. 16). I specifically contributed to phenotypic assessment of the USH1C pig model by organizing pre-clinical sessions, preparation of animals and anesthesia management.

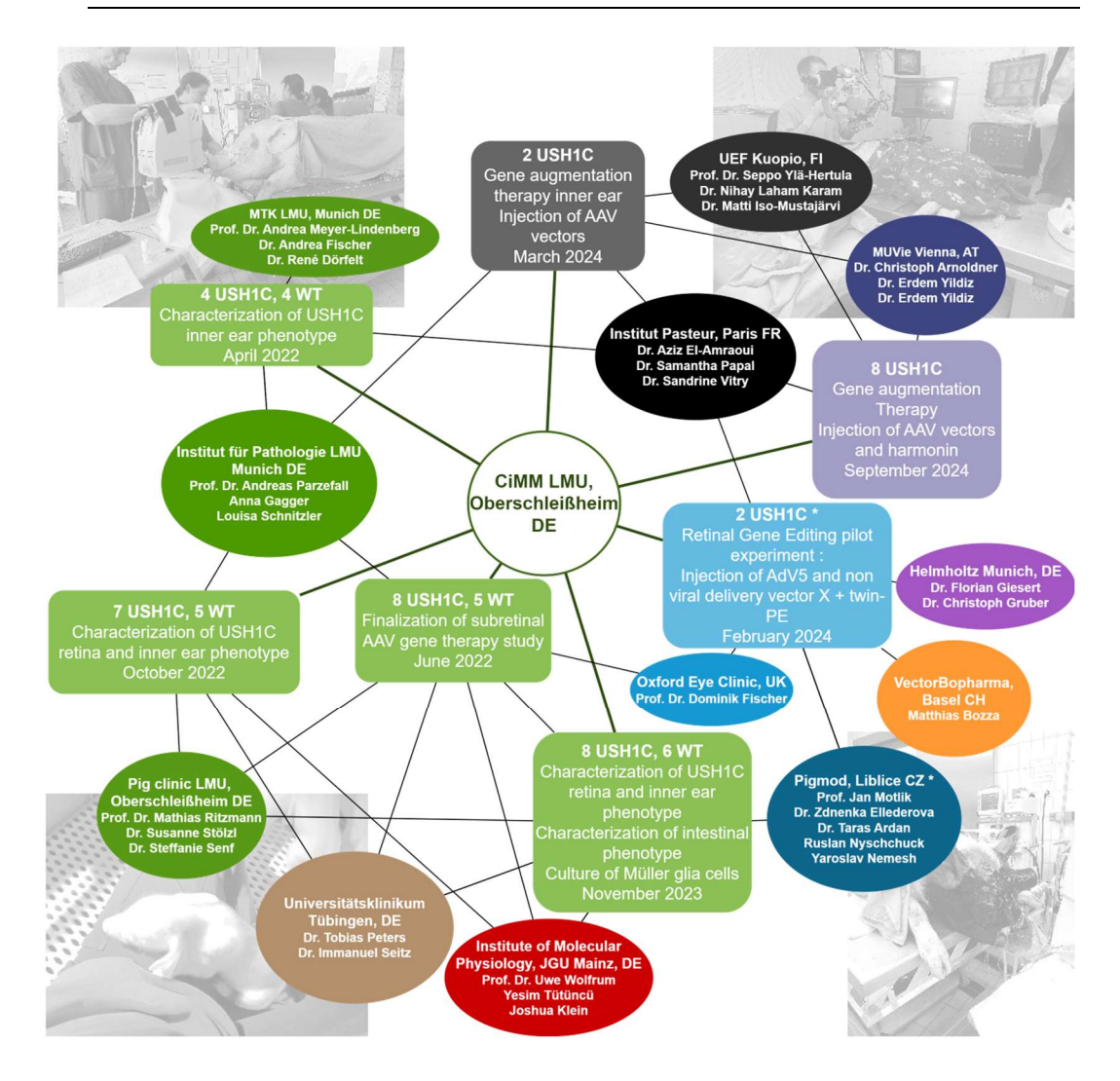


Figure 16: Network of Collaborations and Translational Studies.

In vivo experiments aiming at characterizing the inner ear, retinal and intestinal phenotype as well as inner ear GT attempts were conducted during my thesis work. Numbers indicate animals used and contributing collaboration partners. From a sister herd at PigMod Center, Liblice, primarily aiming at retinal GT, 2 USH1C animals (*) were provided for a pilot experiment on therapeutic GE.

2.3. Functional Assessment of Retina in USH1C pigs

Electroretinography (ERG) measurements were conducted to characterize the retinal phenotype of USH1C pigs and to establish baseline functional parameters for potential assessment of therapeutic interventions. These studies were performed in collaboration with Prof. Dr. Dr. Dominik Fischer (Oxford Eye Hospital), Dr. Tobias Peters and Dr. Immanuel Seitz (Universitätsklinikum Tübingen), and Ruslan Nyshchuck (PigMod, Liblice, CZ).

ERG analysis between USH1C pigs and WT controls revealed considerable variability between animals. However, a consistent pattern emerged for dark-

adapted (scotopic) responses, indicating that USH1C animals exhibited a tendency toward enhanced ERG response, as evidenced by increased absolute b-wave amplitudes compared to WT controls after dark adaptation (Fig. 17). Calculating the relative b-wave values by referring to the maximum stimulatory potential in each experimental series indicated that ERG responses of USH1C pigs peaked at lower light stimuli than their WT counterparts. Interestingly, parents recognize an increased light sensitivity in their USH1C children upon strong light exposure, e.g. when moving from darkness to bright light in daily activities (Susie Trotochaud, USH2020 foundation, personal communication).

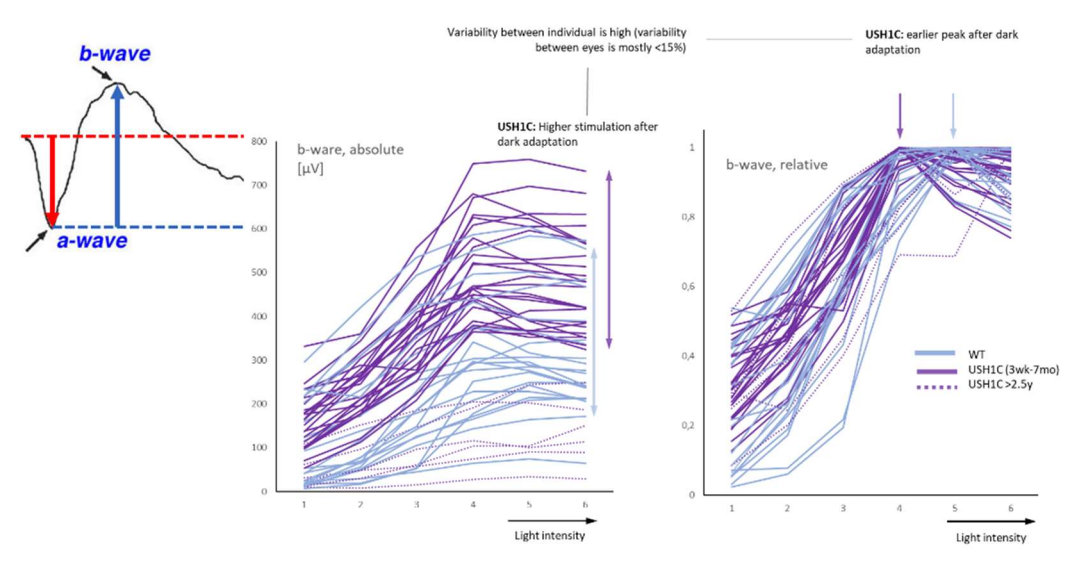


Figure 17: ERG Measurements of USH1C vs. WT animals

ERG measurements were conducted after 30min dark adaptation with a series of 6 increasing light stimuli. Left: determining a- and b-wave from ERG profiles. Middle: b-wave measurements in 14 eyes of USH1C (lilac) and 21 eyes of control (blue) pigs, aging from 3 weeks to 7 months. No clear correlation of ERG potential decrease and age was observed in USH1C pigs during this age. ERG in 6 eyes of USH1C aged >2.5 years showed reduced response (lilac dotted lines). Right: Relative b-wave values, using the maximum in each experimental series as reference. Data measured by Prof. Dr. Dr. M.D. Dominik Fischer (Oxford Eye Hospital, UK), Tobias Peters & Immanuel Seitz (Universitätsklinikum Tübingen) and Ruslan Nyshchuk (PigMod Liblice, CZ) and combined by Prof. Nikolai Klymiuk.

2.4. Auditory Function Assessment

The inner ear phenotype was assessed by Distortion Product Otoacoustic Emission (DPOAE), measuring cochlear hair cell function through sounds the inner ear produces in response to tones, Auditory Steady-State Response (ASSR), determining brain responses to continuous sound to estimate hearing thresholds and Auditory Brainstem Response (ABR) Click and frequency-specific Tone Burst responses, evaluating the auditory pathway from ear to brainstem. Measurements

were conducted by Prof. Dr. Andrea Fischer (LMU) adapting the Sentiero Advanced device (PathMedical, Germering) for pigs. Anesthesia support was provided by Dr. René Dörfelt (LMU). Two distinct age cohorts (1 month and 3 months) (Fig. 18 and 19) corroborated the findings previously reported by (GROTZ et al., 2022). There were technical difficulties for DPOAE, especially with increasing age, reflecting the difficulties in measuring robust sound reflections through the long and complexly organized ear canal of pigs.

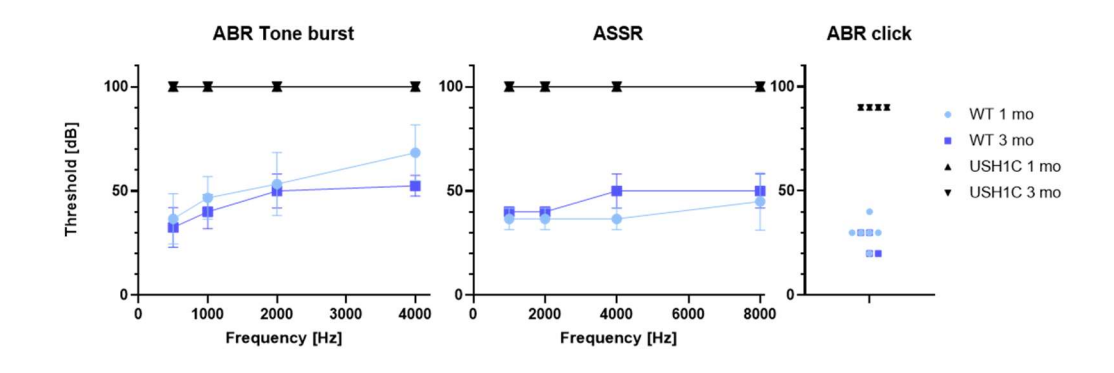


Figure 18: ABR Tone Burst, ABR Click and ASSR Tests in USH1C vs. WT animals

The 1-month-old age group consisted of 3 WT animals and 2 USH1C animals. The 3-month-old group consisted of 2 WT and 2 USH1C animals. Hearing threshold was determined for WT pigs in decibels. USH1C pigs did not respond to the highest test auditory intensity (100dB). In ABR Tone burst and ASSR tests, several sound frequencies were tested.

		1 mo				3 mo				1 mo			3 mo						
		W	T1	W	T2	W	T3	W	T4	W	T5	USH	11C1	USH	1C2	USH	11C3	USH	I1C4
	Frequency	L	R	L	R	L	R	L	R	L	R	L	R	L	R	L	R	L	R
DPOAE 35 dB	1 kHz	n.d.	×	×	×	n.d.	×	n.d.	n.d.	×	×	×	×	×	×	n.d.	n.d.	n.d.	n.d.
	1,5 kHz	n.d.	1	1	1	n.d.	×	n.d.	n.d.	1	1	×	×	×	×	n.d.	n.d.	n.d.	n.d.
	2 kHz	n.d.	1	1	1	n.d.	1	n.d.	n.d.	1	1	×	×	×	×	n.d.	n.d.	n.d.	n.d.
	3 kHz	n.d.	1	✓	1	n.d.	1	n.d.	n.d.	1	1	×	×	×	×	n.d.	n.d.	n.d.	n.d.
	4 kHz	n.d.	1	1	1	n.d.	1	n.d.	n.d.	1	1	×	×	×	×	n.d.	n.d.	n.d.	n.d.
	5 kHz	n.d.	1	1	1	n.d.	1	n.d.	n.d.	1	1	×	×	×	×	n.d.	n.d.	n.d.	n.d.
	6 kHz	n.d.	1	✓	1	n.d.	1	n.d.	n.d.	1	×	×	×	×	×	n.d.	n.d.	n.d.	n.d.
	8 kHz	n.d.	×	×	✓	n.d.	1	n.d.	n.d.	×	×	×	×	×	×	n.d.	n.d.	n.d.	n.d.
DPOAE 45 dB	1 kHz	n.d.	×	×	×	n.d.	×	n.d.	n.d.	×	×	×	×	×	×	n.d.	n.d.	n.d.	n.d.
	1,5 kHz	n.d.	1	✓	1	n.d.	1	n.d.	n.d.	1	1	×	×	×	×	n.d.	n.d.	n.d.	n.d.
	2 kHz	n.d.	1	1	1	n.d.	1	n.d.	n.d.	1	1	×	×	×	×	n.d.	n.d.	n.d.	n.d.
	3 kHz	n.d.	✓	1	1	n.d.	1	n.d.	n.d.	1	1	×	×	×	×	n.d.	n.d.	n.d.	n.d.
	4 kHz	n.d.	1	1	1	n.d.	1	n.d.	n.d.	1	1	×	×	×	×	n.d.	n.d.	n.d.	n.d.
	5 kHz	n.d.	✓	✓	1	n.d.	1	n.d.	n.d.	1	1	×	×	×	×	n.d.	n.d.	n.d.	n.d.
	6 kHz	n.d.	1	1	1	n.d.	1	n.d.	n.d.	1	1	×	×	×	×	n.d.	n.d.	n.d.	n.d.
	8 kHz	n.d.	1	×	1	n.d.	1	n.d.	n.d.	1	×	×	×	×	×	n.d.	n.d.	n.d.	n.d.
DPOAE 55 dB	1 kHz	n.d.	1	1	1	×	×	1	n.d.	1	1	×	×	×	×	×	×	n.d.	×
	1,5 kHz	n.d.	1	1	1	1	1	1	n.d.	1	1	×	×	×	×	×	×	n.d.	×
	2 kHz	n.d.	1	1	1	1	1	×	n.d.	1	1	×	×	×	×	×	×	n.d.	×
	3 kHz	n.d.	1	1	1	1	1	×	n.d.	1	1	×	×	×	×	×	×	n.d.	×
	4 kHz	n.d.	✓	✓	1	1	1	1	n.d.	1	1	×	×	×	×	×	×	n.d.	×
	5 kHz	n.d.	1	✓	1	1	1	1	n.d.	1	1	×	×	×	×	×	×	n.d.	×
	6 kHz	n.d.	✓	1	✓	1	1	1	n.d.	1	1	×	×	×	×	×	×	n.d.	×
	8 kHz	n.d.	1	1	1	1	1	×	n.d.	1	1	×	×	×	×	×	×	n.d.	×
DPOAE 65 dB	1 kHz	n.d.	1	1	1	×	×	1	n.d.	1	1	×	×	×	×	×	×	n.d.	×
	1,5 kHz	n.d.	1	1	1	1	1	1	n.d.	1	1	×	×	×	×	×	×	n.d.	×
	2 kHz	n.d.	1	1	1	1	1	×	n.d.	1	1	×	×	×	×	×	×	n.d.	×
	3 kHz	n.d.	✓	1	1	1	1	×	n.d.	1	1	×	×	×	×	×	×	n.d.	×
	4 kHz	n.d.	1	1	1	1	1	×	n.d.	1	1	×	×	×	×	×	×	n.d.	×
	5 kHz	n.d.	1	1	1	1	1	1	n.d.	1	1	×	×	×	×	×	×	n.d.	×
	6 kHz	n.d.	1	✓	1	1	1	1	n.d.	1	1	×	×	×	×	×	×	n.d.	×
	8 kHz	n.d.	1	1	1	1	1	1	n.d.	✓	1	×	×	×	×	×	×	n.d.	×

Figure 19: DPOAE Measurements of USH1C and WT animals

The same cohorts as in Fig. 18 were assessed in the same experimental session. DPOAE test is considered passed or not passed. A clear difference can be observed between WT and USH1C. Non determined (n.d.) was documented when measurements were not possible (failed leak test).

3. Pre-clinical Assessment of Promising Therapeutic GE and Vector Candidates

Stimulated by *in vitro* work and robust pre-clinical protocols, subretinal injection of GE therapies and vectors was performed in collaboration with experienced retinal surgeon Prof. Dr. Dr. Dominik Fischer (Oxford Eye Hospital, UK) and PigMod Center, Liblice (CZ) providing USH1C animals from a sister herd (AUCH, 2023) and infrastructure for eye surgery. For effective readout and in line with the 3R principles, 3 animals were included in this pilot cohort, with 3 injections performed per eye (Fig. 20). One animal received AdV-mediated therapeutic PE, another received DVX-mediated reporter gene, and one animal served as non-injected control.

Table 14: Injection Protocol of Pilot in vivo Experiment

Animal 1: AdV	5-TwinPE-GFP	Animal 2: Deli	very vector X -	Animal 3: Non injected			
		G	FP	control			
Left eye	Right eye	Left eye	Right eye	Left eye	Right eye		
3 injection	3 injection	3 injection	3 injection				
sites à 100µl	sites à 25µl	sites à 100µl	sites à 100µl	No injection			
each (=HD)	each (=LD)	each	each				

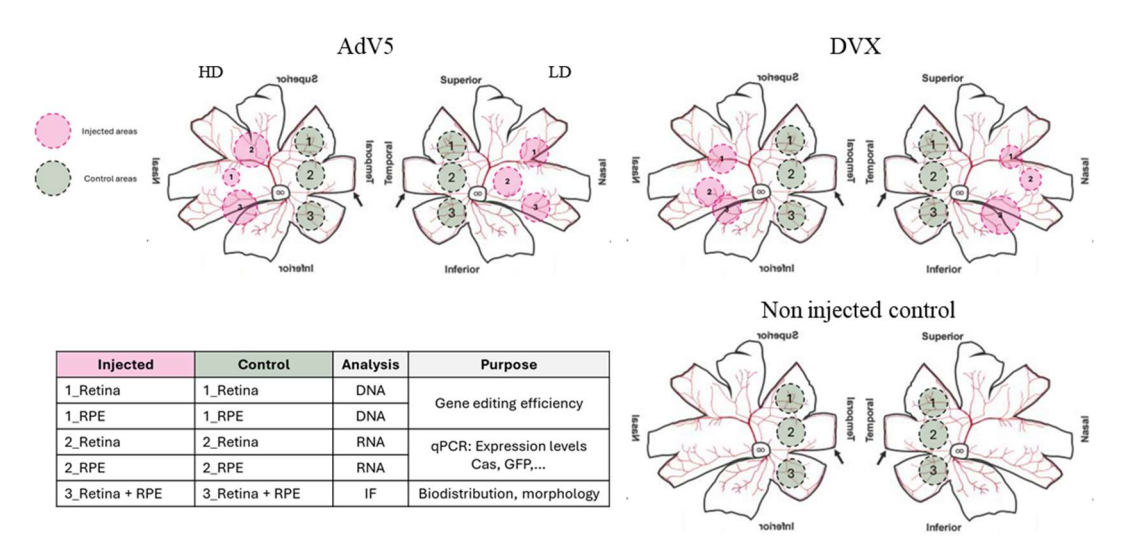


Figure 20: Sampling protocol of pilot in vivo experiment

Injection scheme of each eye and corresponding sampling localization. Each sample was taken as a 8mm biopsy punch. The table represents the usage of samples in downstream analysis.

3.1. AdV5 -mediated Delivery of TwinPE

To deliver the most promising TwinPE with twin-pegRNA set 2 (Fig. 8) as well as a fluorescent reporter, AdV-based delivery was selected for packaging capacity and its retinal permeation capability (CASHMAN et al., 2007; SWEIGARD et al., 2010). Specifically, a gutless high-capacity adenovirus serotype 5 (AdV5) was selected, facilitating pre-clinical work under BioSafety level I. The vector was provided by Matthias Bozza (VectorBiopharma). Two injection volumes were explored, referred to as "high-dose (HD)" and "low-dose (LD)". Three injections per eye were performed by Prof. Dr. Dr. Dominik Fischer (Oxford Eye Hospital, UK), supported by Yaroslav Nemesh (Pigmod, Liblice CZ) (Table 12). Injection sites were documented and after a follow-up of 7 days, animals were assessed by OCT and fundoscopy before euthanization and sample collection (Dr. Taras Ardan, Pigmod, Liblice CZ). The sampling protocol was designed to maximize the scientific output; samples of the injection sites and intra-ocular control sites were taken as tissue punches to facilitate both molecular and structural analysis (Fig. 20).

Optical coherence tomography (OCT) and fundus imaging indicated atrophy at the injection sites of the HD-treated eye (Fig. 21, A-B) but not in the LD-treated eye. Immunofluorescence (IF) staining for GFP demonstrated successful transduction of AdV5 into relevant retinal cell types (RPE, PRC and GCL) and expression of the reporter after HD-AdV5-injection (Fig. 22). In consecutive staining, the spatial distribution of the reporter signal was allocated to a bleb area of maximum diameter 7,2 mm with highest intensities in region of 3,6mm (Fig. 23). In the areas receiving AdV5 in LD, GFP signals were restricted to RPE in IF (Fig. 24).

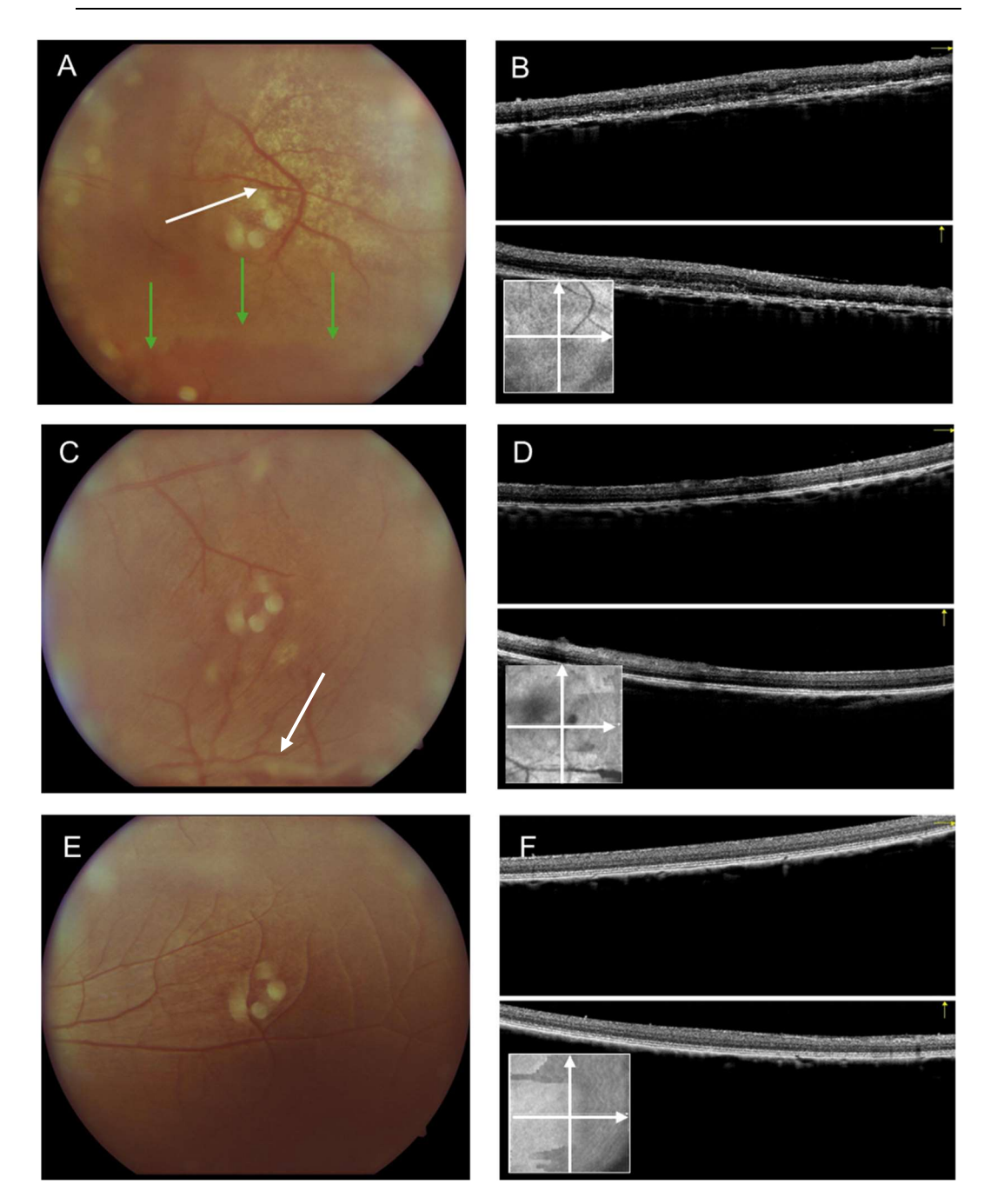


Figure 21: Fundus Image and OCT of the Retina - 1 Week after AdV5 Injection

Fundus (A) of an area receiving HD-AdV-GFP-TwinPE shows atrophy of the retina, as indicated by white spots (white arrow), and remaining border of the injection "bleb" (green arrows). The LD-AdV-GFP treated eye showed some signs of retinal detachment at one injection site but no atrophy (C). The fundus of the non-injected control animal appears normal (E). OCT (B) shows retinal thinning in the vicinity of the HD injection area, compared to the LD (D) and non-injected control animal (F). Analysis performed by Dr Taras Ardan (Pigmod, Liblice, CZ).

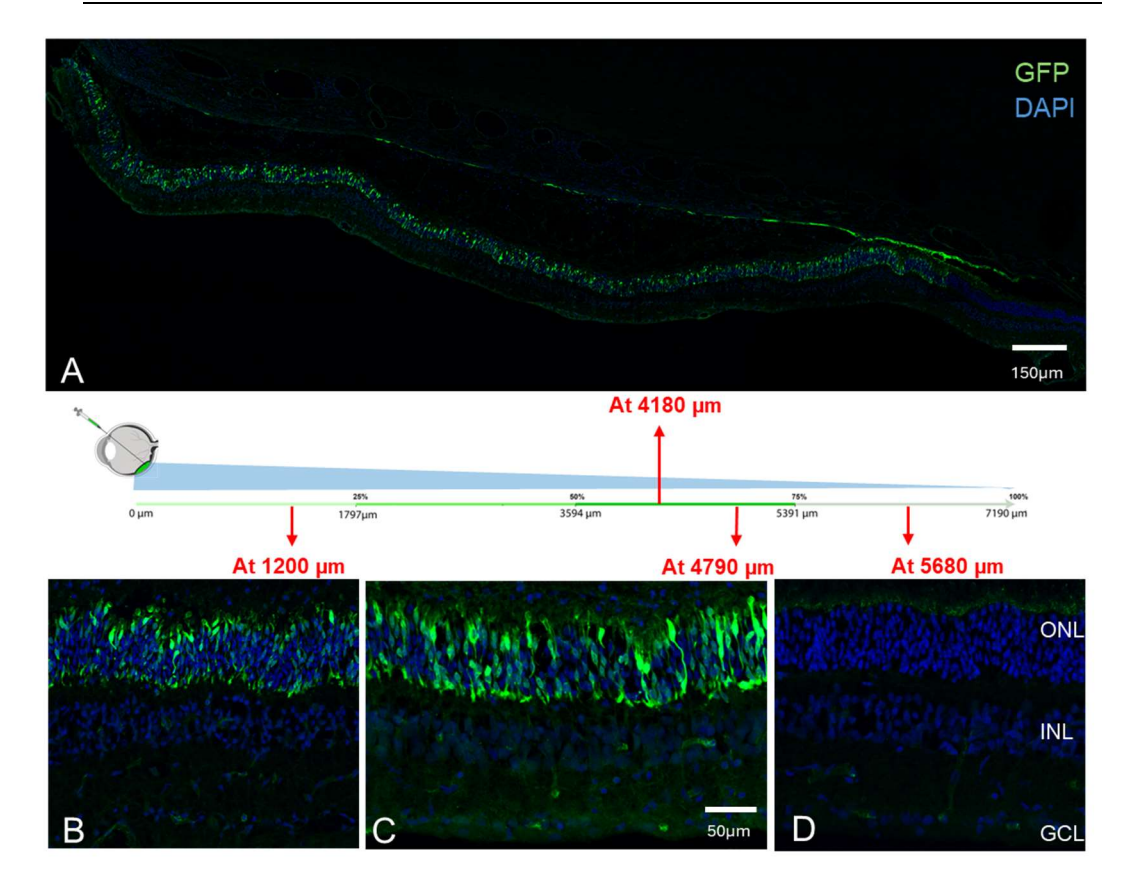


Figure 22: IF Images of the Retina – 1 Week after HD-AdV5 Injection

(A) IF staining of GFP across the injection site indicating homogeneous distribution of the GFP signal in the RPE (upper band), PRC layer (middle band) and GCL (lower band). Detachment of the retina may be due to fixation process or mechanical disruption during the surgical procedure. Close-up images correspond to the periphery of the injected site (B), middle region of the injection site (C) and outside of the injection site reach (D). Staining performed by Dr. Samantha Papal and Dr. Aziz el-Amraoui (Institut Pasteur, Paris, FR).

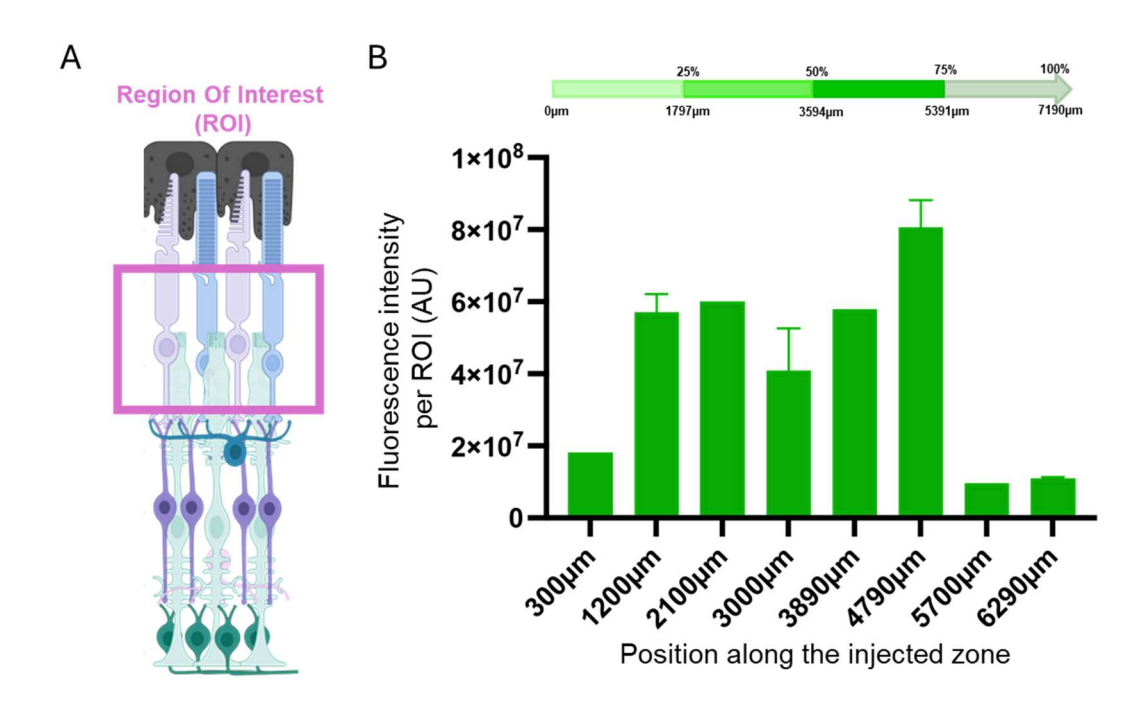


Figure 23: Distribution of GFP Signal at the HD-AdV5-TwinPE-GFP Injection Site

Fluorescence intensity of GFP and DAPI signals were measured at different positions along the ONL (A), giving an approximation of the biodistribution across the injection site (B). Analysis performed by Samantha Papal (Institut Pasteur, Paris, FR).

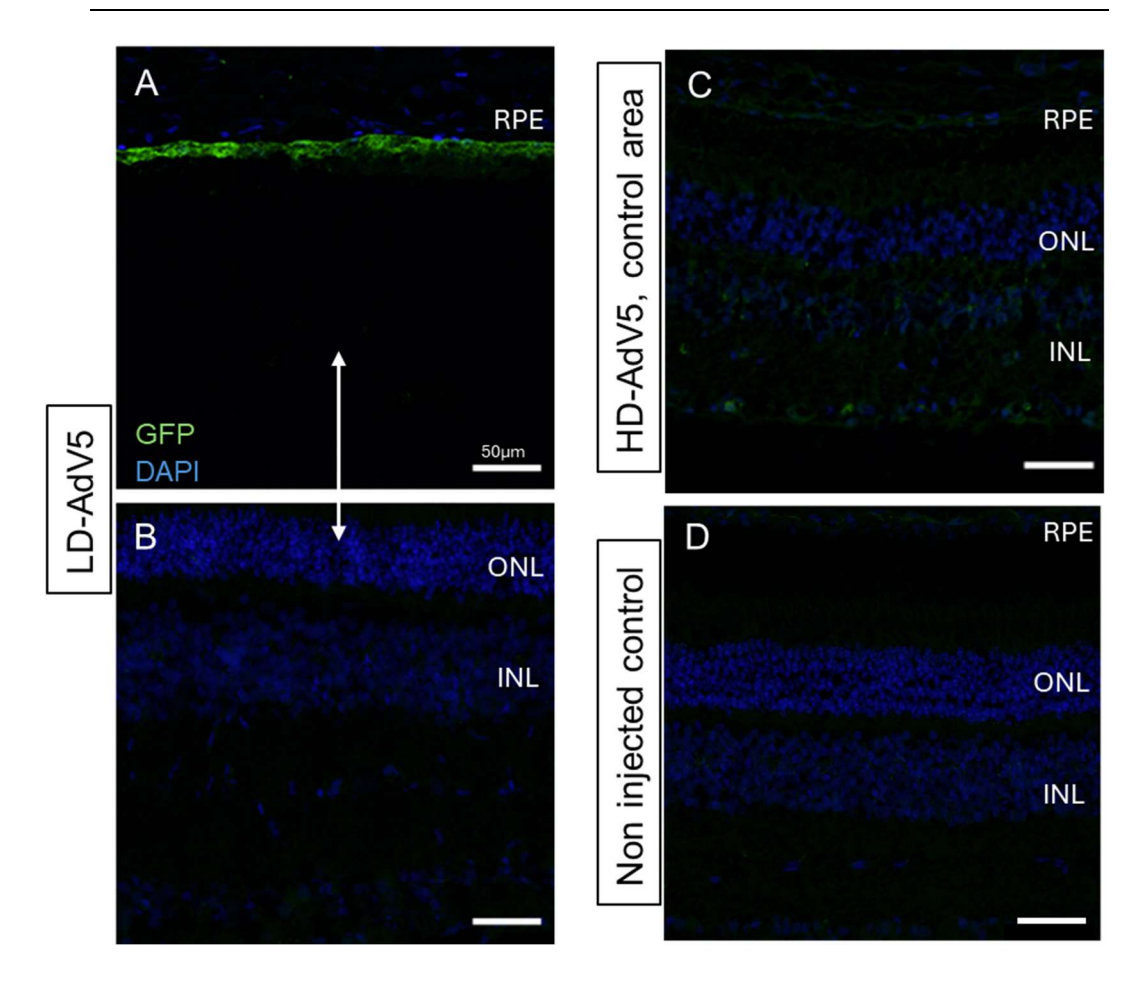


Figure 24: Further IF Images of the Retina - 1 week after AdV5-TwinPE-GFP injection

(A) and (B) are IF images taken from the same region. The gap between RPE and ONL required splitting into separate analysis. GFP signal can be seen in the RPE but not in the PRC. (C) was taken from a control region of the HD-AdV5-injected eye, with weak GFP signal in the RPE, PRC and GCL, suggesting a broader biodistribution. (D) shows the non injected control, where GFP was completely negative. Analysis performed by Samantha Papal and Aziz El-Amraoui (Institut Pasteur, Paris, FR).

qPCR analysis of cryo-preserved punches confirmed the expression of the Cas9, pegRNA, and GFP in the neuroretina of HD-AdV5-treated eye at transcript level, while none were detected in the LD-AdV5 injection areas, highlighting the importance of dosage studies (Fig. 25, A). For the assessment of GE efficiency, DNA from RPE and neuroretina was analyzed separately by NGS. In the LD-AdV5-treated area, no editing was detected. Likewise, no editing was determined in the neuroretina of an HD-AdV5-treated area, while 0,2% of 4,3k reads from the RPE, 0.2% were successfully edited (Fig. 25, B).

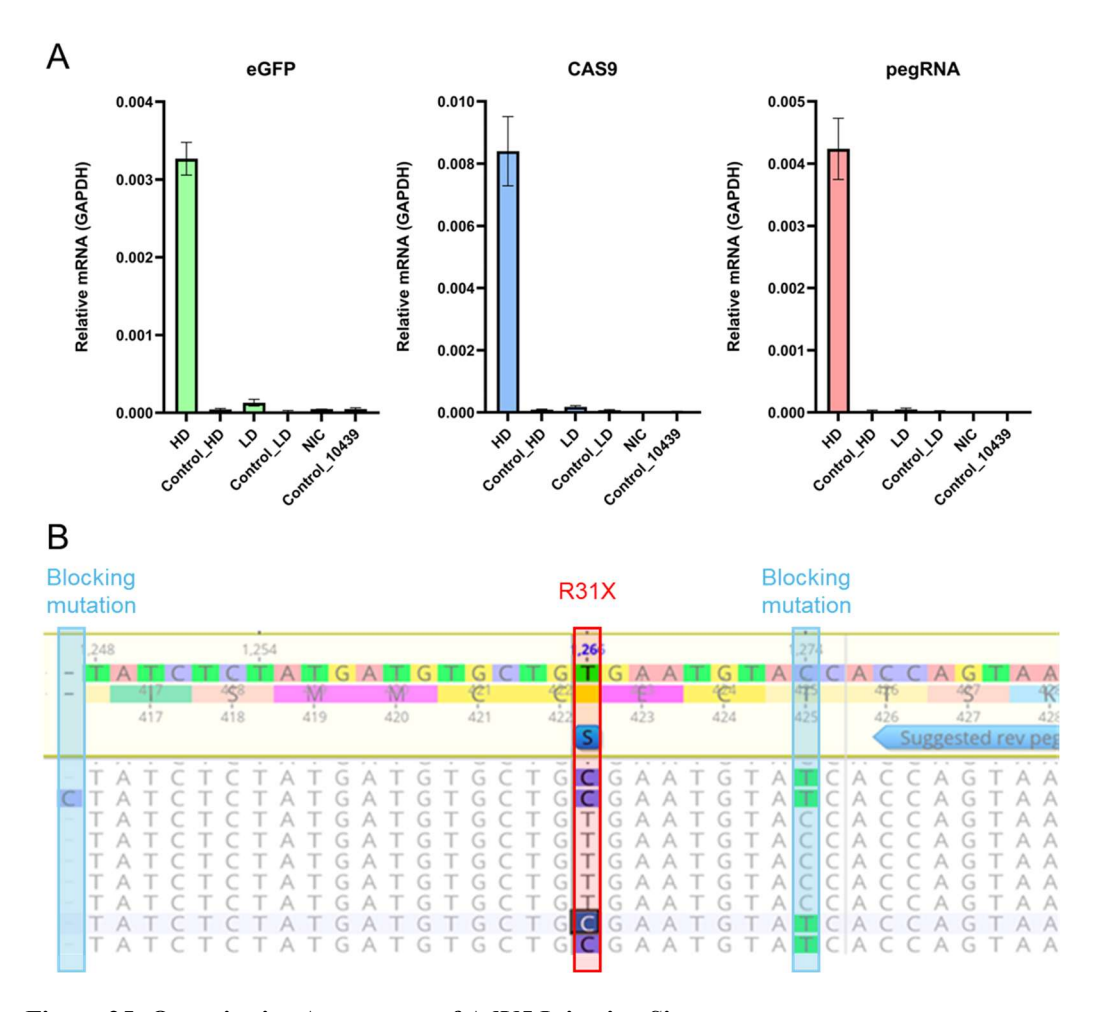


Figure 25: Quantitative Assessment of AdV5 Injection Sites

(A) Specific qPCR for eGFP and Cas9 mRNA as well as pegRNA transcripts were developed by Josep Miquel Cambra, indicating substantial expression only in HD-injected blebs. Expression of PE components is low, but beyond threshold levels. Control samples are from the intra-ocular control areas from HD-AdV5 and LD-AdV5 eyes (Control_HD, Control LD) or from eyes of non-injected animals (NIC and 10439). (B) NGS revealed reads containing the causative (red box) and one or two of the blocking mutations (blue boxes).

3.2. DVX-mediated Delivery of GFP Reporter

In another pilot experiment, the capacity of DVX to deliver mRNA of a GFP-encoding reporter was assessed. DVX particles were provided by Dr. Christoph Gruber and Dr. Florian Giesert (HZM). The intervention, imaging and sampling procedures were carried out as described for AdV5-mediated TwinPE delivery. While the DVX-treated pig did not exhibit any generalized clinical symptoms during the 7-days follow-up, fundus examination revealed a strong inflammatory reaction with atrophy and wrinkling of the retina, indicating profound retinal detachment (Fig. 26). The inflammation extended to the vitreous and precluded

OCT measurement. Tissue sampling confirmed that the retina was grossly detached. Despite these adverse events, the analysis demonstrated successful transduction of the RPE.

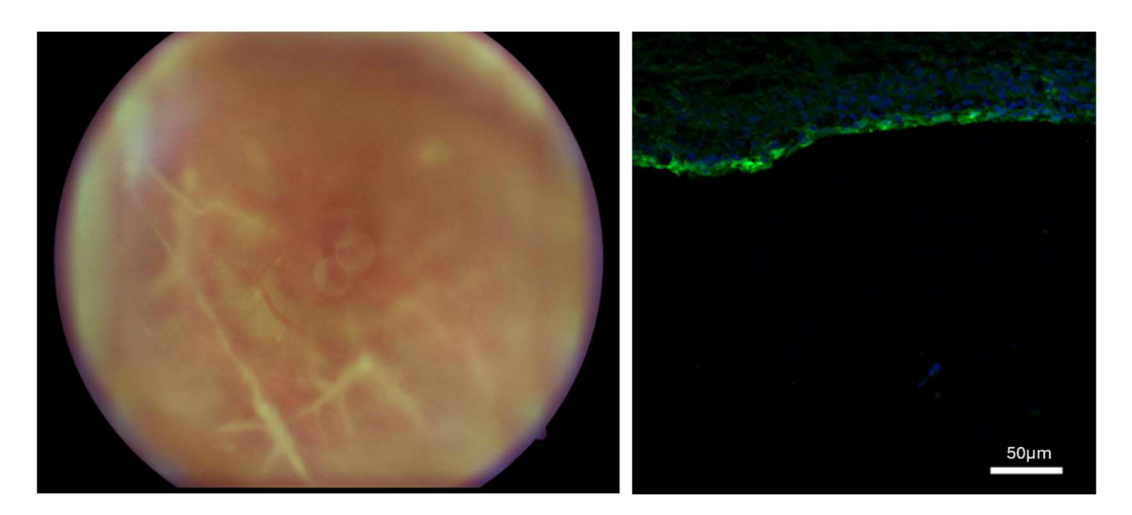


Figure 26: Fundus and IF Images of DVX Treated Retina

Left: Fundus examination showed strong atrophy, retinal wrinkling and turbidity in the vitreous body. Data by Dr Taras Ardan (PigMod Center, Liblice, CZ). Right: GFP signal was detected in RPE. Data provided by Samantha Papal (Institut Pasteur, Paris, France). The complete neuroretina detachment prevented IF assessment of the tissue.

Overall, the pilot experiments in USH1C confirmed the robust pre-clinical pipeline for retinal GT in pig and proved the capacity of TwinPE to correct the USH1C c.91C>T mutation *in vivo*. However, the dramatically decreased GE efficiency in the pig eye, although RPE and PRC were highly transduced, suggested that retinal tissue represents peculiar hurdles that cannot be examined in established cell culture assays. Thus, the third part of my thesis work aimed at evaluating alternative test systems for retina.

3.3. Alternative Test Systems

Aiming to bridge the gap between cell culture work and pre-clinical work, the primary requirements of alternative test systems are their robustness and the mimicking of relevant cell-biology characteristics of the target tissue. The influence of cell cycle status on DNA repair pathway utilization is well-documented, as (CICCIA and ELLEDGE, 2010; HUSTEDT and DUROCHER, 2016) reviewed, with homology-directed repair (HDR) primarily active during S and G2 phases, while non-homologous end joining (NHEJ) remains active throughout the cell

cycle. This differential activity of repair pathways could significantly impact GE outcomes in postmitotic tissues such as the retina. Considering that retina is a terminally differentiated post-mitotic tissue, I hypothesized that recapitulating the cell cycle regulation of the retina is key for alternative test systems. For this purpose, I investigated alternative culture conditions of PKC as well as the possibility to keep REs in culture for a period that allows exploring therapeutic GE.

3.3.1. Establishing an *in vitro* Postmitotic Mimicking Cell Model

I aimed at manipulating PKC to shift from proliferating and dividing cells that undergo the cycle of G1, S, G2 and M phases into non-dividing cells that arrest in G0. Methods to induce a cell cycle arrest in G0/G1 in PKC include serum starvation, contact inhibition (through confluency), chemical inhibitors (HAYES et al., 2005; KHAMMANIT et al., 2008) and hypothermia which is known to block the cell cycle in the G2/M phase (MAURISSEN and WOLTJEN, 2020). In an exploratory experiment, PKC were cultivated under standard (15% serum, 37°C), hypothermic (15% serum, 30°C) or starvation (1,5% serum, 37°C) conditions. After 24h, cells were electroporated with DSB-HDR components as benchmark treatment. At the time point of electroporation, a proportion of cells was fixed, permeabilized and stained with Propidium Iodide (PI) to determine the cell cycle by Flow Cytometry (FC). Although differences were small, hypothermia showed less cells in G1, compared to standard conditions while the proportion of G1 cells were slightly higher under starvation (Fig. 25).

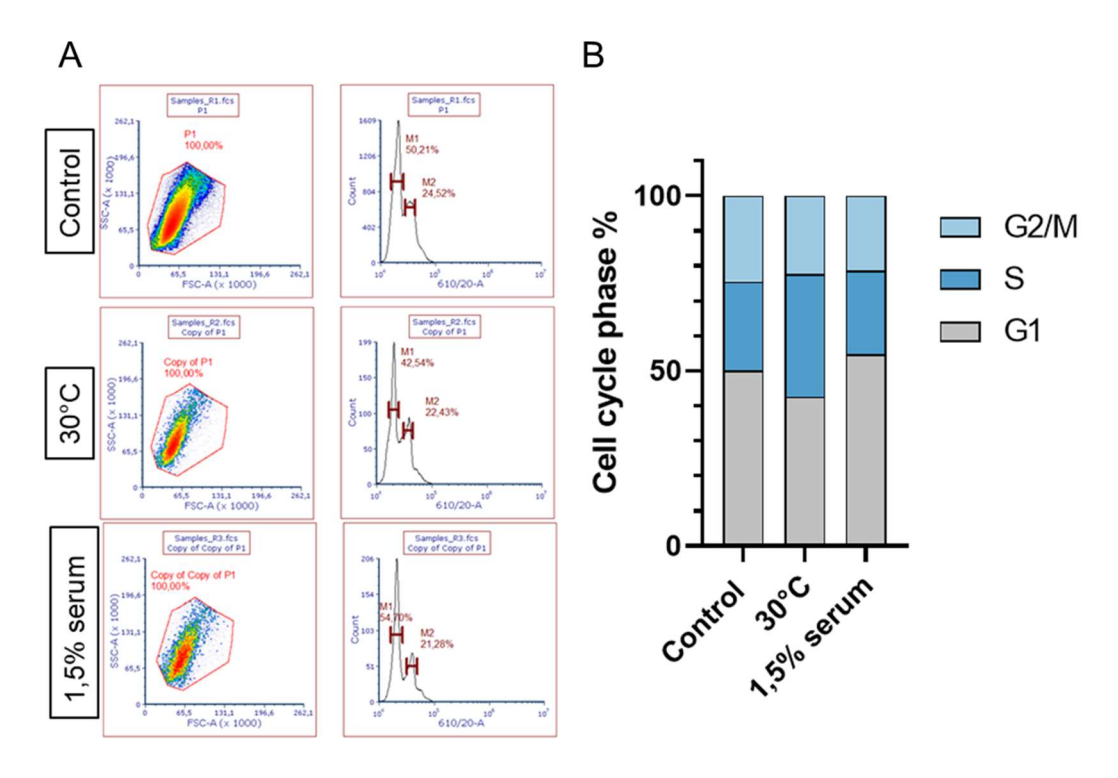


Figure 27: Cell Cycle Assessment in PKC Under Distinct Culture Conditions

(A) Left: Cells were stained with PI and gated for standard FSC and SSC parameters in flow cytometry. Right: To quantify cells in the G1 (low PI) and G2/M phase (high PI), a threshold level was set at the minimum between the peaks. Cells in S phase, presumably showing a blurry signal, were calculated as difference between 100% and the proportions of cells G1 and G2/M phases. (B) overview of cells in the respective cell stages under the experimental conditions.

24 hours after treatment with DSB-HDR components, cells were examined for GE efficiency. Under hypothermic conditions, NHEJ was reduced, while HDR was similar to control conditions. Under starvation, both HDR and NHEJ were reduced. (Fig. 28, A). Relative HDR/NHEJ indicated an increase of HDR under hypothermia, consistent with an increase of cells in the S cell cycle, while the HDR ration in starved cells declined (Fig. 28, B).

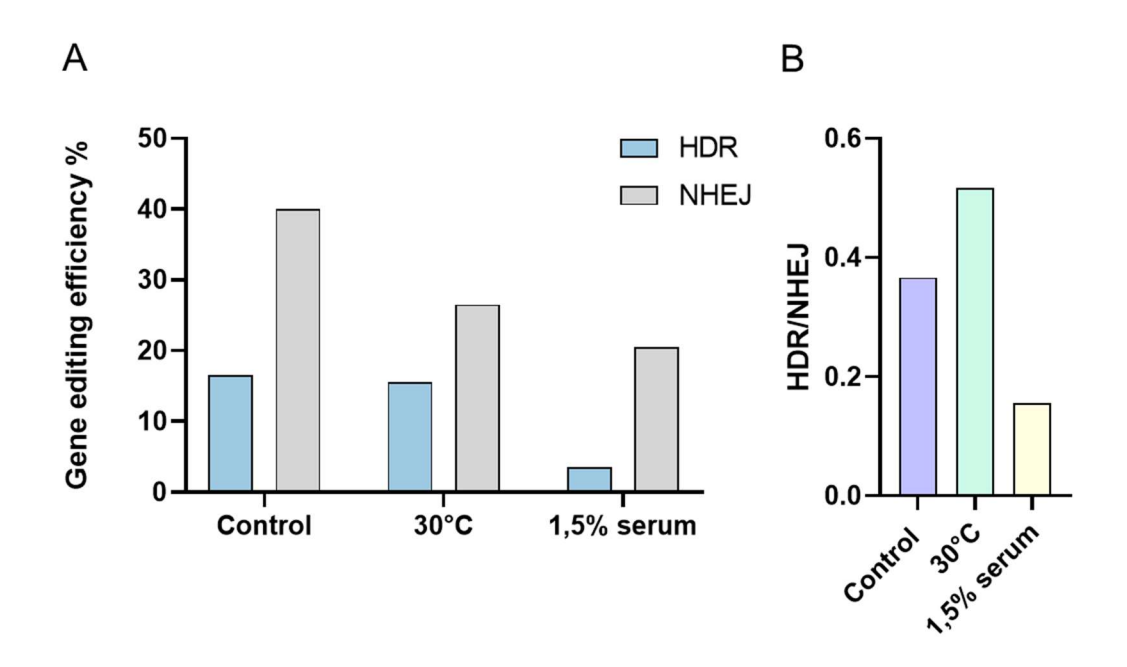


Figure 28: GE Efficiency of DSB-HDR After Cell Cycle Arrest Assays

(A) Frequency of HDR and NHEJ in PKC under control, hypothermic (30°C) and starvation (1,5% serum) conditions, as determined by Synthego Analysis of electropherograms from PCR product Sanger sequencing. (B) Relative HDR/NHEJ ratios for the respective conditions.

In a subsequent experiment, I utilized contact inhibition through increased confluency and more stringent serum starvation (0,5% serum) and compared the benchmark DSB-HDR with the prioritized TwinPE with pegRNA set 2. To determine the electroporation rate, the TwinPE was placed on a plasmid with independent expression of a GFP cassette. Contact inhibition, indicated by increased cell confluency, led to decreased transfection efficiency (Fig. 29) and correlated to a slight reduction in HDR and PE (Fig 30, A). Under starvation, also NHEJ declined but HDR completely diminished (Fig. 30, B). Notably, when the decreased electroporation efficacy was considered (Fig. 29), TwinPE editing rates remained relatively stable across all tested conditions (Fig. 30, C).

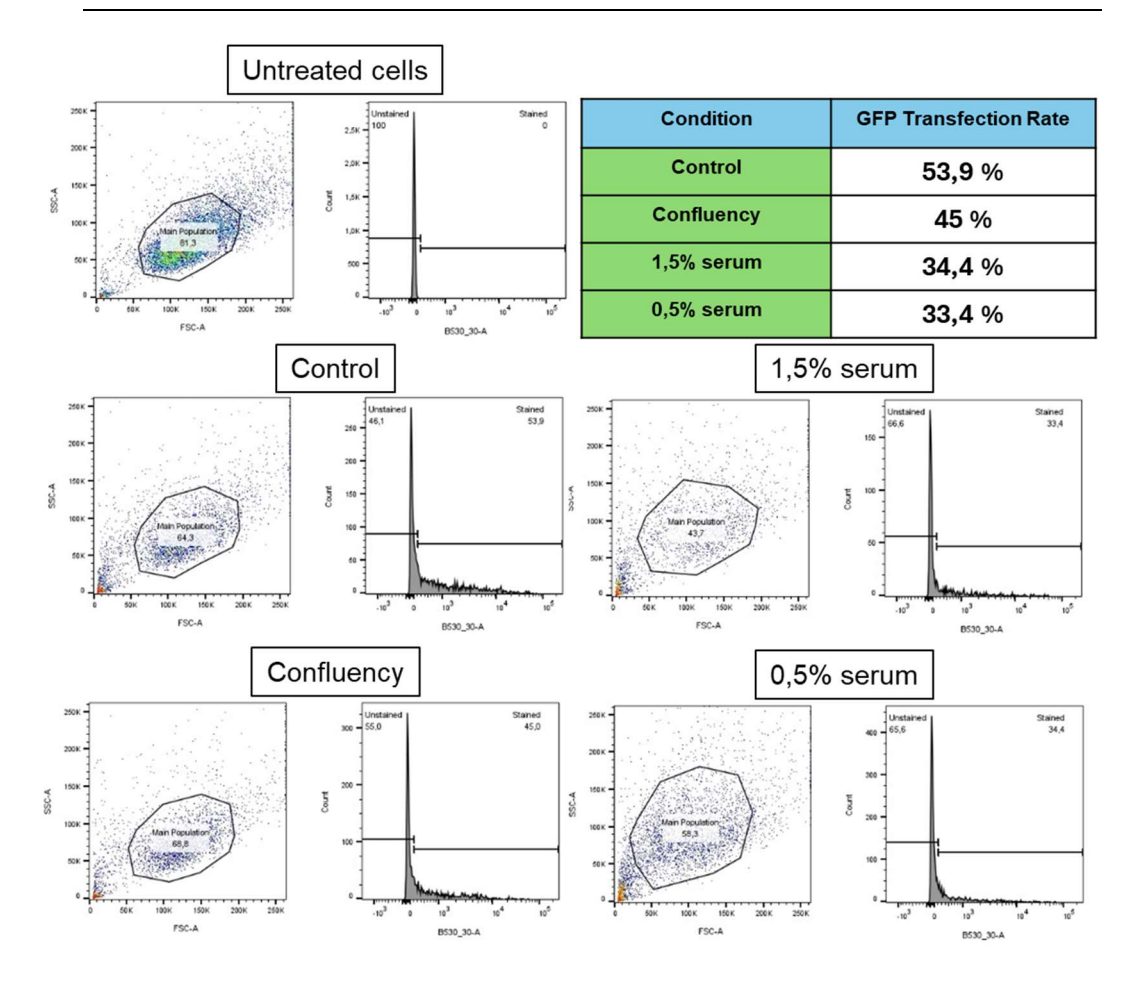


Figure 29: Transfection Rates in PKC under Different Culture Conditions

The electroporation efficiency was assessed by flow cytometry analysis after electroporation with a plasmid carrying a TwinPE and a GFP cassette. Gating and GFP-negative threshold were determined using untreated cells. GFP transfection rates are indicated for the respective culture conditions.

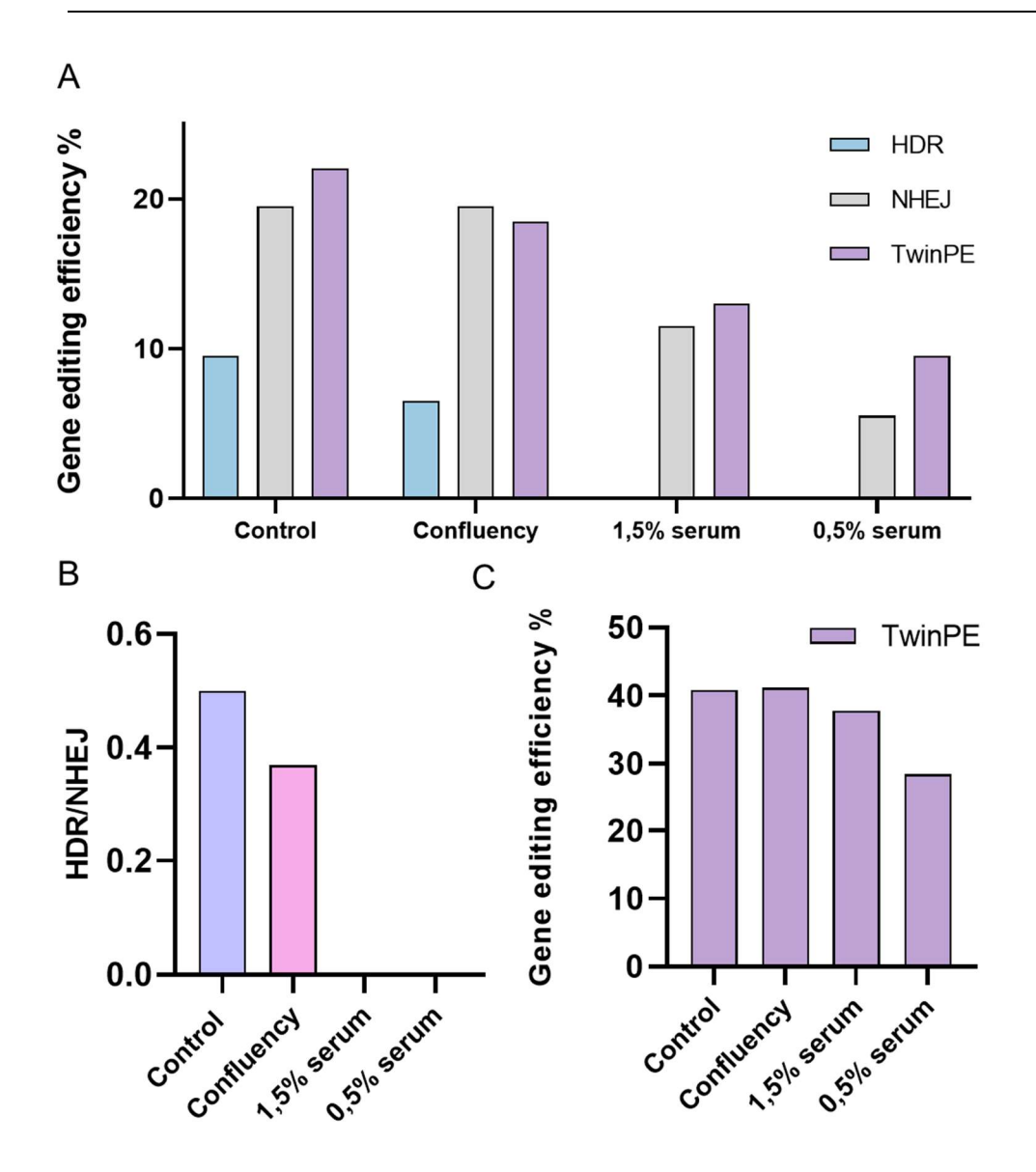


Figure 30: GE Efficiencies under Different Culture Conditions.

(A) HDR and NHEJ rates after nucleofection with DSB-HDR components and PE rates after nucleofection with the TwinPE plus GFP plasmid. (B) Relative HDR/NHEJ ratios. (C) Normalized PE correction after electroporation with the TwinPE plus GFP plasmid, considering the GFP transfection rates (Fig. 29).

3.3.2. Development and Use of Retina Explants (RE)

As an alternative to manipulating the cell cycle in primary cells, I envisaged the cultivation of pig REs to mimic *in vivo* conditions. The protocol was adapted from previous work (WELLER et al., 2024), with help of Dr. Maria Weller, Dr. Brigitte Müller and Dr. Knut Stieger (JLU, Gießen) via a lab exchange and financial support by a seed funding initiative of the DFG-funded SPP2127 "Gene and cell therapies

to counteract neuroretinal diseases". To test therapeutic GE approaches in RE, the main goal was to establish retinal fragments in culture and maintain their integrity and cellular structure under robust and reproducible conditions.

After explorative experiments, REs were consistently taken from the eyes of 6 months old pigs, providing 4-6 excised tissue fragments. REs were kept in culture using the established protocol (WELLER et al., 2024). To validate the viability and structural integrity of the explants, I compared REs after 7 days of cultivation with freshly isolated retina. IF staining for key retinal cell markers demonstrated that the explants maintained their gross structure and cellular composition. Recoverin (RCVRN) and peanut agglutinin (PNA) indicate that PRC are intact (Fig. 31). Remarkably, however, the reduction of RCVRN signals on the apical side of PRC, compared to intact retina, suggests that outer segments (OS) collapse in culture. This may be caused by the preparation process, separating the neuroretina from RPE, by the positioning of the OS on the insert membrane in the culture dishes or a combination of both. Bipolar cells, indicated by CHX10 staining, ganglion cells, indicated by RPBMS staining, and microglia cells, indicated by IBA1 signals, appear in similar numbers in d7 REs and freshly isolated tissue.

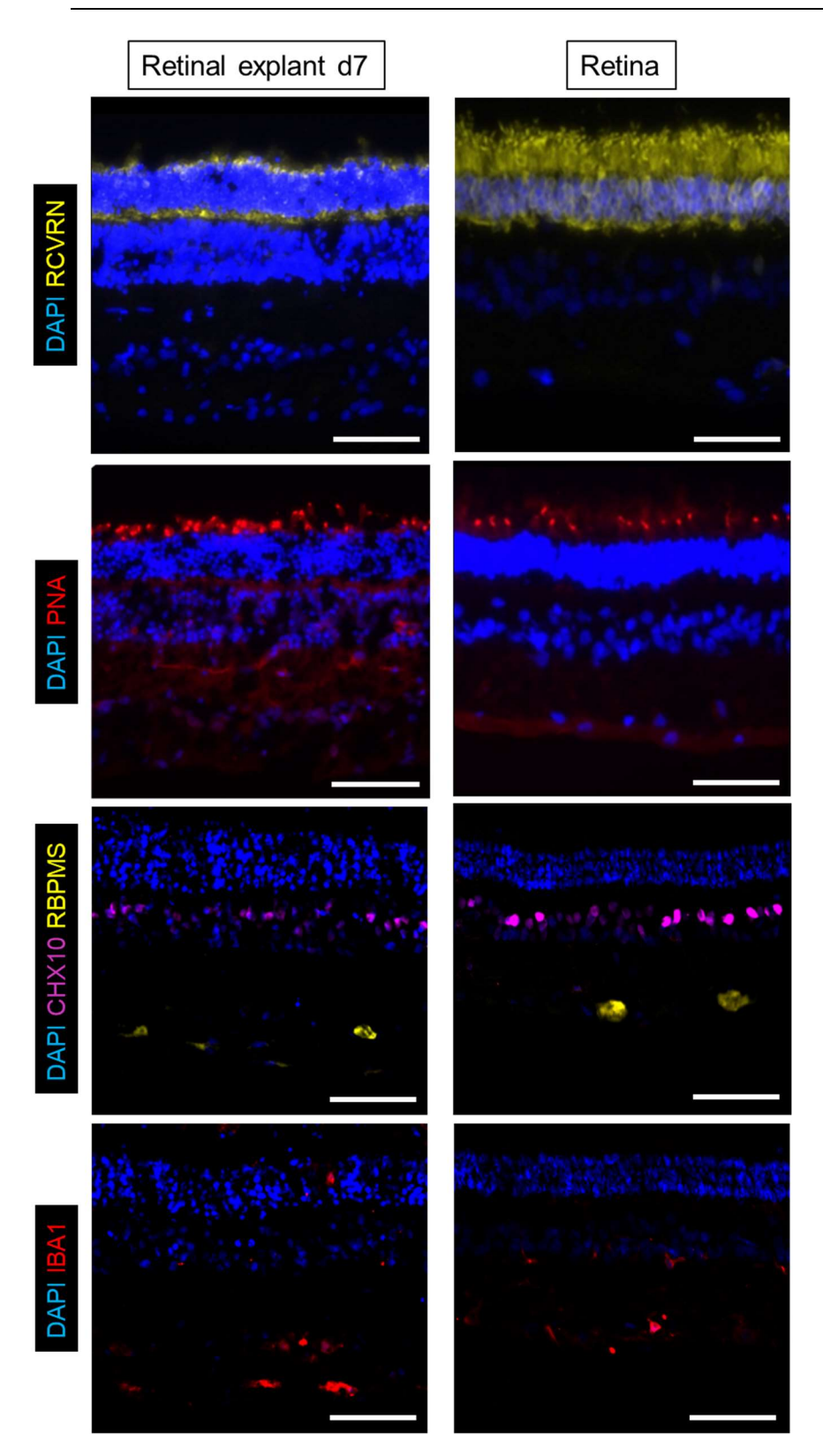


Figure 31: RE Integrity After 7 Days in Culture

Tissue sections were stained with validated markers for retinal cell types: Recoverin (RCVRN) stains PRC without discerning cones and rods. Peanut-Agglutinin (PNA) stains predominantly the IS of cones. CHX10. RBPMS and IBA1 indicate bipolar, ganglion and microglia cells, respectively.

In a complementary approach, REs were assessed at the transcriptional level, using a qPCR-based comprehensive gene expression panel. Compared to freshly isolated tissue from animals and freshly cultivated RE (d0), cytokines (Fig. 32, A), inflammatory markers (Fig. 32, B) cellular stress response and survival pathways (Fig. 32, E) were upregulated, while cell-specific markers were downregulated, except the Müller Glia cell marker RLBP1 (Fig. 32, D) after the 1st week of culture. Notably, the Usher syndrome interactome genes, involved in the structural maintenance of PRC, remained relatively stable (Fig. 32, C). Integrating the examined markers in Principle Component Analysis (PCA) reflected a picture of substantial adaptation to culture conditions and gross stability after 1 week of culture (Fig. 32, F).

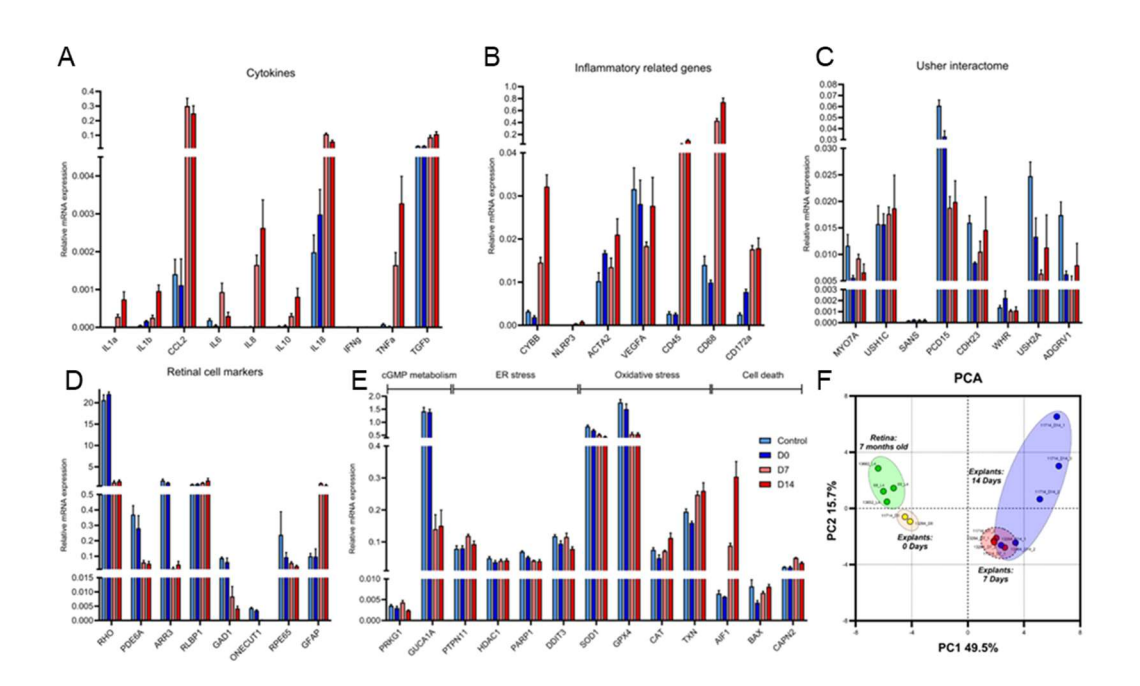


Figure 32: Transcriptional Assessment of REs

A qPCR-based panel established for retinal research by Dr. Josep Miquel Cambra, comprising cytokine (A), inflammatory (B), Usher interactome (C), retinal cell markers (D) and cell stress makers (E) was applied to REs. A combination of PPIA, RLP19, and GAPDH was used as most stable house keeping genes to determine the relative mRNA expression level of the different markers. (F) PCA of validated markers for freshly isolated retinal tissue, freshly cultivated RE and RE after 7 and 14 days respectively.

3.3.2.1. Testing AdV-mediated Transduction in REs

The first application of validated pig REs was to determine the delivery of GE components with the AdV5-GFP vector, provided by Matthias Bozza (Vector BioPharma). Live imaging of RE revealed successful GFP expression across the explant tissue, with fluorescence increasing with amount of vector applied and considerably stronger GFP intensity along the borders of the explants (Fig. 30). qPCR demonstrated GFP expression at the transcriptional level (Fig. 31).

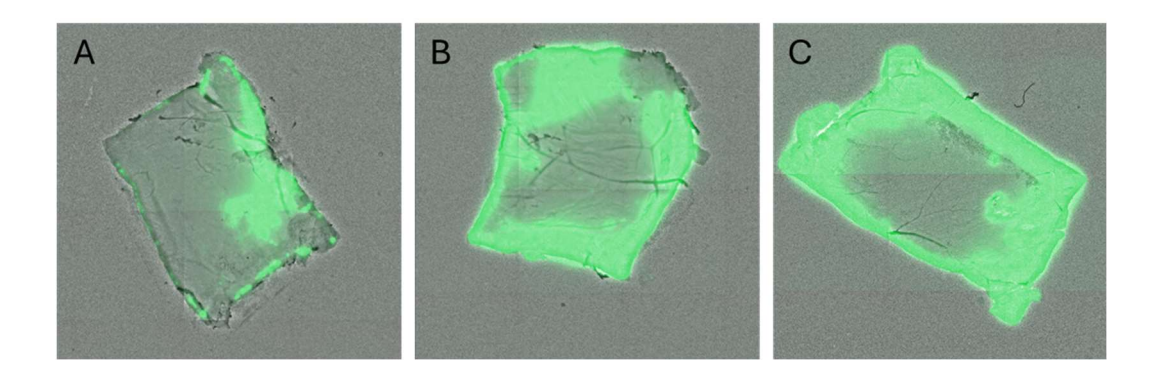


Figure 33: Live Fluorescence Imaging of RE after AdV5-GFP treatment RE were cultivated and treated at d0 with $5\mu L$ (A), $15\mu L$ (B) and $45\mu L$ (C) of AdV5-GFP were applied.

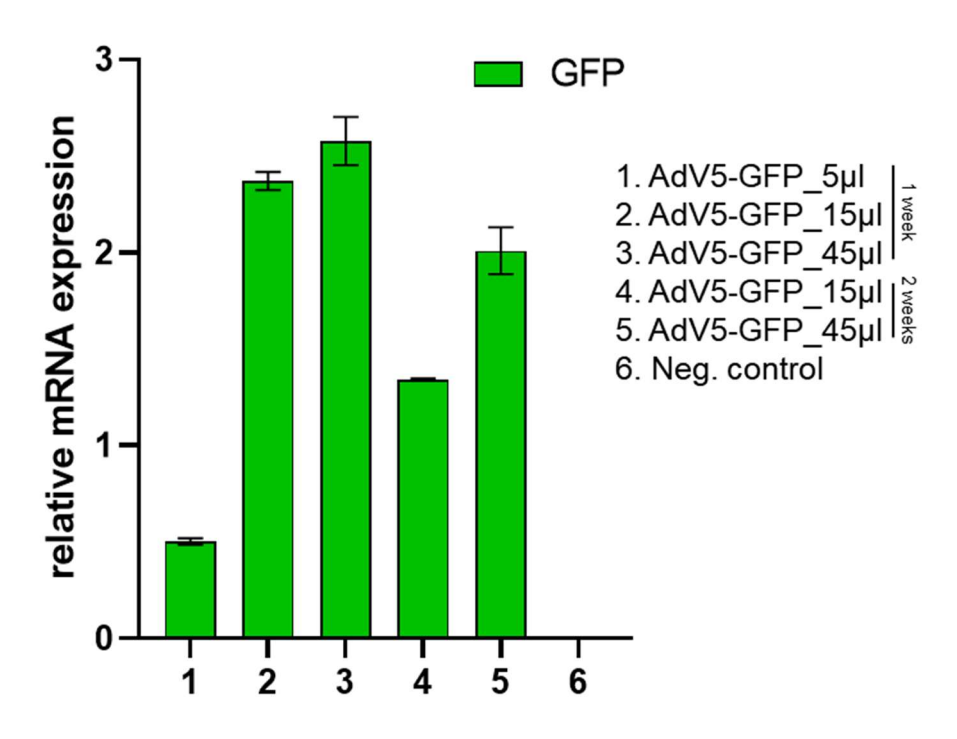


Figure 34: qPCR after AdV5 Application on RE

This figure shows the relative mRNA expression of GFP in different conditions. 1-3 were analyzed 1 week after AdV5 application, 4 and 5 were analyzed 2 weeks after application. The expression rises with increasing volume of AdV5 and was lower in samples analyzed 2 weeks after application. The expression levels are relative to the most stable housekeeping gene GAPDH.

To allow subsequent flow cytometry analysis for transfection rate assessment, I established a tissue dissociation protocol adapted from (MULLER et al., 2025). After the dissociation, the cells were fixed, permeabilized and stained with DAPI. A fluorescence microscopy image post dissociation shows that the cells preserved their shape and single GFP positive cells can be seen (Fig. 35).

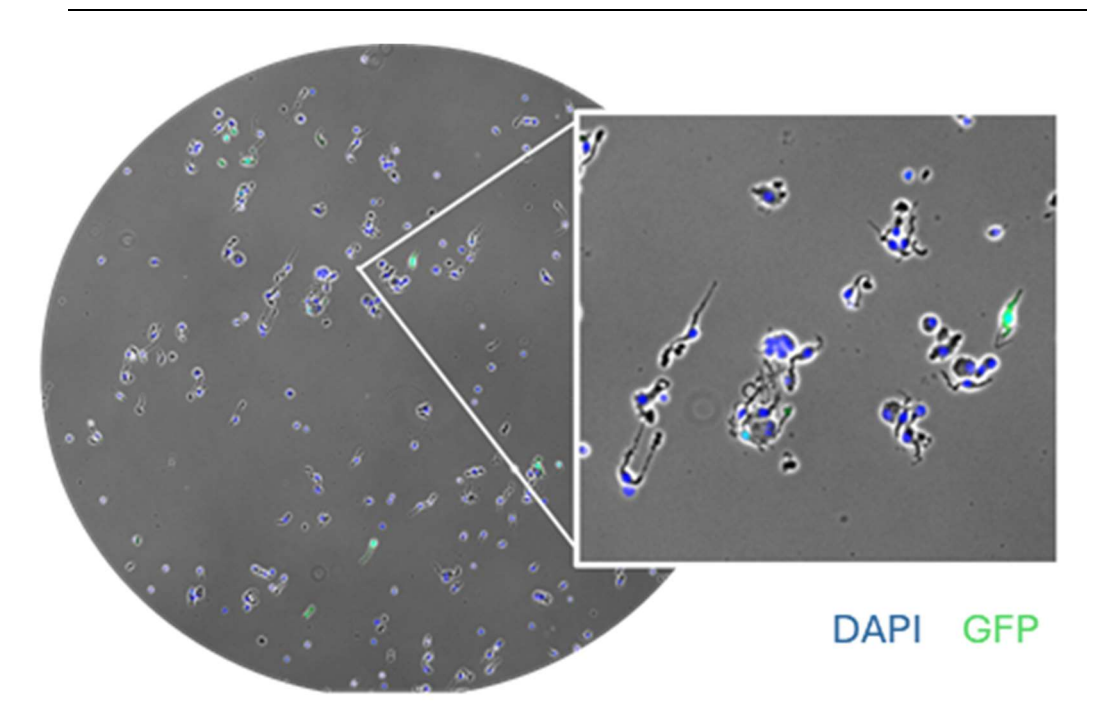


Figure 35: Fluorescence Microscopy Image of Dissociated RE after AdV5-GFP Treatment
The cells were dissociated, permeabilized fixed and stained with DAPI. Their morphology was well
preserved. Single GFP-positive cells with different fluorescence intensity can be seen.

Flow cytometry analysis of dissociated explants helped quantify overall transfection efficiency (Fig. 36).

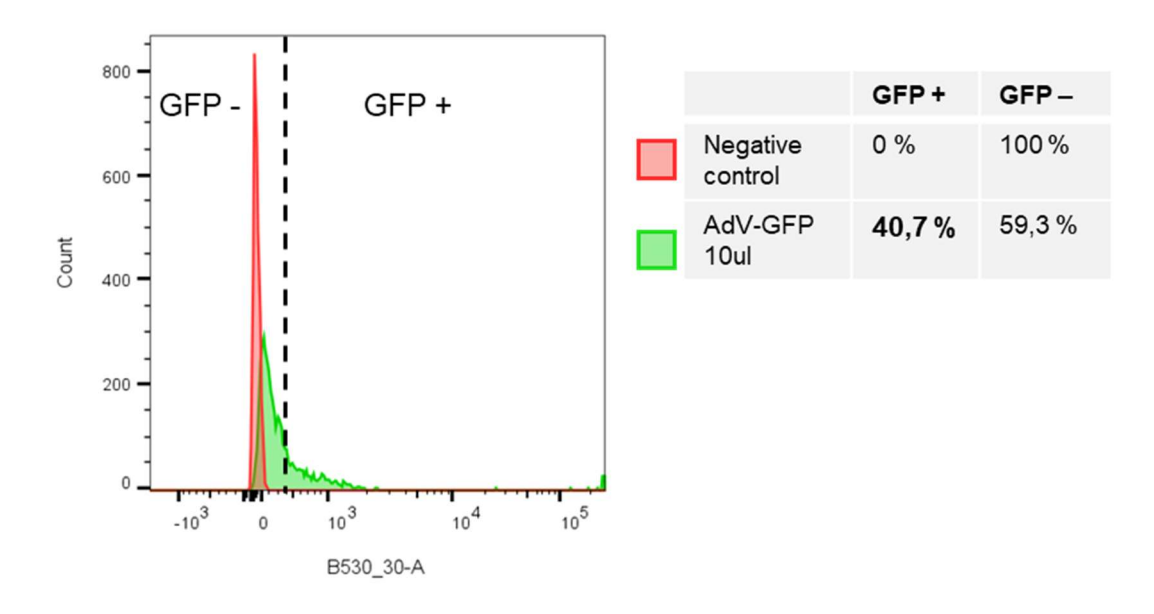


Figure 36: Flow cytometry analysis of dissociated AdV5-treated REs

An untreated RE was analysed and used to set the negative GFP threshold. The flow cytometry analysis revealed 40,7% of positive GFP events in a RE treated with 10 μ L of AdV-GFP (native GFP signal). Among these 40,7%, approximately 1% of the events show a much higher fluorescence intensity (bottom right corner).

For 3D visualization of REs, I collaborated with Teresa Rogler and Dr. Friedhelm Serwane (Institute of Biophysics, University of Ulm) based on their recent preprint (ROGLER et al., 2024). A confocal imaging protocol was adapted to integrate the spatial resolution advantages of IF with the quantitative capabilities of flow cytometry. This methodology, originally developed for Retina Organoids (ROs), was optimized to quantify vector transduction efficiency through the combination of 3D confocal imaging reconstruction and a computational algorithm for nuclear segmentation, enumeration, and colocalization analysis with GFP signal in situ.

A preliminary analysis was conducted on an explant treated with 45µl of AdV5-GFP (Fig. 37). It revealed some improvements needs, notably due to incomplete DAPI penetration that resulted in preferential staining of the ONL.

Quantitative analysis identified 871 individual nuclei within the imaging field, of which 517 demonstrated colocalization with GFP signal, which indicated a transduction efficiency of 59% within the ONL of the RE.

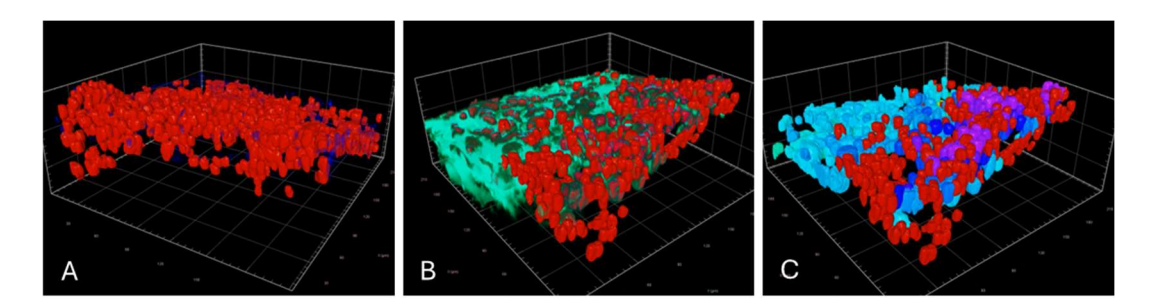


Figure 37: Initial Quantitative 3D analysis of Vector Transduction in RE

(A) Visualization of DAPI-stained nuclei in the ONL of a retinal explant treated with 45μL of AdV5-GFP, with computational segmentation overlay. (B) Native GFP fluorescence signal distribution within the same field of view. (C) Colocalization analysis showing segmented nuclei with overlapping DAPI and GFP signals (green to purple), indicating successful transduction. The red nuclei remaining represent non transfected PRCs.

3.3.2.2. Non-Viral Delivery Vectors

After successfully testing VLPs and DVX in PKC, I decided to apply them on REs. These two types of delivery vectors didn't transfect any cells of the neuroretina. This finding was confirmed by live imaging and flow cytometry analysis (Fig. 38).

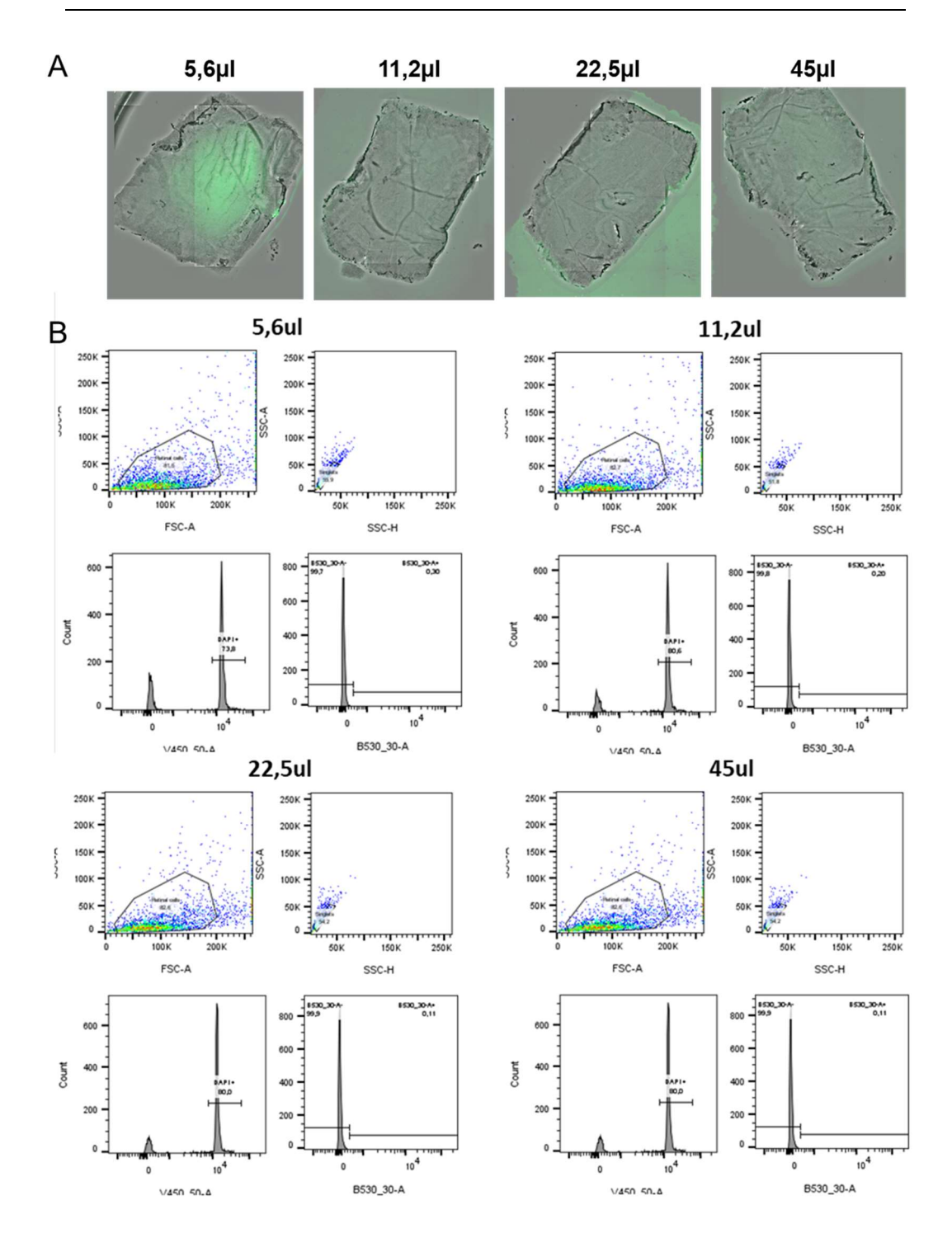


Figure 38: Fluorescence Live Imaging and Flow Cytometry Analysis of VLP Transfection in REs

(A) Live imaging pictures revealed a strong background fluorescence, probably due to the production process of the VLPs. No transfection was observed with this method. The finding was confirmed by flow cytometry analysis.

V. DISCUSSION

1. Considerations for Gene Therapy Preclinical Studies in Inherited Retinal Diseases

The development of effective gene therapy (GT) modalities for inherited retinal diseases (IRDs) represents one of the most promising yet methodologically complex frontiers in contemporary ophthalmological research. Recent years have witnessed remarkable progress in this therapeutic domain, commencing with the landmark approval of voretigene neparvovec-rzyl (Luxturna), the first FDA-sanctioned gene therapy for RPE65-mediated retinal dystrophy (RUSSELL et al., 2017; MAGUIRE et al., 2019). This milestone has catalyzed exponential growth in the field, culminating in approximately 159 registered clinical trials investigating gene therapy approaches for various IRDs (AMERI et al., 2023).

The BRILLIANCE clinical trial (NCT03872479) constitutes a significant advancement as the inaugural Phase I/II investigation applying CRISPR-Cas9 gene editing technology to address an IRD. Under the aegis of Editas Medicine, this pioneering study evaluates EDIT-101, an AAV5-delivered CRISPR-based therapeutic targeting the intronic c.2991+1655A>G mutation in the CEP290 gene-the predominant genetic etiology of Leber Congenital Amaurosis 10 (LCA10) (MAEDER et al., 2019). Interim analyses as of May 2024 indicate that among 14 enrolled participants, 11 (78.6%) demonstrated statistically significant improvements in visual function parameters and vision-related quality of life metrics without evidence of irreversible adverse events (PIERCE et al., 2024).

Concurrently to these encouraging clinical developments, a substantial translational gap persists between preclinical efficacy and clinical outcomes. Preclinical successes observed in murine models have been reported to fail to recapitulate in several human clinical trials, a phenomenon attributable to interspecies differences in retinal architecture, cellular composition, and genetic background (GARAFALO et al., 2020; SHAMSHAD et al., 2023). This translational disparity is further exemplified by the longitudinal clinical experience with Luxturna. Patient responses exhibit marked heterogeneity, with some individuals experiencing substantial improvements in visual acuity and visual field sensitivity while others derive suboptimal therapeutic benefit (CHIU et al., 2021).

Emerging reports document therapy-related adverse events following subretinal administration of Luxturna, including macular hole formation, foveal attenuation, chorioretinal atrophy, ocular hypertension, and cataract development (PENNESI et al., 2018; FISCHER et al., 2024). Additional complications have been observed following contralateral administration and in extended post-treatment surveillance, including inflammatory responses and progressive retinal thinning (MAGUIRE et al., 2019). These observations highlight critical limitations in current preclinical research methodologies - specifically, the absence of validated long-term preclinical studies capable of predicting therapy-emergent effects and the anatomical and immunological differences between murine models and human retinal tissue that influence translatability of gene therapy interventions (SHAMSHAD et al., 2023).

The progression beyond conventional murine systems toward more physiologically relevant models that accurately recapitulate human retinal pathophysiology represents an essential step to guarantee the success of clinical trials. Integration of these advanced preclinical models with comprehensive longitudinal assessment protocols may substantially enhance the predictive value of preclinical studies, ultimately improving therapeutic outcomes for patients with IRDs (BASSOLS et al., 2014; HOFFE and HOLAHAN, 2019; HOU et al., 2022; MCCALL, 2024).

1.1. Positioning the Pig as a Valuable Species for Translational Research in IRDs

The pig has emerged as a particularly valuable animal model in ophthalmic research, occupying a strategic middle ground between small laboratory animals and humans (SOMMER et al., 2011; ROSS et al., 2012; MCCALL, 2024). This value stems from its remarkable anatomical and physiological similarities to the human eye (SANCHEZ et al., 2011; KOSTIC and ARSENIJEVIC, 2016). Unlike rodent eyes, porcine eyes feature comparable size, layered retinal structure, and importantly, a cone-rich visual streak that functionally resembles the human macula. These structural parallels extend to cellular and molecular levels, with porcine PRCs exhibiting similar morphology and distribution to their human counterparts.

Perhaps most significantly, pigs can be genetically modified to effectively recapitulate human disease mechanisms and progression, allowing for patient relevant therapeutic strategies (AIGNER et al., 2010; GROTZ et al., 2022; STIRM et al., 2022; JAUDAS et al., 2025). This capability has been conclusively demonstrated through successful generation comprehensive the and characterization of humanized porcine models for several conditions, including Duchenne-Muscular-Dystrophy, Cystic fibrosis and of course Usher Syndrome - a critical capability not readily available in other large animal models such as canines and NHPs. The establishment of such comprehensive models strengthens the position of pigs in biomedical research while simultaneously expanding our understanding of porcine physiological and metabolic parameters through the collection of increasingly comprehensive datasets, ultimately providing deeper insights into inflammatory responses, immune system dynamics, and speciesspecific drug metabolism relevant to translational medicine (VAN DER LAAN et al., 2010; BASSOLS et al., 2014; YOSHIMATSU et al., 2016; TANG and MAYERSOHN, 2018). While such extensive reference datasets have long been available for murine models, their relative scarcity for porcine systems reflects the more recent emergence of the pig as a translational model organism, a gap that continues to narrow as adoption of these models accelerates.

Another compelling advantage of pigs for IRD research is their suitability for long-term studies, enabled by their significantly longer lifespan compared to murine models. This extended timeframe better reflects the progressive degenerative nature of retinal diseases in patients while remaining more economical than other large animal models such as NHPs. The value of porcine models for longitudinal investigations has been validated by their successful implementation in neurodegenerative research (HOFFE and HOLAHAN, 2019; YANG et al., 2021), where similar requirements for tracking slow disease progression and treatment effects over extended periods are essential.

1.2. Pilot Preclinical Testing of Gene Editing to Treat IRDs Using the USH1C Pig Model

In line with the advantages of the pig in translational research for IRD treatment, the USH1C pig model provides a valuable opportunity to investigate GE approaches (GROTZ et al., 2022; AUCH, 2023). My research explored this potential through a pilot experiment that addressed several crucial aspects of GT for IRDs. This comprehensive investigation encompassed the preliminary development of efficient GE strategies targeting a specific locus, the selection and testing of appropriate delivery vectors, determination of optimal application routes, and preliminary evaluation of effective dosages (DICARLO et al., 2018; DRAG et al., 2023). Through this multifaceted approach, my work establishes a foundation for advancing GE therapies in a clinically relevant large animal model that closely resembles human retinal physiology and disease progression and gives us insights on side-effects and necessary improvements.

After achieving promising results *in vitro* (Fig. 8-10), I proceeded to test TwinPE *in vivo*. This progression required a delivery vector capable of packaging the large PE components and effectively transfecting retinal cells. The only established delivery vector meeting these requirements is an AdV. Consequently, I selected the high-capacity gutless AdV5 for this critical phase of the investigation, as it offers the necessary cargo capacity while maintaining the ability to transduce retinal tissue (SWEIGARD et al., 2010; HAN et al., 2021; MCDONALD et al., 2024).

For the application, the subretinal application route was chosen for several reasons. It provides a more localized delivery directly adjacent to the target PRC cells. It also requires fewer vector particles compared to intravitreal application, where the substantial volume of the vitreous causes significant dilution of the therapeutic agent (IGARASHI et al., 2013; KIRALY et al., 2025).

This approach proved fruitful, as I demonstrated that high-capacity gutless AdV5 vectors successfully delivered a substantial 35 kb genetic payload encompassing the dsDNA coding for both the TwinPE components and the GFP-reporter - to retinal cells, as evidenced by IF (Fig. 22-24). The expression of all components in retinal cells was confirmed by qPCR (Fig. 25, A), and although only minimal editing activity was observed in the RPE of the HD-treated eye (Fig. 25, B), this

experiment established the potential of this approach in a large animal model physiologically similar to humans - a significant advancement for the field.

This investigation also revealed important findings. Retinal atrophy was observed following subretinal injections in the pilot experiment, particularly in the HDtreated eye (Fig. 21), a finding that has been documented in the literature and reminds of emerging clinical reports from Luxturna administration in patients (HAN et al., 2019; KU et al., 2024). The primary cause of this atrophy remains difficult to determine. During subretinal application, mechanical disruption of retinal layers occurs through the creation of a localized retinal detachment, temporarily separating the neuroretina from the RPE (PENG et al., 2017). With increasing injection volumes, this mechanical disruption can be exacerbated, exerting greater pressure and tension on retinal tissue and potentially causing damage, which could explain the more pronounced atrophy in the HD-treated eye. Alternatively, the atrophy could result from dose-dependent vector toxicity and secondary inflammatory responses to the treatment, also emphasizing the need of dosage optimization and prophylactic corticosteroids regimen (MAGUIRE et al., 2009; MACLACHLAN et al., 2018; KVANTA et al., 2024). In this study, injections were performed in the same eye to maximize outcomes, potentially intensifying adverse effects. An important parameter of vector preparation linked to atrophy in ocular applications is endotoxin contamination during production (ZHENG et al., 2021). Although the AdV5 vectors were produced under standard pharmaceutical conditions, where endotoxin levels must remain below 10 EU/mL of vector suspension, personal communication with Prof. Dr. Dr. Dominik Fischer (Oxford Eye Hospital), who performed the surgical procedure, suggested that even this low level might exceed the tolerance threshold of the sensitive retinal tissue. This hypothesis could be confirmed by the strong reaction observed with the injection of the DVX subretinally (Fig. 26). While this vector had been previously tested in mice by systemic injection and did not provoke any strong advert immune response, this vector was prepared under biomedical research conditions and showed a strong reaction in the eye. It is important to determine if this effect is due to inherent vector toxicity or vector preparation.

AdV5 showed a bounded vector biodistribution, with high expression levels visible within approximately 0.36 cm diameter around the injection site (Fig. 23). This restricted spread indicates that targeting larger retinal areas would require multiple

injection sites with the current approach, substantially increasing risks of retinal atrophy and detachment - a question that must be addressed in future experiments and maybe motivate a reconsideration of alternative application route to expend the biodistribution (PAVLOU et al., 2021; KELLISH et al., 2023) or refine the technique, with recent literature emphasizing the positive effect of an intravitreal air tamponade on vector distribution following subretinal injection (DUCLOYER et al., 2023).

These findings collectively highlight the importance of technical aspects in ocular GT, including application routes and vector preparation. Comprehensive preclinical studies are key to improving treatment efficacy and safety, and pig models represent excellent candidates for exploring these open questions and minimizing unexpected side effects in subsequent clinical studies.

1.3. Considerations in Functional Assessments of the USH1C Pig Model

Functional measurements are fundamental to my research, serving dual purposes: characterizing the USH1C animal model and establishing crucial baselines for assessing future therapeutic interventions. Throughout my PhD, I collaborated with field experts who provided invaluable insights into these methodological approaches. The sophisticated equipment employed for these assessments originates from human clinical settings, where measurements are typically performed on cooperative patients (BINNS and MARGRAIN, 2005; ZHANG et al., 2019; TEAL et al., 2024). This creates a unique translational opportunity by using the same devices as patients but necessitates thoughtful adaptations for application in animal models (GONÇALVES et al., 2012; PASMANTER et al., 2021; GROTZ et al., 2022). In porcine studies, these procedures require carefully managed anaesthesia protocols, specialized equipment, and dedicated facilities. While this introduces variables that must be controlled, it also creates opportunities for standardization across research centres.

Electroretinography (ERG) measurements are particularly sensitive to anaesthesia conditions, as different agents and depths can alter waveforms, potentially influencing the interpretation of therapeutic effects (NAIR et al., 2011). This sensitivity highlights the critical role of veterinary expertise in ensuring stable

anaesthesia protocols and comprehensive monitoring during functional assessments.

When analysing ERG measurements, I observed inter-animal variability that reflects another important characteristic of porcine models - their greater biological diversity compared to inbred laboratory mice. Within littermates, I documented notable weight differences influenced by both sex and phenotype, with WT controls generally larger than their USH1C counterparts. These physical differences, which more accurately mirror the heterogeneity seen in human populations, influence parameters such as drug distribution and could affect the outcome of measurements. Future refinements to the approach could incorporate additional precise measures of anaesthesia depth to eliminate this factor from our measurements or help correlate findings. One candidate includes use of an electroencephalogram (EEG) monitoring, which has shown promise in rats (BLOKHINA et al., 2023), though standardized protocols for porcine applications don't exist yet and would need establishment (MIRRA et al., 2023).

Our experience with distortion product otoacoustic emissions (DPOAE) further illustrates the adaptability required for translational research. This technique, widely used for its efficiency and convenience in human subjects - including awake newborns (MADZIVHANDILA et al., 2024) - requires improvements for porcine applications. The anatomical differences in ear canals affected the proper fitting of ear inserts provided and normally meant for humans, particularly in larger animals (WANG et al., 2022). After testing various inserts and positioning approaches, DPOAE was often not possible due to an incomplete leak check as can be seen in the (Fig. 19). This observation is important for future analysis as it can be easily solved with adapted inserts.

Adaptations are required for functional assessments in large animal models, but the pig represents an optimal compromise between translational relevance and experimental practicality. The significant advantages of human-like ocular and auditory anatomy outweigh the methodological modifications needed, especially as these protocols become increasingly standardized.

2. 3R Principle Considerations in Porcine Retinal Research

The anatomical, physiological, and genetic similarities between porcine and human visual systems position these models as valuable intermediaries between rodent-based preclinical research and clinical application. These attributes suggest that porcine models may accelerate the preclinical validation of therapeutic candidates for IRDs by reducing species-specific translational barriers and that their position in translational research will therefore strengthen in the future (AIGNER et al., 2010; BASSOLS et al., 2014; HOU et al., 2022; MEYERHOLZ et al., 2024).

The advantages of porcine models are accompanied by specific ethical considerations. Their neurophysiological complexity, including well-documented cognitive capabilities, advanced sensory processing, and social behaviour necessitates rigorous ethical frameworks for experimental design (GIELING et al., 2011; KORNUM and KNUDSEN, 2011; LUCAS et al., 2024). This consideration is particularly relevant for studies involving sensory systems directly linked to environmental interaction and cognitive function.

These scientific and ethical dimensions converge in the application of the 3R principle - Replacement, Reduction, and Refinement - which provides a framework for optimizing experimental protocols (WEBSTER et al., 2010). Systematic application of these principles enhances both the ethical standing and scientific validity of porcine models in retinal research, as demonstrated by improved data consistency and reproducibility in 3R-optimized experimental designs (TÖRNQVIST et al., 2014)

2.1. Maximization of research outcome from each animal

Through careful planning and coordination, I made sure to maximize the scientific value derived from each animal. In one exemplary cohort (Figure 16, Cohort of November 2023), we performed for each animal: a comprehensive retinal phenotyping via ERG and OCT with the help of Dr. Tobias Peters (Universitätsklinikum Tübingen) and Ruslan Nychshuk (Pigmod, Liblice, CZ), collected retinal tissue for molecular and histological analysis of disease progression for our own characterization projects, established Müller glia cell cultures from rests of retinal tissue (Yesim Tütüncü, JGU Mainz), took extensive

samples to characterize a potential intestinal phenotype in USH1C animals (Prof. Dr. Andreas Parzefall, LMU Munich) and collected inner ear samples for Dr. Aziz El-Amraoui (Institut Pasteur, Paris, FR).

This approach demands significant organizational effort and coordination between research teams. However, the scientific and ethical benefits are substantial, ensuring that each animal contributes to multiple research objectives simultaneously (GROTZ et al., 2022; SEITZ et al., 2024). Furthermore, the collaborative framework ensures that breeding is meticulously planned to align with research timelines, guaranteeing that no animals are produced without specific scientific purpose.

2.2. Improvement of Postnatal Management

This is especially important for USH1C piglets who show a strong phenotype from birth and shouldn't be born without a comprehensive scientific purpose. During my work on this thesis, I made sure to improve the well being of homozygous piglets postpartum by finding a middle-ground between natural social behaviour, including interaction with mother and healthy littermates, while providing them a gentler environment for the first critical hours of life (Fig. 15). A temporary separation from the mother and implementation of straw and milk buckets allowed our piglets to show a faster improvement of coordination compared to our previous protocol, helping them with their independence and wellbeing.

2.3. Further functional assessment options

The functional measurements of USH1C pigs during my thesis were all performed under anaesthesia. Although very valuable, the process of sedation and awakening from anaesthesia can be a source of stress for the animals. Pigs are very intelligent and social animals with cognitive capabilities that can be leveraged to develop welfare-friendly evaluation methods through training (GIELING et al., 2011; KORNUM and KNUDSEN, 2011).

Behavioural testing represents a promising refinement strategy that capitalizes on the cognitive abilities of pigs while potentially providing more naturalistic functional assessments. (GROTZ et al., 2022) implemented innovative behavioural tests to evaluate visual acuity in USH1C pigs, demonstrating the feasibility of such

approaches despite the complications introduced by their vestibular phenotype. In their study, the authors developed a behaviour-based visual navigation test that could distinguish between WT and USH1C pigs based on their ability to navigate a maze using visual cues. This approach not only reduced reliance on invasive procedures but also provided functional data more representative of actual visual performance.

Recent advances in automated assessment technologies further illustrate the potential for refined testing methodologies. (BARONE et al., 2024) described a sophisticated visual psychophysics method for measuring visual function in minipigs. Their approach utilized a touchscreen interface paired with a reward system to train pigs on contrast sensitivity discrimination tasks. The system progressed to a self-running configuration where animals could complete multiple consecutive trials without human intervention. This automated approach reduced handling stress while generating detailed contrast sensitivity data comparable to that obtained in human psychophysical testing.

By incorporating playful interactions and reward-based learning into the research context, such approaches align scientific objectives with animal welfare considerations. Although implementing these techniques presents logistical challenges, particularly for animals with sensory or motor impairments, they deserve greater prominence in translational research programs.

2.4. Development of Intermediate Test Systems

In the context of retinal research, intermediate test systems that bridge the gap between cell culture and whole-animal studies offer promising opportunities to reduce reliance on *in vivo* experiments (ALSALLOUM et al., 2024).

RE cultures represent a particularly valuable reduction strategy for addressing fundamental research questions (WANG et al., 2011; RETTINGER and WANG, 2018; WELLER et al., 2024). While still requiring animal tissue, explant cultures dramatically increase experimental efficiency. A single porcine eye can yield up to six explants, each serving as an independent experimental unit. This approach enables the evaluation of multiple treatment conditions or timepoints from a single

donor animal, substantially reducing the number of animals required and minimizing the stress related to a treatment *in vivo*.

By continuing to use explant culture techniques and establishing clear correlations between ex vivo and *in vivo* outcomes, I can progressively shift more research questions to these intermediate systems, reserving whole-animal studies for latestage validation of therapeutic approaches.

3. Therapeutic GE: Critical Barriers in Achieving Efficient Genetic Modification

Successful GE requires overcoming multiple biological barriers to ensure therapeutic efficacy, particularly in specialized post-mitotic cells like PRCs. My work demonstrates that these barriers exist at three critical levels: accessing the target cell, ensuring the correct reassembly of GE components in the target cell, and enabling CRISPR-Cas9 access to the target DNA.

3.1. Access to the Target Cell

The selection of an appropriate delivery vector is fundamental to successful GE, as different vectors exhibit distinct cell-type tropisms. In this thesis, I demonstrated that AdV5 vectors successfully transduced both RPE and PRC *in vivo*. In contrast, DVX and VLPs - which were developed based on different viruses – failed to transduce neuroretinal cells (Fig. 21, 25, 38) (KALESNYKAS et al., 2017; BANSKOTA et al., 2022).

PRC transduction by different vectors offers exciting research opportunities, as the mechanisms remain only partially understood. (PETIT et al., 2017) provided evidence suggesting the OS serves as an entry point for AAV vectors in PRCs. This insight opens intriguing pathways for investigation, as vectors entering through this route undertake a fascinating intracellular journey - navigating from the OS through the connecting cilium and ultimately reaching the nucleus where therapeutic expression can occur.

The natural adaptability of PRCs adds another interesting dimension to gene delivery research. Under stress conditions, these specialized cells can shed their OS, demonstrating a remarkable evolutionary adaptation that, while protective for the

cell, presents a creative challenge for vector design to ensure successful nuclear entry before shedding occurs (BAZAN et al., 1992; VARGAS and FINNEMANN, 2022). The adjacent RPE actively participates in retinal homeostasis by phagocytosing shed OS. This activity, combined with the RPE's accessible single-cell layer structure, may preferentially capture vectors intended for PRC transduction.

Alternative entry routes, such as uptake through the cell body, can be considered, yet these also encounter structural barriers - including the OLM in subretinal delivery or ILM in intravitreal delivery (TAKAHASHI et al., 2017; TEO et al., 2018).

The interplay of these multiple factors likely contributes to the observed inefficiencies in PRC targeting, underscoring the need for further research to elucidate the optimal strategies for gene vector delivery in the retina (MULLER et al., 2025).

3.2. Assembly of GE Components in the target cell

For DNA-based delivery methods, such as the AdV5 vector I used in the pilot *in vivo* experiment, the genetic cargo must enter the nucleus for transcription. As (DEAN et al., 2005) explained, nuclear entry is considerably more efficient in dividing cells, where the nuclear envelope temporarily disassembles during mitosis. In non-dividing cells, this barrier necessitates active transport mechanisms. The AdV5 have naturally evolved to actively transfer their genetic material into the nucleus of both dividing and non-dividing cells (GREBER and SUOMALAINEN, 2022). This ability is confirmed by the GFP signal observed in the IF images of the retina post treatment (Fig. 19).

The choice of promoter in DNA delivery also significantly impacts expression levels and specificity. Studies by (BELTRAN et al., 2010; HULLIGER et al., 2020) demonstrated that PRC-specific promoters offer targeted expression, although the expression levels are lower than ubiquitous promoters, that drive robust expression within a broader diversity of cells, such as the one used in the *in vivo* pilot experiment (CMV).

RNA-based delivery approaches, which we investigated using VLPs and DVX, offer the advantage of bypassing nuclear entry requirements before translation (XIAO et al., 2022; POPOVITZ et al., 2023).

In eukaryotic cells, cytoplasmic ribosomes translate mRNA transcripts into their corresponding polypeptide chains. GFP, following translation, remains predominantly localized within the cytoplasmic compartment until its eventual degradation via ubiquitin-proteasome pathway mechanisms. CRISPR-Cas9 GE components require post-translational assembly, with Cas9 nuclease protein and guide RNA (gRNA) forming a functional ribonucleoprotein complex. According to (NISHIMASU et al., 2014) this assembly involves specific structural rearrangements in Cas9 upon gRNA binding, essential for subsequent target DNA recognition.

3.3. Access of CRISPR-Cas9 to the DNA in the nucleus of the target cell

(JIANG et al., 2015) demonstrated that the Cas9-gRNA complex must subsequently translocate to the nucleus via nuclear localization signals (NLS) to access genomic DNA. This nucleocytoplasmic transport is mediated specifically by NLS peptide sequences integrated within the Cas9 protein structure. The enhanced PE systems evaluated in my *in vitro* experiments, PE2Max and PE4Max, incorporate bipartite SV40 NLS sequences with optimized positioning and flanking amino acid composition that demonstrably facilitate nuclear import efficiency (CHEN et al., 2021). These structural modifications facilitate more effective nucleocytoplasmic transport particularly in post-mitotic cells - where nuclear envelope breakdown does not occur- potentially increasing editing efficiency (DEAN et al., 2005).

Within the nucleus, the CRISPR-Cas9 ribonucleoprotein complex employs a multistep target search mechanism. This process begins with Cas9 scanning the DNA for protospacer adjacent motif (PAM) sequences, followed by local DNA unwinding to facilitate gRNA base pairing with the target strand, dissociation upon detection of critical mismatches, and iterative repetition of this interrogation process along the genomic DNA until complete binding of the gRNA at its target sequence (JINEK et al., 2012). Target search efficiency is demonstrably impeded in postmitotic cells due to heightened chromatin compaction and restricted nucleosome accessibility of target loci (DAER et al., 2017). Cell-type specific variations in

chromatin architecture, including differential nucleosome positioning, density, and epigenetic modifications, have been extensively mapped by (TEIF et al., 2012), providing a mechanistic explanation for the heterogeneous editing efficiencies observed across different cell types and loci despite employing identical GE methodologies.

The GE testings I performed *in vitro* provided compelling evidence for the locus-specific differences in editing efficiency. When targeting the B2M locus with adenine base editors (ABE), I observed 100% editing efficiency using VLP delivery in PKC. However, the same delivery system and editing approach showed no detectable editing at the USH1C locus of PKC. Similarly, my collaborators consistently tested the approaches in HEK293 cells to test USH1C targeting prior to my testing in PKC. The GE efficiencies I detected were always significantly lower than in HEK293 cells. The differential editing efficiency we observed between loci and cell types cannot be attributed solely to delivery challenges, as we confirmed successful vector transduction in cases where no editing occurred (Fig. 11).

Differences in GE between cell types was also reported *in vivo* by (MULLER et al., 2025), who demonstrated dramatic differences in editing rates between RPE and PRCs using similar approaches and targeting comparable genomic loci.

A critical consideration often overlooked in translational research is the distinctive nuclear morphology of PRCs, which varies significantly between species. As described by (SOLOVEI et al., 2009; FEODOROVA et al., 2020), in nocturnal mammals, rod photoreceptors exhibit an inverted arrangement of chromatin compared to most eukaryotic cells - an adaptation that reduces light scattering. This fundamental difference may contribute to the variable efficiency observed between nocturnal and diurnal species, potentially explaining why promising results in nocturnal rodent models often fail to translate to larger diurnal animal models like pigs and humans especially in the context of GE therapy.

These observations also make me consider other GE components and strategies. While CRISPR-Cas9 offers significant advantages, especially due to its high flexibility and shows great efficiency in dividing cells, I am now wondering if the

mechanism of other systems, such as TALENs or ZFN may be more efficient at targeting tightly compacted chromatin (LI et al., 2023; GARCIA et al., 2025)

4. Intermediate Test Systems to Model Clinical Application

Developing appropriate intermediate test systems is essential for bridging the gap between simplified *in vitro* experiments and complex *in vivo* studies. My work explored multiple approaches to create more relevant experimental platforms while maintaining practical feasibility.

4.1. Cell Cycle Shift in Proliferative PKC

One fundamental challenge in developing relevant test systems for retinal GE lies in mimicking the postmitotic state of PRC. Given the difficulties associated with culturing and manipulating primary retinal cells, I worked on an efficient approach for testing GE using my established USH1C PKC system.

By inducing a cell cycle arrest through various methods, I aimed to create a more relevant screening platform for evaluating GE strategies intended for retinal application. This approach offered several key advantages: it utilized cells derived directly from the USH1C pig model and allowed for controlled manipulation of cell cycle status while preserving the established experimental pipeline for preliminary GE optimization.

This model allowed me to prove the impact of cell cycle manipulation on GE efficiency. Even though the cycle shift assessed by flow cytometry was minimal after 24h of cell cycle arrest, the effect on HDR/NHEJ ratio was concurrent to the literature (Fig. 26-29). Indeed, it proved the inefficiency of HDR in cells predominantly in the phase G1 of the cell cycle (CICCIA and ELLEDGE, 2010; HUSTEDT and DUROCHER, 2016; LEAL et al., 2024) and the lower impact of the cell cycle of TwinPE efficiency – that doesn't rely on HDR and NHEJ repair mechanisms.

The observed decline in transfection efficiency and overall editing efficiency across experimental conditions represents an intriguing finding (Fig. 29). The diminished GFP signal may not necessarily indicate reduced overall electroporation efficiency of the plasmid itself. Rather, this phenomenon could reflect decreased nuclear

import efficiency in non-dividing cells where the nuclear membrane remains intact throughout the cell cycle, thus preventing the transcription of GFP and GE plasmids (DEAN et al., 2005). Further exploration of this test system could give some additional insights on metabolic aspects of non dividing cells.

A significant advantage of this approach is that it enables numerous experiments without requiring additional animals, aligning with the 3R principles discussed earlier. This ethical consideration, combined with the practical benefits of working with an established cell line, made this approach an attractive first step.

4.2. RE Culture as a Superior Intermediate System

REs offer significant advantages over cell-based systems by maintaining the complex three-dimensional tissue architecture and cellular diversity of the native retina. It consists of collecting the retina of animals, dissecting it in pieces of approximately 5x4mm, that can then be placed on cell culture inserts and cultured for several weeks using a neural cells optimized medium (WELLER et al., 2024). It allows the testing of different GE approaches in a separate and controlled manner, especially convenient for dosage assessment.

(DI LAURO et al., 2016) demonstrated improved retinal tissue preservation through co-culture with RPE cells, better maintaining the tissue's natural cellular interactions. Another group has explored the benefits of light exposure on explant survival, suggesting that maintaining physiological light cycles can enhance tissue viability and function (CHUCHUY et al., 2019).

While these optimization approaches are interesting to understand cell to cell interactions and the influence of environmental factors on the viability of the explants, my focus with the use of REs was to answer the following questions: Can the vectors effectively transduce the tissue, and does GE work in the target cells. Acknowledging that explant cultures cannot recapitulate all aspects of the *in vivo* environment, particularly immune responses and long-term effects, I determined that a simpler explant system was sufficient for addressing these fundamental questions. This decision allowed me to balance physiological relevance with experimental throughput and reproducibility.

Following evaluation of the pilot *in vivo* study, it became evident that immunofluorescence (IF) techniques alone proved insufficient for accurate quantitative assessment of transfection efficiency within the highly structured architecture of the retinal tissue (Fig. 22-23). The complex cellular stratification and dense organizational characteristics of the retina necessitate complementary analytical methodologies to achieve precise quantification of transgene expression and cellular targeting specificity.

To build upon these initial observations and develop a more comprehensive analytical approach, I established a standardized protocol for dissociating porcine REs into single-cell suspensions based on the methodology published by (MULLER et al., 2025). The protocol incorporated a carefully optimized enzymatic digestion process using papain, which preserved cell viability while effectively separating the tightly interconnected retinal cells. This technique enabled comprehensive flow cytometric analysis of transduction efficiency at the single-cell level (Fig. 35-36).

The flow cytometry data allowed us to determine the successful transduction of 40,7% of cells, it also revealed an intriguing finding: approximately 1% of GFP-positive cells exhibited fluorescence intensity significantly higher than the remainder of the transduced population (Fig. 36). This subset of highly fluorescent cells represents a critical area for further investigation. The marked difference in GFP expression could indicate either preferential transduction of specific retinal cell types, differential promoter activity across various cell populations, or potential variations in vector processing within certain cells. Determining the identity of these intensely fluorescent cells could provide valuable insights into cellular tropism and vector behaviour in the complex retinal environment.

Building on these observations, a logical advancement of this methodology would be the implementation of cell-specific marker staining in conjunction with flow cytometry. This approach would allow precise identification of which retinal cell types are successfully transduced and at what efficiency. By integrating antibodies against markers into the flow cytometry protocol, we could develop a comprehensive map of vector tropism across the diverse retinal cell populations.

Furthermore, fluorescence-activated cell sorting (FACS) of transduced versus non-transduced cells of each type would enable detailed investigation of how vector uptake differs between cell populations and correlates with GE efficiency—a question of paramount importance for therapeutic development. This refined approach would allow us to distinguish whether observed variations in editing outcomes stem primarily from delivery limitations or from intrinsic cellular barriers to the editing process itself, thereby providing critical guidance for optimizing both vector design and editing strategies.

The 3D-quantification technique also holds promise for subsequent experiments as a complementary and in-depth analysis strategy (ROGLER et al., 2024).

The methodological advances established through this RE system provide a versatile platform for rapid, high-throughput screening of therapeutic approaches before progressing to more complex and resource-intensive *in vivo* studies.

5. Perspectives and Future Directions

Building on the findings presented in this thesis, my future research will focus on several complementary approaches to advance GE therapy for IRD:

1. RE Characterization and Optimization for publication:

- Conduct comprehensive characterization of RE properties and transduction efficiency of various delivery vectors
- Implement RNA sequencing analyses and long-term IF assessment to further validate the RE system
- Develop refined cell dissociation protocols and FACS methodologies for precise assessment of cell type-specific transfection and editing efficiencies

2. PRC-Targeted Vector Development:

- Leverage findings on differential transduction patterns to engineer delivery vectors with enhanced PRC tropism
- Evaluate newly developed tropism-enhanced vectors in the validated RE system before progressing to *in vivo* studies

 Collaborate with vector design specialists to systematically improve cellular access

3. GE Optimization for Retinal Application:

- Test improved GE systems in the RE platform to address identified barriers of nuclear entry and DNA accessibility
- Optimize vector-GE combinations for maximal efficiency in postmitotic retinal cells

4. Translation to Preclinical in vivo Studies:

- Transfer optimized vector-GE combinations to preclinical porcine models
- Address technical aspects of GT application including vector preparation quality suitable for clinical standards
- Refine delivery routes and optimize dosing strategies based on RE findings
- Develop improved functional assessment methodologies, including refinements to anaesthesia-dependent measurements (ERG) and alternative approaches
- Conduct parallel investigations into gene supplementation approaches for inner ear, enabling comparative analysis between different sensory tissues
- Identify common principles and tissue-specific considerations for therapeutic design in sensory systems

V. Summary 103

VI. SUMMARY

Inherited retinal diseases (IRDs) affect approximately 1 in 2000 individuals worldwide, causing progressive loss of vision with limited treatment options. While gene supplementation approaches have shown promise, they face significant limitations including packaging constraints and inability to address certain mutation types. Gene editing (GE) technologies offer a revolutionary alternative by enabling precise modification of the genome itself, potentially providing more comprehensive and durable solutions for patients. This thesis investigates innovative GE strategies for treating IRDs, using Usher Syndrome Type 1C (USH1C) as a model disease with a specific focus on correcting the c.91C>T mutation in the USH1C gene. The work progresses systematically from *in vitro* testing to preclinical studies in a porcine model.

In vitro development of GE strategies in porcine kidney cells (PKC) from USH1C pigs revealed that Twin Prime Editing (TwinPE) achieved the highest efficiency (25-32%) compared to other approaches such as Double Strand Break-Homology Directed Repair (16.3% HDR, 41.4% NHEJ) and Adenine Base Editing (14.5% but with bystander mutations).

Novel delivery methods were evaluated, including Virus-Like Particles (VLPs) and Delivery Vector X (DVX). While VLPs showed excellent transfection capabilities for reporter genes (>99%), they demonstrated limited efficiency (6%) for USH1C gene editing. DVX achieved up to 80% gene modification in PKC but is not yet capable of efficiently deliver and allow editing using the TwinPE approach.

The management of the USH1C pig model was refined through improved postnatal management protocols. Extensive phenotypic assessments conducted with international collaborators confirmed the USH1C phenotype through electroretinography (ERG) and auditory tests, with ERG revealing increased light sensitivity in USH1C pigs.

Preclinical assessment of GE therapy involved subretinal injection of TwinPE via adenovirus (AdV5) into USH1C pig eyes. Analysis demonstrated successful transduction of retinal cells (RPE, PRC, GCL) but limited editing efficiency (0.2%) in RPE. Retinal atrophy was observed at injection sites, indicating the need for improved delivery methods and dosage optimization.

V. Summary 104

Alternative test systems were developed to bridge the gap between *in vitro* and *in vivo* studies. Cell cycle manipulation in PKC attempted to mimic post-mitotic conditions through various methods. Retina explants were established as a promising intermediate platform that maintains retinal structure while allowing controlled experimentation.

This research advances GE approaches for inherited retinal diseases and establishes important methodological frameworks for translation to clinical applications. Future work will focus on optimizing retinal explant systems, developing photoreceptor-targeted delivery vectors, enhancing GE efficiency in post-mitotic cells, and refining preclinical studies with improved delivery methods and functional assessment

VII. ZUSAMMENFASSUNG

Weiterentwicklung therapeutischer Genbearbeitungsstrategien für vererbte Netzhauterkrankungen: Von der *in-vitro-*Entwicklung zur präklinischen Bewertung in einem USH1C-Schweinemodell

Erbliche Netzhauterkrankungen (Inherited Retinal Diseases, IRDs) betreffen etwa 1 von 2000 Menschen weltweit und führen zu fortschreitendem Sehverlust mit begrenzten Behandlungsmöglichkeiten. Während Genergänzungsansätze vielversprechende Ergebnisse gezeigt haben, stoßen sie auf erhebliche Einschränkungen, darunter Verpackungsbeschränkungen und die Unfähigkeit, bestimmte Mutationstypen zu behandeln. Genome Editing (GE)-Technologien bieten eine revolutionäre Alternative, indem sie eine präzise Modifikation des Genoms selbst ermöglichen und potenziell umfassendere und nachhaltigere Lösungen für Patienten bieten. Diese Dissertation untersucht innovative GE-Strategien zur Behandlung von IRDs und verwendet das Usher-Syndrom Typ 1C (USH1C) als Modellerkrankung mit speziellem Fokus auf die Korrektur der c.91C>T-Mutation im USH1C-Gen. Die Arbeit schreitet systematisch von In-vitro-Tests zu präklinischen Studien in einem Schweinemodell voran.

Die In-vitro-Entwicklung von GE-Strategien in Schweinenierenzellen (PKC) von USH1C-Schweinen zeigte, dass Twin Prime Editing (TwinPE) die höchste Effizienz (25-32%) im Vergleich zu anderen Ansätzen wie Double Strand Break-Homology Directed Repair (16,3% HDR, 41,4% NHEJ) und Adenine Base Editing (14,5%, aber mit unbeabsichtigten Begleitmutationen) erreichte.

Neuartige Übertragungsmethoden wurden evaluiert, darunter Virus-Like Particles (VLPs) und Delivery Vector X (DVX). Während VLPs hervorragende Transfektionsfähigkeiten für Reportergene (>99%) zeigten, wiesen sie eine begrenzte Effizienz (6%) für USH1C-Genbearbeitung auf. DVX erreichte bis zu 80% Genmodifikation in PKC, ist jedoch noch nicht in der Lage, den TwinPE-Ansatz effizient zu übertragen und die Bearbeitung zu ermöglichen.

Die Betreuung des USH1C-Schweinemodells wurde durch verbesserte postnatale Managementprotokolle verfeinert. Umfangreiche phänotypische Beurteilungen, die in Zusammenarbeit mit internationalen Kollaborateuren durchgeführt wurden,

VII. Zusammenfassung 106

bestätigten den USH1C-Phänotyp durch Elektroretinographie (ERG) und Hörtests, wobei ERG eine erhöhte Lichtempfindlichkeit bei USH1C-Schweinen zeigte.

Die präklinische Bewertung der GE-Therapie umfasste die subretinale Injektion von TwinPE mittels Adenovirus (AdV5) in USH1C-Schweineaugen. Die Analyse zeigte eine erfolgreiche Transduktion von Netzhautzellen (RPE, PRC, GCL), aber eine begrenzte Bearbeitungseffizienz (0,2%) im RPE. An den Injektionsstellen wurde eine Netzhautatrophie beobachtet, was auf die Notwendigkeit verbesserter Übertragungsmethoden und Dosisoptimierung hinweist.

Alternative Testsysteme wurden entwickelt, um die Lücke zwischen *in-vitro-* und *in-vivo-*Studien zu überbrücken. Die Zellzyklusmanipulation in PKC versuchte, postmitotische Bedingungen durch verschiedene Methoden nachzuahmen. Netzhautexplantate wurden als vielversprechende Zwischenplattform etabliert, die die Netzhautstruktur erhält und gleichzeitig kontrollierte Experimente ermöglicht.

Diese Forschung fördert GE-Ansätze für erbliche Netzhauterkrankungen und etabliert wichtige methodische Rahmenbedingungen für die Translation in klinische Anwendungen. Zukünftige Arbeiten werden sich auf die Optimierung von Netzhautexplantatsystemen, die Entwicklung von Photorezeptor-gezielten Übertragungsvektoren, die Verbesserung der GE-Effizienz in postmitotischen Zellen und die Verfeinerung präklinischer Studien mit verbesserten Übertragungsmethoden und funktionellen Bewertungen konzentrieren.

VIII. REFERENCES

Afanasyeva TAV, Corral-Serrano JC, Garanto A, Roepman R, Cheetham ME, Collin RWJ. A look into retinal organoids: methods, analytical techniques, and applications. Cell Mol Life Sci 2021; 78: 6505-32.

Ahmed Z. Preparation of Retinal Explant Cultures. Methods Mol Biol 2023; 2708: 25-31.

Aigner B, Renner S, Kessler B, Klymiuk N, Kurome M, Wünsch A, Wolf E. Transgenic pigs as models for translational biomedical research. J Mol Med (Berl) 2010; 88: 653-64.

Alarautalahti V, Ragauskas S, Hakkarainen JJ, Uusitalo-Järvinen H, Uusitalo H, Hyttinen J, Kalesnykas G, Nymark S. Viability of Mouse Retinal Explant Cultures Assessed by Preservation of Functionality and Morphology. Invest Ophthalmol Vis Sci 2019; 60: 1914-27.

Alipanahi R, Safari L, Khanteymoori A. CRISPR genome editing using computational approaches: A survey. Frontiers in Bioinformatics 2023;

Alsalloum A, Gornostal E, Mingaleva N, Pavlov R, Kuznetsova E, Antonova E, Nadzhafova A, Kolotova D, Kadyshev V, Mityaeva O, Volchkov P. A Comparative Analysis of Models for AAV-Mediated Gene Therapy for Inherited Retinal Diseases. Cells 2024; 13

Ameri H, Kesavamoorthy N, Bruce DN. Frequency and Pattern of Worldwide Ocular Gene Therapy Clinical Trials up to 2022. Biomedicines 2023; 11

Anzalone AV, Randolph PB, Davis JR, Sousa AA, Koblan LW, Levy JM, Chen PJ, Wilson C, Newby GA, Raguram A, Liu DR. Search-and-replace genome editing without double-strand breaks or donor DNA. Nature 2019; 576: 149-57.

Anzalone AV, Koblan LW, Liu DR. Genome editing with CRISPR-Cas nucleases,

base editors, transposases and prime editors. Nat Biotechnol 2020; 38: 824-44.

Anzalone AV, Gao XD, Podracky CJ, Nelson AT, Koblan LW, Raguram A, Levy JM, Mercer JAM, Liu DR. Programmable deletion, replacement, integration and inversion of large DNA sequences with twin prime editing. Nat Biotechnol 2022; 40: 731-40.

Arbabi A, Liu A, Ameri H. Gene Therapy for Inherited Retinal Degeneration. J Ocul Pharmacol Ther 2019; 35: 79-97.

Athanasiou D, Aguila M, Bellingham J, Li W, McCulley C, Reeves PJ, Cheetham ME. The molecular and cellular basis of rhodopsin retinitis pigmentosa reveals potential strategies for therapy. Prog Retin Eye Res 2018; 62: 1-23.

Auch H. Gene Editing in pig models of inherited retinal diseases. Diss. med. vet. 2023.

Baden T, Euler T, Berens P. Understanding the retinal basis of vision across species. Nat Rev Neurosci 2020; 21: 5-20.

Bairqdar A, Karitskaya PE, Stepanov GA. Expanding Horizons of CRISPR/Cas Technology: Clinical Advancements, Therapeutic Applications, and Challenges in Gene Therapy. Int. J. Mol. Sci. 2024;

Banou L, Sarrafpour S, Teng CC, Liu J. Ocular Gene Therapy: An Overview of Viral Vectors, Immune Responses, and Future Directions. Yale J Biol Med 2024; 97: 491-503.

Banskota S, Raguram A, Suh S, Du SW, Davis JR, Choi EH, Wang X, Nielsen SC, Newby GA, Randolph PB, Osborn MJ, Musunuru K, Palczewski K, Liu DR. Engineered virus-like particles for efficient in vivo delivery of therapeutic proteins. Cell 2022; 185: 250-65.e16.

Barone F, Bunea I, Creel K, Sharma R, Amaral J, Maminishkis A, Bharti K. An Automated Visual Psychophysics Method to Measure Visual Function in Swine Preclinical Animal Model. Transl Vis Sci Technol 2024; 13: 8.

Bassols A, Costa C, Eckersall PD, Osada J, Sabrià J, Tibau J. The pig as an animal model for human pathologies: A proteomics perspective. Proteomics Clin Appl 2014; 8: 715-31.

Bazan NG, Gordon WC, Rodriguez de Turco EB. Docosahexaenoic acid uptake and metabolism in photoreceptors: retinal conservation by an efficient retinal pigment epithelial cell-mediated recycling process. Adv Exp Med Biol 1992; 318: 295-306.

Belhadj S, Tolone A, Christensen G, Das S, Chen Y, Paquet-Durand F. Long-Term, Serum-Free Cultivation of Organotypic Mouse Retina Explants with Intact Retinal Pigment Epithelium. J Vis Exp 2020;

Beltran WA, Boye SL, Boye SE, Chiodo VA, Lewin AS, Hauswirth WW, Aguirre GD. rAAV2/5 gene-targeting to rods:dose-dependent efficiency and complications associated with different promoters. Gene Ther 2010; 17: 1162-74.

Binns A, Margrain TH. Evaluation of retinal function using the Dynamic Focal Cone ERG. Ophthalmic Physiol Opt 2005; 25: 492-500.

Blaese RM, Culver KW, Miller AD, Carter CS, Fleisher T, Clerici M, Shearer G, Chang L, Chiang Y, Tolstoshev P, Greenblatt JJ, Rosenberg SA, Klein H, Berger M, Mullen CA, Ramsey WJ, Muul L, Morgan RA, Anderson WF. T lymphocyte-directed gene therapy for ADA- SCID: initial trial results after 4 years. Science 1995; 270: 475-80.

Blokhina IA, Koronovskii AA, Jr., Dmitrenko AV, Elizarova IV, Moiseikina TV, Tuzhilkin MA, Semyachkina-Glushkovskaya OV, Pavlov AN. Characterization of Anesthesia in Rats from EEG in Terms of Long-Range Correlations. Diagnostics (Basel) 2023; 13

Bucher K, Rodríguez-Bocanegra E, Dauletbekov D, Fischer MD. Immune responses to retinal gene therapy using adeno-associated viral vectors - Implications for treatment success and safety. Prog Retin Eye Res 2021; 83: 100915.

Bunel M, Chaudieu G, Hamel C, Lagoutte L, Manes G, Botherel N, Brabet P, Pilorge P, André C, Quignon P. Natural models for retinitis pigmentosa: progressive retinal atrophy in dog breeds. Hum Genet 2019; 138: 441-53.

Burnight ER, Wiley LA, Mullin NK, Adur MK, Lang MJ, Cranston CM, Jiao C, Russell SR, Sohn EH, Han IC, Ross JW, Stone EM, Mullins RF, Tucker BA. CRISPRi-Mediated Treatment of Dominant Rhodopsin-Associated Retinitis Pigmentosa. Crispr j 2023; 6: 502-13.

Byosiere SE, Chouinard PA, Howell TJ, Bennett PC. What do dogs (Canis familiaris) see? A review of vision in dogs and implications for cognition research. Psychon Bull Rev 2018; 25: 1798-813.

Caffé AR, Ahuja P, Holmqvist B, Azadi S, Forsell J, Holmqvist I, Söderpalm AK, van Veen T. Mouse retina explants after long-term culture in serum free medium. J Chem Neuroanat 2001; 22: 263-73.

Campbell BC, Nabel EM, Murdock MH, Lao-Peregrin C, Tsoulfas P, Blackmore MG, Lee FS, Liston C, Morishita H, Petsko GA. mGreenLantern: a bright monomeric fluorescent protein with rapid expression and cell filling properties for neuronal imaging. Proc Natl Acad Sci U S A 2020; 117: 30710-21.

Campbell JP, McFarland TJ, Stout JT. Ocular Gene Therapy. Dev Ophthalmol 2016; 55: 317-21.

Carvalho C, Lemos L, Antas P, Seabra MC. Gene therapy for inherited retinal diseases: exploiting new tools in genome editing and nanotechnology. Frontiers in Ophthalmology 2023; 3

Carvalho LS, Turunen HT, Wassmer SJ, Luna-Velez MV, Xiao R, Bennett J, Vandenberghe LH. Evaluating Efficiencies of Dual AAV Approaches for Retinal Targeting. Front Neurosci 2017; 11: 503.

Cashman SM, McCullough L, Kumar-Singh R. Improved retinal transduction in vivo and photoreceptor-specific transgene expression using adenovirus vectors with modified penton base. Mol Ther 2007; 15: 1640-6.

Castiglione A, Möller C. Usher Syndrome. Audiology Research 2022; 12: 42-65.

Chader GJ. Animal models in research on retinal degenerations: past progress and future hope. Vision Res 2002; 42: 393-9.

Chen L, Zhang S, Xue N, Hong M, Zhang X, Zhang D, Yang J, Bai S, Huang Y, Meng H, Wu H, Luan C, Zhu B, Ru G, Gao H, Zhong L, Liu M, Liu M, Cheng Y, Yi C, Wang L, Zhao Y, Song G, Li D. Engineering a precise adenine base editor with minimal bystander editing. Nat Chem Biol 2023; 19: 101-10.

Chen PJ, Hussmann JA, Yan J, Knipping F, Ravisankar P, Chen PF, Chen C, Nelson JW, Newby GA, Sahin M, Osborn MJ, Weissman JS, Adamson B, Liu DR. Enhanced prime editing systems by manipulating cellular determinants of editing outcomes. Cell 2021; 184: 5635-52.e29.

Cheng SY, Caiazzi J, Biscans A, Alterman JF, Echeverria D, McHugh N, Hassler M, Jolly S, Giguere D, Cipi J, Khvorova A, Punzo C. Single intravitreal administration of a tetravalent siRNA exhibits robust and efficient gene silencing in mouse and pig photoreceptors. Mol Ther Nucleic Acids 2024; 35: 102088.

Chhetri J, Jacobson G, Gueven N. Zebrafish--on the move towards ophthalmological research. Eye (Lond) 2014; 28: 367-80.

Chichagova V, Georgiou M, Carter M, Dorgau B, Hilgen G, Collin J, Queen R, Chung G, Ajeian J, Moya-Molina M, Kustermann S, Pognan F, Hewitt P, Schmitt

M, Sernagor E, Armstrong L, Lako M. Incorporating microglia-like cells in human induced pluripotent stem cell-derived retinal organoids. J Cell Mol Med 2023; 27: 435-45.

Chiu W, Lin T-Y, Chang Y-C, Lai HIM, Lin S-C, Ma C, Yarmishyn AA, Lin S-C, Chang K-J, Chou Y-B, Hsu C-C, Lin T-C, Chen S-J, Chien Y, Yang Y-P, Hwang D-K. An Update on Gene Therapy for Inherited Retinal Dystrophy: Experience in Leber Congenital Amaurosis Clinical Trials. Int. J. Mol. Sci. 2021;

Choi EH, Suh S, Sears AE, Hołubowicz R, Kedhar SR, Browne AW, Palczewski K. Genome editing in the treatment of ocular diseases. Exp Mol Med 2023; 55: 1678-90.

Chuchuy J, Achberger K, Probst C, Haderspeck J, Antkowiak L, Liebau S, Loskill P. Controlled illumination of a PDMS-free Retina-on-a-Chip for the proximity-culture of retinal organoids with pigment epithelial cells. Investigative Ophthalmology & Visual Science 2019; 60: 35-.

Ciccia A, Elledge SJ. The DNA damage response: making it safe to play with knives. Mol Cell 2010; 40: 179-204.

Clevers H. Modeling Development and Disease with Organoids. Cell 2016; 165: 1586-97.

Collin GB, Gogna N, Chang B, Damkham N, Pinkney J, Hyde LF, Stone L, Naggert JK, Nishina PM, Krebs MP. Mouse Models of Inherited Retinal Degeneration with Photoreceptor Cell Loss. Cells 2020; 9

Colombo L, Baldesi J, Martella S, Quisisana C, Antico A, Mapelli L, Montagner S, Primon A, Rossetti L. Managing Retinitis Pigmentosa: A Literature Review of Current Non-Surgical Approaches. Journal of Clinical Medicine 2025; 14: 330.

Cukras C, Wiley HE, Jeffrey BG, Sen HN, Turriff A, Zeng Y, Vijayasarathy C,

Marangoni D, Ziccardi L, Kjellstrom S, Park TK, Hiriyanna S, Wright JF, Colosi P, Wu Z, Bush RA, Wei LL, Sieving PA. Retinal AAV8-RS1 Gene Therapy for X-Linked Retinoschisis: Initial Findings from a Phase I/IIa Trial by Intravitreal Delivery. Mol Ther 2018; 26: 2282-94.

Cullis PR, Felgner PL. The 60-year evolution of lipid nanoparticles for nucleic acid delivery. Nat Rev Drug Discov 2024; 23: 709-22.

D'Amanda CS, Nolen R, Huryn LA, Turriff A. Psychosocial impacts of Mendelian eye conditions: A systematic literature review. Surv Ophthalmol 2020; 65: 562-80.

Daer RM, Cutts JP, Brafman DA, Haynes KA. The Impact of Chromatin Dynamics on Cas9-Mediated Genome Editing in Human Cells. ACS Synth Biol 2017; 6: 428-38.

Dawson LM, Alshawabkeh M, Schröer K, Arakrak F, Ehrhardt A, Zhang W. Role of homologous recombination/recombineering on human adenovirus genome engineering: Not the only but the most competent solution. Eng Microbiol 2024; 4: 100140.

Dean DA, Strong DD, Zimmer WE. Nuclear entry of nonviral vectors. Gene Ther 2005; 12: 881-90.

Di Lauro S, Rodriguez-Crespo D, Gayoso MJ, Garcia-Gutierrez MT, Pastor JC, Srivastava GK, Fernandez-Bueno I. A novel coculture model of porcine central neuroretina explants and retinal pigment epithelium cells. Mol Vis 2016; 22: 243-53.

DiCarlo JE, Mahajan VB, Tsang SH. Gene therapy and genome surgery in the retina. J Clin Invest 2018; 128: 2177-88.

Doench JG, Fusi N, Sullender M, Hegde M, Vaimberg EW, Donovan KF, Smith I, Tothova Z, Wilen C, Orchard R, Virgin HW, Listgarten J, Root DE. Optimized

sgRNA design to maximize activity and minimize off-target effects of CRISPR-Cas9. Nat Biotechnol 2016; 34: 184-91.

Drag S, Dotiwala F, Upadhyay AK. Gene Therapy for Retinal Degenerative Diseases: Progress, Challenges, and Future Directions. Invest Ophthalmol Vis Sci 2023; 64: 39.

Ducloyer JB, Pichard V, Mevel M, Galy A, Lefevre GM, Brument N, Alvarez-Dorta D, Deniaud D, Mendes-Madeira A, Libeau L, Le Guiner C, Cronin T, Adjali O, Weber M, Le Meur G. Intravitreal air tamponade after AAV2 subretinal injection modifies retinal EGFP distribution. Mol Ther Methods Clin Dev 2023; 28: 387-93.

Egerer S, Fiebig U, Kessler B, Zakhartchenko V, Kurome M, Reichart B, Kupatt C, Klymiuk N, Wolf E, Denner J, Bähr A. Early weaning completely eliminates porcine cytomegalovirus from a newly established pig donor facility for xenotransplantation. Xenotransplantation 2018; 25: e12449.

Ehrke-Schulz E, Schiwon M, Leitner T, Dávid S, Bergmann T, Liu J, Ehrhardt A. CRISPR/Cas9 delivery with one single adenoviral vector devoid of all viral genes. Sci Rep 2017; 7: 17113.

Eldred KC, Reh TA. Human retinal model systems: Strengths, weaknesses, and future directions. Dev Biol 2021; 480: 114-22.

Feldman D, Singh A, Schmid-Burgk JL, Carlson RJ, Mezger A, Garrity AJ, Zhang F, Blainey PC. Optical Pooled Screens in Human Cells. Cell 2019; 179: 787-99.e17.

Feo A, Ramtohul P, Govetto A, Borrelli E, Sacconi R, Corradetti G, Querques G, Romano MR, Rosenfeld PJ, Spaide RF, Freund KB, Sadda S, Sarraf D. En face OCT: Breakthroughs in understanding the pathoanatomy of retinal disease and clinical applications. Prog Retin Eye Res 2025; 106: 101351.

Feodorova Y, Falk M, Mirny LA, Solovei I. Viewing Nuclear Architecture through

the Eyes of Nocturnal Mammals. Trends Cell Biol 2020; 30: 276-89.

Ferreira MV, Fernandes S, Almeida AI, Neto S, Mendes JP, Silva RJS, Peixoto C, Coroadinha AS. Extending AAV Packaging Cargo through Dual Co-Transduction: Efficient Protein Trans-Splicing at Low Vector Doses. Int J Mol Sci 2023; 24

Fischer MD, Simonelli F, Sahni J, Holz FG, Maier R, Fasser C, Suhner A, Stiehl DP, Chen B, Audo I, Leroy BP. Real-World Safety and Effectiveness of Voretigene Neparvovec: Results up to 2 Years from the Prospective, Registry-Based PERCEIVE Study. Biomolecules 2024; 14

Ford JL, Karatza E, Mody H, Nagaraja Shastri P, Khajeh Pour S, Yang TY, Swanson M, Chao D, Devineni D. Clinical Pharmacology Perspective on Development of Adeno-Associated Virus Vector-Based Retina Gene Therapy. Clin Pharmacol Ther 2024; 115: 1212-32.

Friedmann T, Roblin R. Gene therapy for human genetic disease? Science (New York, N.Y.) 1972; 175: 949-55.

Gao ML, Wang TY, Lin X, Tang C, Li M, Bai ZP, Liu ZC, Chen LJ, Kong QR, Pan SH, Zeng SS, Guo Y, Cai JQ, Huang XF, Zhang J. Retinal Organoid Microenvironment Enhanced Bioactivities of Microglia-Like Cells Derived From HiPSCs. Invest Ophthalmol Vis Sci 2024; 65: 19.

Garafalo AV, Cideciyan AV, Héon E, Sheplock R, Pearson A, WeiYang Yu C, Sumaroka A, Aguirre GD, Jacobson SG. Progress in treating inherited retinal diseases: Early subretinal gene therapy clinical trials and candidates for future initiatives. Prog Retin Eye Res 2020; 77: 100827.

Garcia DA, Pierre AF, Quirino L, Acharya G, Vasudevan A, Pei Y, Chung E, Chang JYH, Lee S, Endow M, Kuakini K, Bresnahan M, Chumpitaz M, Rajappan K, Parker S, Chivukula P, Boehme SA, Diaz-Trelles R. Lipid nanoparticle delivery of TALEN mRNA targeting LPA causes gene disruption and plasma lipoprotein(a) reduction in transgenic mice. Mol Ther 2025; 33: 90-103.

Gaudelli NM, Komor AC, Rees HA, Packer MS, Badran AH, Bryson DI, Liu DR. Programmable base editing of A•T to G•C in genomic DNA without DNA cleavage. Nature 2017; 551: 464-71.

Gehrke JM, Cervantes O, Clement MK, Wu Y, Zeng J, Bauer DE, Pinello L, Joung JK. An APOBEC3A-Cas9 base editor with minimized bystander and off-target activities. Nat Biotechnol 2018; 36: 977-82.

Gieling ET, Nordquist RE, van der Staay FJ. Assessing learning and memory in pigs. Anim Cogn 2011; 14: 151-73.

Gonçalves R, McBrearty A, Pratola L, Calvo G, Anderson TJ, Penderis J. Clinical evaluation of cochlear hearing status in dogs using evoked otoacoustic emissions. J Small Anim Pract 2012; 53: 344-51.

Greber UF, Suomalainen M. Adenovirus entry: Stability, uncoating, and nuclear import. Mol Microbiol 2022; 118: 309-20.

Grotz S. Characterization of a pig model of Usher syndrome. Diss. med. vet. 2021.

Grotz S, Schäfer J, Wunderlich KA, Ellederova Z, Auch H, Bähr A, Runa-Vochozkova P, Fadl J, Arnold V, Ardan T, Veith M, Santamaria G, Dhom G, Hitzl W, Kessler B, Eckardt C, Klein J, Brymova A, Linnert J, Kurome M, Zakharchenko V, Fischer A, Blutke A, Döring A, Suchankova S, Popelar J, Rodríguez-Bocanegra E, Dlugaiczyk J, Straka H, May-Simera H, Wang W, Laugwitz KL, Vandenberghe LH, Wolf E, Nagel-Wolfrum K, Peters T, Motlik J, Fischer MD, Wolfrum U, Klymiuk N. Early disruption of photoreceptor cell architecture and loss of vision in a humanized pig model of usher syndromes. EMBO Mol Med 2022; 14: e14817.

Hald Albertsen C, Kulkarni JA, Witzigmann D, Lind M, Petersson K, Simonsen JB. The role of lipid components in lipid nanoparticles for vaccines and gene therapy. Adv Drug Deliv Rev 2022; 188: 114416.

Han IC, Burnight ER, Ulferts MJ, Worthington KS, Russell SR, Sohn EH, Mullins RF, Stone EM, Tucker BA, Wiley LA. Helper-Dependent Adenovirus Transduces the Human and Rat Retina but Elicits an Inflammatory Reaction When Delivered Subretinally in Rats. Hum Gene Ther 2019; 30: 1371-84.

Han IC, Burnight ER, Kaalberg EE, Boyce TM, Stone EM, Fingert JH, Mullins RF, Tucker BA, Wiley LA. Chimeric Helper-Dependent Adenoviruses Transduce Retinal Ganglion Cells and Müller Cells in Human Retinal Explants. J Ocul Pharmacol Ther 2021; 37: 575-9.

Hanany M, Rivolta C, Sharon D. Worldwide carrier frequency and genetic prevalence of autosomal recessive inherited retinal diseases. Proc Natl Acad Sci U S A 2020; 117: 2710-6.

Hayes O, Ramos B, Rodríguez LL, Aguilar A, Badía T, Castro FO. Cell confluency is as efficient as serum starvation for inducing arrest in the G0/G1 phase of the cell cycle in granulosa and fibroblast cells of cattle. Anim Reprod Sci 2005; 87: 181-92.

Hille F, Richter H, Wong SP, Bratovič M, Ressel S, Charpentier E. The Biology of CRISPR-Cas: Backward and Forward. Cell 2018; 172: 1239-59.

Hochstrasser ML, Doudna JA. Cutting it close: CRISPR-associated endoribonuclease structure and function. Trends Biochem Sci 2015; 40: 58-66.

Hoffe B, Holahan MR. The Use of Pigs as a Translational Model for Studying Neurodegenerative Diseases. Front Physiol 2019; 10: 838.

Holm IE, Alstrup AK, Luo Y. Genetically modified pig models for neurodegenerative disorders. J Pathol 2016; 238: 267-87.

Hoon M, Okawa H, Della Santina L, Wong RO. Functional architecture of the retina: development and disease. Prog Retin Eye Res 2014; 42: 44-84.

Hou N, Du X, Wu S. Advances in pig models of human diseases. Animal Model Exp Med 2022; 5: 141-52.

Hu ML, Edwards TL, O'Hare F, Hickey DG, Wang JH, Liu Z, Ayton LN. Gene therapy for inherited retinal diseases: progress and possibilities. Clin Exp Optom 2021; 104: 444-54.

Huang H, Saddala MS, Mukwaya A, Mohan RR, Lennikov A. Association of Placental Growth Factor and Angiopoietin in Human Retinal Endothelial Cell-Pericyte co-Cultures and iPSC-Derived Vascular Organoids. Curr Eye Res 2023; 48: 297-311.

Hulliger EC, Hostettler SM, Kleinlogel S. Empowering Retinal Gene Therapy with a Specific Promoter for Human Rod and Cone ON-Bipolar Cells. Mol Ther Methods Clin Dev 2020; 17: 505-19.

Hustedt N, Durocher D. The control of DNA repair by the cell cycle. Nat Cell Biol 2016; 19: 1-9.

Igarashi T, Miyake K, Asakawa N, Miyake N, Shimada T, Takahashi H. Direct comparison of administration routes for AAV8-mediated ocular gene therapy. Curr Eye Res 2013; 38: 569-77.

Inagaki S, Nakamura S, Kuse Y, Aoshima K, Funato M, Shimazawa M, Hara H. Establishment of vascularized human retinal organoids from induced pluripotent stem cells. Stem Cells 2025;

J. Pulman JS, D. Dalkara. New Editing Tools for Gene Therapy in Inherited Retinal Dystrophies. The CRISPR Journal 2022;

Jain R, Daigavane S. Advances and Challenges in Gene Therapy for Inherited Retinal Dystrophies: A Comprehensive Review. Cureus 2024; 16: e69895.

Jalil A, Ferrara M, Lippera M, Parry N, Black GC, Banderas S, Ashworth J, Biswas S, Hall G, Gray J, Newman W, Ivanova T. Real-world outcomes of Voretigene Neparvovec: a single-centre consecutive case series. Eye (Lond) 2025;

Jaudas F, Bartenschlager F, Shashikadze B, Santamaria G, Reichart D, Schnell A, Stöckl JB, Degroote RL, Cambra JM, Graeber SY, Bähr A, Kartmann H, Stefanska M, Liu H, Naumann-Bartsch N, Bruns H, Berges J, Hanselmann L, Stirm M, Krebs S, Deeg CA, Blum H, Schulz C, Zawada D, Janda M, Caballero-Posadas I, Kunzelmann K, Moretti A, Laugwitz KL, Kupatt C, Saalmüller A, Fröhlich T, Wolf E, Mall MA, Mundhenk L, Gerner W, Klymiuk N. Perinatal dysfunction of innate immunity in cystic fibrosis. Sci Transl Med 2025; 17: eadk9145.

Jiang F, Zhou K, Ma L, Gressel S, Doudna JA. STRUCTURAL BIOLOGY. A Cas9-guide RNA complex preorganized for target DNA recognition. Science 2015; 348: 1477-81.

Jinek M, Chylinski K, Fonfara I, Hauer M, Doudna JA, Charpentier E. A programmable dual-RNA-guided DNA endonuclease in adaptive bacterial immunity. Science 2012;

Kalesnykas G, Kokki E, Alasaarela L, Lesch HP, Tuulos T, Kinnunen K, Uusitalo H, Airenne K, Yla-Herttuala S. Comparative Study of Adeno-associated Virus, Adenovirus, Bacu lovirus and Lentivirus Vectors for Gene Therapy of the Eyes. Curr Gene Ther 2017; 17: 235-47.

Kelley RA, Wu Z. Utilization of the retinal organoid model to evaluate the feasibility of genetic strategies to ameliorate retinal disease(s). Vision Res 2023; 210: 108269.

Kellish PC, Marsic D, Crosson SM, Choudhury S, Scalabrino ML, Strang CE, Hill J, McCullough KT, Peterson JJ, Fajardo D, Gupte S, Makal V, Kondratov O, Kondratova L, Iyer S, Witherspoon CD, Gamlin PD, Zolotukhin S, Boye SL, Boye SE. Intravitreal injection of a rationally designed AAV capsid library in non-human primate identifies variants with enhanced retinal transduction and neutralizing

antibody evasion. Mol Ther 2023; 31: 3441-56.

Khammanit R, Chantakru S, Kitiyanant Y, Saikhun J. Effect of serum starvation and chemical inhibitors on cell cycle synchronization of canine dermal fibroblasts. Theriogenology 2008; 70: 27-34.

Kiraly P, Klein J, Seitz IP, Reichel FF, Peters T, Ardan T, Juhasova J, Juhás S, Ellederova Z, Nemesh Y, Nyshchuk R, Klymiuk N, Nagel-Wolfrum K, Winslow AR, Wolfrum U, Motlik J, Fischer MD. Safety of Human USH1C Transgene Expression Following Subretinal Injection in Wild-Type Pigs. Invest Ophthalmol Vis Sci 2025; 66: 48.

Knott GJ, Doudna JA. CRISPR-Cas guides the future of genetic engineering. Science 2018; 361: 866-9.

Komor AC, Kim YB, Packer MS, Zuris JA, Liu DR. Programmable editing of a target base in genomic DNA without double-stranded DNA cleavage. Nature 2016;

Kornum BR, Knudsen GM. Cognitive testing of pigs (Sus scrofa) in translational biobehavioral research. Neurosci Biobehav Rev 2011; 35: 437-51.

Kostic C, Lillico SG, Crippa SV, Grandchamp N, Pilet H, Philippe S, Lu Z, King TJ, Mallet J, Sarkis C, Arsenijevic Y, Whitelaw CB. Rapid cohort generation and analysis of disease spectrum of large animal model of cone dystrophy. PLoS One 2013; 8: e71363.

Kostic C, Arsenijevic Y. Animal modelling for inherited central vision loss. J Pathol 2016; 238: 300-10.

Kremers J, Tanimoto N. Measuring Retinal Function in the Mouse. Methods Mol Biol 2018; 1753: 27-40.

Ku CA, Igelman AD, Huang SJ, Bailey ST, Lauer AK, Duncan JL, Weleber RG,

Yang P, Pennesi ME. Perimacular Atrophy Following Voretigene Neparvovec-Rzyl Treatment in the Setting of Previous Contralateral Eye Treatment With a Different Viral Vector. Transl Vis Sci Technol 2024; 13: 11.

Kurome M, Kessler B, Wuensch A, Nagashima H, Wolf E. Nuclear transfer and transgenesis in the pig. Methods Mol Biol 2015; 1222: 37-59.

Kvanta A, Rangaswamy N, Holopigian K, Watters C, Jennings N, Liew MSH, Bigelow C, Grosskreutz C, Burstedt M, Venkataraman A, Westman S, Geirsdottir A, Stasi K, André H. Interim safety and efficacy of gene therapy for RLBP1-associated retinal dystrophy: a phase 1/2 trial. Nat Commun 2024; 15: 7438.

Kweon J, Kim Y. High-throughput genetic screens using CRISPR-Cas9 system. Arch Pharm Res 2018; 41: 875-84.

Lam S, Cao H, Wu J, Duan R, Hu J. Highly efficient retinal gene delivery with helper-dependent adenoviral vectors. Genes and Diseases 2014;

Leal AF, Herreno-Pachón AM, Benincore-Flórez E, Karunathilaka A, Tomatsu S. Current Strategies for Increasing Knock-In Efficiency in CRISPR/Cas9-Based Approaches. Int J Mol Sci 2024; 25

Leclerc D, Siroky MD, Miller SM. Next-generation biological vector platforms for in vivo delivery of genome editing agents. Curr Opin Biotechnol 2024; 85: 103040.

Leeb T, Bannasch D, Schoenebeck JJ. Identification of Genetic Risk Factors for Monogenic and Complex Canine Diseases. Annu Rev Anim Biosci 2023; 11: 183-205.

Leinonen H, Tanila H. Vision in laboratory rodents-Tools to measure it and implications for behavioral research. Behav Brain Res 2018; 352: 172-82.

Li Y, Guha C, Asp P, Wang X, Tchaikovskya TL, Kim K, Mendel M, Cost GJ,

Perlmutter DH, Roy-Chowdhury N, Fox IJ, Conway A, Roy-Chowdhury J. Resolution of hepatic fibrosis after ZFN-mediated gene editing in the PiZ mouse model of human α1-antitrypsin deficiency. Hepatol Commun 2023; 7: e0070.

Lin S, Vermeirsch S, Pontikos N, Martin-Gutierrez MP, Daich Varela M, Malka S, Schiff E, Knight H, Wright G, Jurkute N, Simcoe MJ, Yu-Wai-Man P, Moosajee M, Michaelides M, Mahroo OA, Webster AR, Arno G. Spectrum of Genetic Variants in the Most Common Genes Causing Inherited Retinal Disease in a Large Molecularly Characterized United Kingdom Cohort. Ophthalmol Retina 2024; 8: 699-709.

Ling J, Jenny LA, Zhou A, Tsang SH. Therapeutic Gene Editing in Inherited Retinal Disorders. Cold Spring Harb Perspect Med 2023; 13

Liu Q, Muruve DA. Molecular basis of the inflammatory response to adenovirus vectors. Gene Ther 2003; 10: 935-40.

Lorenz B, Tavares J, van den Born L, Marques J, Scholl H-, Group tEn. Current Management of Inherited Retinal Degeneration Patients in Europe: Results of a Multinational Survey by the European Vision Institute Clinical Research Network. Ophthalmic Research 2021; 64: 622-38.

Lucas ME, Hemsworth LM, Butler KL, Morrison RS, Tilbrook AJ, Marchant JN, Rault JL, Galea RY, Hemsworth PH. Early human contact and housing for pigs - part 1: responses to humans, novelty and isolation. Animal 2024; 18: 101164.

Luo S, Jiang H, Li Q, Qin Y, Yang S, Li J, Xu L, Gou Y, Zhang Y, Liu F, Ke X, Zheng Q, Sun X. An adeno-associated virus variant enabling efficient ocular-directed gene delivery across species. Nat Commun 2024; 15: 3780.

MacLachlan TK, Milton MN, Turner O, Tukov F, Choi VW, Penraat J, Delmotte MH, Michaut L, Jaffee BD, Bigelow CE. Nonclinical Safety Evaluation of scAAV8-RLBP1 for Treatment of RLBP1 Retinitis Pigmentosa. Mol Ther Methods Clin Dev 2018; 8: 105-20.

Madzivhandila AG, le Roux T, Biagio de Jager L. Neonatal hearing screening using a smartphone-based otoacoustic emission device: A comparative study. Int J Pediatr Otorhinolaryngol 2024; 177: 111862.

Maeder ML, Stefanidakis M, Wilson CJ, Baral R, Barrera LA, Bounoutas GS, Bumcrot D, Chao H, Ciulla DM, DaSilva JA, Dass A, Dhanapal V, Fennell TJ, Friedland AE, Giannoukos G, Gloskowski SW, Glucksmann A, Gotta GM, Jayaram H, Haskett SJ, Hopkins B, Horng JE, Joshi S, Marco E, Mepani R, Reyon D, Ta T, Tabbaa DG, Samuelsson SJ, Shen S, Skor MN, Stetkiewicz P, Wang T, Yudkoff C, Myer VE, Albright CF, Jiang H. Development of a gene-editing approach to restore vision loss in Leber congenital amaurosis type 10. Nat Med 2019; 25: 229-33.

Maguire AM, High KA, Auricchio A, Wright JF, Pierce EA, Testa F, Mingozzi F, Bennicelli JL, Ying GS, Rossi S, Fulton A, Marshall KA, Banfi S, Chung DC, Morgan JI, Hauck B, Zelenaia O, Zhu X, Raffini L, Coppieters F, De Baere E, Shindler KS, Volpe NJ, Surace EM, Acerra C, Lyubarsky A, Redmond TM, Stone E, Sun J, McDonnell JW, Leroy BP, Simonelli F, Bennett J. Age-dependent effects of RPE65 gene therapy for Leber's congenital amaurosis: a phase 1 dose-escalation trial. Lancet 2009; 374: 1597-605.

Maguire AM, Russell S, Wellman JA, Chung DC, Yu ZF, Tillman A, Wittes J, Pappas J, Elci O, Marshall KA, McCague S, Reichert H, Davis M, Simonelli F, Leroy BP, Wright JF, High KA, Bennett J. Efficacy, Safety, and Durability of Voretigene Neparvovec-rzyl in RPE65 Mutation-Associated Inherited Retinal Dystrophy: Results of Phase 1 and 3 Trials. Ophthalmology 2019; 126: 1273-85.

Mandai M. Pluripotent stem cell-derived retinal organoid/cells for retinal regeneration therapies: A review. Regen Ther 2023; 22: 59-67.

Matet A, Kostic C, Bemelmans AP, Moulin A, Rosolen SG, Martin S, Mavilio F, Amirjanians V, Stieger K, Lorenz B, Behar-Cohen F, Arsenijevic Y. Evaluation of tolerance to lentiviral LV-RPE65 gene therapy vector after subretinal delivery in non-human primates. Transl Res 2017; 188: 40-57.e4.

Mathis N, Allam A, Kissling L, Marquart KF, Schmidheini L, Solari C, Balázs Z, Krauthammer M, Schwank G. Predicting prime editing efficiency and product purity by deep learning. Nat Biotechnol 2023; 41: 1151-9.

Maurissen TL, Woltjen K. Synergistic gene editing in human iPS cells via cell cycle and DNA repair modulation. Nat Commun 2020; 11: 2876.

McCall MA. Pig Models in Retinal Research and Retinal Disease. Cold Spring Harb Perspect Med 2024; 14

McClements ME, MacLaren RE. Adeno-associated Virus (AAV) Dual Vector Strategies for Gene Therapy Encoding Large Transgenes. Yale J Biol Med 2017; 90: 611-23.

McClements ME, Elsayed M, Major L, de la Camara CM, MacLaren RE. Gene Therapies in Clinical Development to Treat Retinal Disorders. Mol Diagn Ther 2024; 28: 575-91.

McDonald A, Gallego C, Andriessen C, Orlová M, Gonçalves M, Wijnholds J. Conventional and Tropism-Modified High-Capacity Adenoviral Vectors Exhibit Similar Transduction Profiles in Human iPSC-Derived Retinal Organoids. Int J Mol Sci 2024; 26

McDonald A, Wijnholds J. Retinal Ciliopathies and Potential Gene Therapies: A Focus on Human iPSC-Derived Organoid Models. Int J Mol Sci 2024; 25

McDowell CM, Kizhatil K, Elliott MH, Overby DR, van Batenburg-Sherwood J, Millar JC, Kuehn MH, Zode G, Acott TS, Anderson MG, Bhattacharya SK, Bertrand JA, Borras T, Bovenkamp DE, Cheng L, Danias J, De Ieso ML, Du Y, Faralli JA, Fuchshofer R, Ganapathy PS, Gong H, Herberg S, Hernandez H, Humphries P, John SWM, Kaufman PL, Keller KE, Kelley MJ, Kelly RA, Krizaj D, Kumar A, Leonard BC, Lieberman RL, Liton P, Liu Y, Liu KC, Lopez NN, Mao W, Mavlyutov T, McDonnell F, McLellan GJ, Mzyk P, Nartey A, Pasquale LR, Patel GC, Pattabiraman PP, Peters DM, Raghunathan V, Rao PV, Rayana N,

Raychaudhuri U, Reina-Torres E, Ren R, Rhee D, Chowdhury UR, Samples JR, Samples EG, Sharif N, Schuman JS, Sheffield VC, Stevenson CH, Soundararajan A, Subramanian P, Sugali CK, Sun Y, Toris CB, Torrejon KY, Vahabikashi A, Vranka JA, Wang T, Willoughby CE, Xin C, Yun H, Zhang HF, Fautsch MP, Tamm ER, Clark AF, Ethier CR, Stamer WD. Consensus Recommendation for Mouse Models of Ocular Hypertension to Study Aqueous Humor Outflow and Its Mechanisms. Invest Ophthalmol Vis Sci 2022; 63: 12.

Meyerholz DK, Burrough ER, Kirchhof N, Anderson DJ, Helke KL. Swine models in translational research and medicine. Vet Pathol 2024; 61: 512-23.

Mirra A, Gamez Maidanskaia E, Carmo LP, Levionnois O, Spadavecchia C. How is depth of anaesthesia assessed in experimental pigs? A scoping review. PLoS One 2023; 18: e0283511.

Muller A, Sullivan J, Schwarzer W, Wang M, Park-Windhol C, Hasler PW, Janeschitz-Kriegl L, Duman M, Klingler B, Matsell J, Hostettler SM, Galliker P, Hou Y, Balmer P, Virág T, Barrera LA, Young L, Xu Q, Magda DP, Kilin F, Khadka A, Moreau PH, Fellmann L, Azoulay T, Quinodoz M, Karademir D, Leppert J, Fratzl A, Kosche G, Sharma R, Montford J, Cattaneo M, Croyal M, Cronin T, Picelli S, Grison A, Cowan CS, Kusnyerik Á, Anders P, Renner M, Nagy ZZ, Szabó A, Bharti K, Rivolta C, Scholl HPN, Bryson D, Ciaramella G, Roska B, György B. High-efficiency base editing in the retina in primates and human tissues. Nat Med 2025; 31: 490-501.

Murali A, Ramlogan-Steel CA, Andrzejewski S, Steel JC, Layton CJ. Retinal explant culture: A platform to investigate human neuro-retina. Clin Exp Ophthalmol 2019; 47: 274-85.

Murphy R, Martin KR. Genetic engineering and the eye. Eye (Lond) 2025; 39: 57-68.

Murro V, Banfi S, Testa F, Iarossi G, Falsini B, Sodi A, Signorini S, Iolascon A, Russo R, Mucciolo DP, Caputo R, Bacci GM, Bargiacchi S, Turco S, Fortini S,

Simonelli F. A multidisciplinary approach to inherited retinal dystrophies from diagnosis to initial care: a narrative review with inputs from clinical practice. Orphanet J Rare Dis 2023; 18: 223.

Nair G, Kim M, Nagaoka T, Olson DE, Thulé PM, Pardue MT, Duong TQ. Effects of common anesthetics on eye movement and electroretinogram. Doc Ophthalmol 2011; 122: 163-76.

Nikolaidou A, Sandali A, Chatzidimitriou E, Pantelaki D, Gianni T, Lamprogiannis L. Virtual Reality With Eye Tracking for Pediatric Ophthalmology: A Systematic Review. J Pediatr Ophthalmol Strabismus 2024; 61: 381-90.

Nishimasu H, Ran FA, Hsu PD, Konermann S, Shehata SI, Dohmae N, Ishitani R, Zhang F, Nureki O. Crystal structure of Cas9 in complex with guide RNA and target DNA. Cell 2014; 156: 935-49.

Nooraei S, Bahrulolum H, Hoseini ZS, Katalani C, Hajizade A, Easton AJ, Ahmadian G. Virus-like particles: preparation, immunogenicity and their roles as nanovaccines and drug nanocarriers. J Nanobiotechnology 2021; 19: 59.

Palanova A. The genetics of inherited retinal disorders in dogs: implications for diagnosis and management. Vet Med (Auckl) 2016; 7: 41-51.

Parameswarappa DC, Kulkarni A, Sahoo NK, Padhy SK, Singh SR, Héon E, Chhablani J. From Cellular to Metabolic: Advances in Imaging of Inherited Retinal Diseases. Diagnostics (Basel) 2024; 15

Parums DV. Editorial: First Regulatory Approvals for CRISPR-Cas9 Therapeutic Gene Editing for Sickle Cell Disease and Transfusion-Dependent β-Thalassemia. Med Sci Monit 2024; 30: e944204.

Pasmanter N, Occelli LM, Petersen-Jones SM. ERG assessment of altered retinal function in canine models of retinitis pigmentosa and monitoring of response to

translatable gene augmentation therapy. Doc Ophthalmol 2021; 143: 171-84.

Pavlou M, Schön C, Occelli LM, Rossi A, Meumann N, Boyd RF, Bartoe JT, Siedlecki J, Gerhardt MJ, Babutzka S, Bogedein J, Wagner JE, Priglinger SG, Biel M, Petersen-Jones SM, Büning H, Michalakis S. Novel AAV capsids for intravitreal gene therapy of photoreceptor disorders. EMBO Mol Med 2021; 13: e13392.

Peng Y, Tang L, Zhou Y. Subretinal Injection: A Review on the Novel Route of Therapeutic Delivery for Vitreoretinal Diseases. Ophthalmic Res 2017; 58: 217-26.

Pennesi ME, Weleber RG, Yang P, Whitebirch C, Thean B, Flotte TR, Humphries M, Chegarnov E, Beasley KN, Stout JT, Chulay JD. Results at 5 Years After Gene Therapy for RPE65-Deficient Retinal Dystrophy. Hum Gene Ther 2018; 29: 1428-37.

Petersen-Jones SM, Komáromy AM. Dog models for blinding inherited retinal dystrophies. Hum Gene Ther Clin Dev 2015; 26: 15-26.

Petit L, Ma S, Cheng SY, Gao G, Punzo C. Rod Outer Segment Development Influences AAV-Mediated Photoreceptor Transduction After Subretinal Injection. Hum Gene Ther 2017; 28: 464-81.

Petters RM, Alexander CA, Wells KD, Collins EB, Sommer JR, Blanton MR, Rojas G, Hao Y, Flowers WL, Banin E, Cideciyan AV, Jacobson SG, Wong F. Genetically engineered large animal model for studying cone photoreceptor survival and degeneration in retinitis pigmentosa. Nat Biotechnol 1997; 15: 965-70.

Pickar-Oliver A, Gersbach CA. The next generation of CRISPR-Cas technologies and applications. Nat Rev Mol Cell Biol 2019; 20: 490-507.

Pierce EA, Aleman TS, Jayasundera KT, Ashimatey BS, Kim K, Rashid A,

Jaskolka MC, Myers RL, Lam BL, Bailey ST, Comander JI, Lauer AK, Maguire AM, Pennesi ME. Gene Editing for CEP290-Associated Retinal Degeneration. N Engl J Med 2024; 390: 1972-84.

Poh WT, Stanslas J. The new paradigm in animal testing - "3Rs alternatives". Regul Toxicol Pharmacol 2024; 153: 105705.

Popovitz J, Sharma R, Hoshyar R, Soo Kim B, Murthy N, Lee K. Gene editing therapeutics based on mRNA delivery. Adv Drug Deliv Rev 2023; 200: 115026.

Quadrato G, Nguyen T, Macosko EZ, Sherwood JL, Min Yang S, Berger DR, Maria N, Scholvin J, Goldman M, Kinney JP, Boyden ES, Lichtman JW, Williams ZM, McCarroll SA, Arlotta P. Cell diversity and network dynamics in photosensitive human brain organoids. Nature 2017; 545: 48-53.

Quinn J, Musa A, Kantor A, McClements M, Cehajic-Kapetanovic J, MacLaren R, Xue K. Genome-Editing Strategies for Treating Human Retinal Degenerations. Human Gene Therapy 2021;

Raguram A, Banskota S, Liu DR. Therapeutic in vivo delivery of gene editing agents. Cell 2022; 185: 2806-27.

Ramachandran PS, Lee V, Wei Z, Song JY, Casal G, Cronin T, Willett K, Huckfeldt R, Morgan JI, Aleman TS, Maguire AM, Bennett J. Evaluation of Dose and Safety of AAV7m8 and AAV8BP2 in the Non-Human Primate Retina. Hum Gene Ther 2017; 28: 154-67.

Raper SE, Chirmule N, Lee FS, Wivel NA, Bagg A, Gao GP, Wilson JM, Batshaw ML. Fatal systemic inflammatory response syndrome in a ornithine transcarbamylase deficient patient following adenoviral gene transfer. Mol Genet Metab 2003; 80: 148-58.

Ravi NS, George A, Mohankumar KM. Protocol for arrayed gRNA screening by

base editors in mammalian cell lines using lentiviral system. STAR Protoc 2023; 4: 102668.

Rettinger CL, Wang HC. Quantitative Assessment of Retina Explant Viability in a Porcine Ex Vivo Neuroretina Model. J Ocul Pharmacol Ther 2018; 34: 521-30.

Richter A, Kurome M, Kessler B, Zakhartchenko V, Klymiuk N, Nagashima H, Wolf E, Wuensch A. Potential of primary kidney cells for somatic cell nuclear transfer mediated transgenesis in pig. BMC Biotechnol 2012; 12: 84.

Richter MF, Zhao KT, Eton E, Lapinaite A, Newby GA, Thuronyi BW, Wilson C, Koblan LW, Zeng J, Bauer DE, Doudna JA, Liu DR. Phage-assisted evolution of an adenine base editor with improved Cas domain compatibility and activity. Nat Biotechnol 2020; 38: 883-91.

Riedmayr LM, Hinrichsmeyer KS, Thalhammer SB, Mittas DM, Karguth N, Otify DY, Böhm S, Weber VJ, Bartoschek MD, Splith V, Brümmer M, Ferreira R, Boon N, Wögenstein GM, Grimm C, Wijnholds J, Mehlfeld V, Michalakis S, Fenske S, Biel M, Becirovic E. mRNA trans-splicing dual AAV vectors for (epi)genome editing and gene therapy. Nat Commun 2023; 14: 6578.

Rinwa P, Eriksson M, Cotgreave I, Bäckberg M. 3R-Refinement principles: elevating rodent well-being and research quality. Lab Anim Res 2024; 40: 11.

Rogler TS, Salbaum KA, Sonntag SM, James R, Shelton ER, Brinkop AT, Klopstock T, Babutzka S, Michalakis S, Serwane F. 3D quantification of viral transduction efficiency in living human retinal organoids. bioRxiv 2024: 2024.03.06.583795.

Ross JW, Fernandez de Castro JP, Zhao J, Samuel M, Walters E, Rios C, Bray-Ward P, Jones BW, Marc RE, Wang W, Zhou L, Noel JM, McCall MA, DeMarco PJ, Prather RS, Kaplan HJ. Generation of an inbred miniature pig model of retinitis pigmentosa. Invest Ophthalmol Vis Sci 2012; 53: 501-7.

Russell S, Bennett J, Wellman JA, Chung DC, Yu ZF, Tillman A, Wittes J, Pappas J, Elci O, McCague S, Cross D, Marshall KA, Walshire J, Kehoe TL, Reichert H, Davis M, Raffini L, George LA, Hudson FP, Dingfield L, Zhu X, Haller JA, Sohn EH, Mahajan VB, Pfeifer W, Weckmann M, Johnson C, Gewaily D, Drack A, Stone E, Wachtel K, Simonelli F, Leroy BP, Wright JF, High KA, Maguire AM. Efficacy and safety of voretigene neparvovec (AAV2-hRPE65v2) in patients with RPE65-mediated inherited retinal dystrophy: a randomised, controlled, open-label, phase 3 trial. Lancet 2017; 390: 849-60.

Sainz-Ramos M, Gallego I, Villate-Beitia I, Zarate J, Maldonado I, Puras G, Pedraz JL. How Far Are Non-Viral Vectors to Come of Age and Reach Clinical Translation in Gene Therapy? Int J Mol Sci 2021; 22

Sakurai H, Kawabata K, Sakurai F, Nakagawa S, Mizuguchi H. Innate immune response induced by gene delivery vectors. Int J Pharm 2008; 354: 9-15.

Sampson TR, Weiss DS. Exploiting CRISPR/Cas systems for biotechnology. Bioessays 2014; 36: 34-8.

Sanchez I, Martin R, Ussa F, Fernandez-Bueno I. The parameters of the porcine eyeball. Graefes Arch Clin Exp Ophthalmol 2011; 249: 475-82.

Schneider N, Sundaresan Y, Gopalakrishnan P, Beryozkin A, Hanany M, Levanon E, Banin E, Ben-Aroya S, Sharon D. Inherited retinal diseases: Linking genes, disease-causing variants, and relevant therapeutic modalities. Progress in retinal and eye research 2021;

Schnichels S, Paquet-Durand F, Löscher M, Tsai T, Hurst J, Joachim SC, Klettner A. Retina in a dish: Cell cultures, retinal explants and animal models for common diseases of the retina. Prog Retin Eye Res 2021; 81: 100880.

Schön C, Biel M, Michalakis S. Retinal gene delivery by adeno-associated virus (AAV) vectors: Strategies and applications. Eur J Pharm Biopharm 2015; 95: 343-52.

Seah I, Goh D, Chan HW, Su X. Developing Non-Human Primate Models of Inherited Retinal Diseases. Genes (Basel) 2022; 13

Seitz IP, Peters T, Reichel F, Bähr A, Auch H, Motlik J, Ardan T, Juhasova J, Nemesh Y, Juhás S, Klymiuk N, Fischer MD. Optimizing Subretinal Bleb Formation for Visual Streak Involvement in a Porcine Model for Retinal Gene Therapy. Invest Ophthalmol Vis Sci 2024; 65: 41.

Shalem O, Sanjana NE, Zhang F. High-throughput functional genomics using CRISPR-Cas9. Nat Rev Genet 2015; 16: 299-311.

Shamshad A, Kang C, Jenny LA, Persad-Paisley EM, Tsang SH. Translatability barriers between preclinical and clinical trials of AAV gene therapy in inherited retinal diseases. Vision Res 2023; 210: 108258.

Simon DA, Tálas A, Kulcsár PI, Biczók Z, Krausz SL, Várady G, Welker E. PEAR, a flexible fluorescent reporter for the identification and enrichment of successfully prime edited cells. Elife 2022; 11

Simonelli F, Sodi A, Falsini B, Bacci G, Iarossi G, Di Iorio V, Giorgio D, Placidi G, Andrao A, Reale L, Fiorencis A, Aoun M. Narrative medicine to investigate the quality of life and emotional impact of inherited retinal disorders through the perspectives of patients, caregivers and clinicians: an Italian multicentre project. BMJ Open 2022; 12: e061080.

Solovei I, Kreysing M, Lanctôt C, Kösem S, Peichl L, Cremer T, Guck J, Joffe B. Nuclear architecture of rod photoreceptor cells adapts to vision in mammalian evolution. Cell 2009; 137: 356-68.

Sommer JR, Estrada JL, Collins EB, Bedell M, Alexander CA, Yang Z, Hughes G, Mir B, Gilger BC, Grob S, Wei X, Piedrahita JA, Shaw PX, Petters RM, Zhang K. Production of ELOVL4 transgenic pigs: a large animal model for Stargardt-like macular degeneration. Br J Ophthalmol 2011; 95: 1749-54.

Song X, Liu J, Chen T, Zheng T, Wang X, Guo X. Gene therapy and gene editing strategies in inherited blood disorders. J Genet Genomics 2024; 51: 1162-72.

Stirm M, Fonteyne LM, Shashikadze B, Stöckl JB, Kurome M, Keßler B, Zakhartchenko V, Kemter E, Blum H, Arnold GJ, Matiasek K, Wanke R, Wurst W, Nagashima H, Knieling F, Walter MC, Kupatt C, Fröhlich T, Klymiuk N, Blutke A, Wolf E. Pig models for Duchenne muscular dystrophy - from disease mechanisms to validation of new diagnostic and therapeutic concepts. Neuromuscul Disord 2022; 32: 543-56.

Suh S, Choi EH, Raguram A, Liu DR, Palczewski K. Precision genome editing in the eye. Proceedings of the National Academy of Sciences of the United States of America 2022;

Sweigard JH, Cashman SM, Kumar-Singh R. Adenovirus vectors targeting distinct cell types in the retina. Invest Ophthalmol Vis Sci 2010; 51: 2219-28.

Szabó V, Varsányi B, Barboni M, Takács Á, Knézy K, Molnár MJ, Nagy ZZ, György B, Rivolta C. Insights into eye genetics and recent advances in ocular gene therapy. Mol Cell Probes 2025; 79: 102008.

Takahashi K, Igarashi T, Miyake K, Kobayashi M, Yaguchi C, Iijima O, Yamazaki Y, Katakai Y, Miyake N, Kameya S, Shimada T, Takahashi H, Okada T. Improved Intravitreal AAV-Mediated Inner Retinal Gene Transduction after Surgical Internal Limiting Membrane Peeling in Cynomolgus Monkeys. Mol Ther 2017; 25: 296-302.

Tang H, Mayersohn M. Porcine Prediction of Pharmacokinetic Parameters in People: A Pig in a Poke? Drug Metab Dispos 2018; 46: 1712-24.

Teal PD, Shera CA, Abdala C. Whole Stimulus DPOAE Analysis. AIP Conf Proc 2024; 3062

Teif VB, Vainshtein Y, Caudron-Herger M, Mallm JP, Marth C, Höfer T, Rippe K. Genome-wide nucleosome positioning during embryonic stem cell development. Nat Struct Mol Biol 2012; 19: 1185-92.

Teo KYC, Lee SY, Barathi AV, Tun SBB, Tan L, Constable IJ. Surgical Removal of Internal Limiting Membrane and Layering of AAV Vector on the Retina Under Air Enhances Gene Transfection in a Nonhuman Primate. Invest Ophthalmol Vis Sci 2018; 59: 3574-83.

Testa F, Bacci G, Falsini B, Iarossi G, Melillo P, Mucciolo DP, Murro V, Salvetti AP, Sodi A, Staurenghi G, Simonelli F. Voretigene neparvovec for inherited retinal dystrophy due to RPE65 mutations: a scoping review of eligibility and treatment challenges from clinical trials to real practice. Eye (Lond) 2024; 38: 2504-15.

Thangaraj G, Greif A, Layer PG. Simple explant culture of the embryonic chicken retina with long-term preservation of photoreceptors. Exp Eye Res 2011; 93: 556-64.

Tornabene P, Trapani I, Minopoli R, Centrulo M, Lupo M, de Simone S, Tiberi P, Dell'Aquila F, Marrocco E, Iodice C, Iuliano A, Gesualdo C, Rossi S, Giaquinto L, Albert S, Hoyng CB, Polishchuk E, Cremers FPM, Surace EM, Simonelli F, De Matteis MA, Polishchuk R, Auricchio A. Intein-mediated protein trans-splicing expands adeno-associated virus transfer capacity in the retina. Sci Transl Med 2019; 11

Törnqvist E, Annas A, Granath B, Jalkesten E, Cotgreave I, Öberg M. Strategic focus on 3R principles reveals major reductions in the use of animals in pharmaceutical toxicity testing. PLoS One 2014; 9: e101638.

Truong DJ, Kühner K, Kühn R, Werfel S, Engelhardt S, Wurst W, Ortiz O. Development of an intein-mediated split-Cas9 system for gene therapy. Nucleic Acids Res 2015; 43: 6450-8.

Usui-Ouchi A, Giles S, Harkins-Perry S, Mills EA, Bonelli R, Wei G, Ouchi Y,

Ebihara N, Nakao S, Friedlander M, Eade KT. Integrating human iPSC-derived macrophage progenitors into retinal organoids to generate a mature retinal microglial niche. Glia 2023; 71: 2372-82.

van der Laan JW, Brightwell J, McAnulty P, Ratky J, Stark C. Regulatory acceptability of the minipig in the development of pharmaceuticals, chemicals and other products. J Pharmacol Toxicol Methods 2010; 62: 184-95.

van der Oost J, Patinios C. The genome editing revolution. Trends Biotechnol 2023; 41: 396-409.

Vargas JA, Finnemann SC. Probing Photoreceptor Outer Segment Phagocytosis by the RPE In Vivo: Models and Methodologies. Int J Mol Sci 2022; 23

Vats A, Xi Z, Byrne LC, Chen Y. Retinal Explant Culture from Mouse, Human, and Nonhuman Primates and Its Applications in Vision Research. Methods Mol Biol 2025; 2848: 169-86.

Wang J, Kolomeyer AM, Zarbin MA, Townes-Anderson E. Organotypic culture of full-thickness adult porcine retina. J Vis Exp 2011;

Wang J, He A, Yin D, Zhu Y, Zhou G, Zhang T. Comparative study of the external auditory canal in humans and large mammals. Anat Rec (Hoboken) 2022; 305: 436-45.

Wang JH, Gessler DJ, Zhan W, Gallagher TL, Gao G. Adeno-associated virus as a delivery vector for gene therapy of human diseases. Signal Transduct Target Ther 2024; 9: 78.

Wang JY, Doudna JA. CRISPR technology: A decade of genome editing is only the beginning. Science 2023; 379: eadd8643.

Watanabe M, Nishikawaji Y, Kawakami H, Kosai KI. Adenovirus Biology,

Recombinant Adenovirus, and Adenovirus Usage in Gene Therapy. Viruses 2021; 13

Webster J, Bollen P, Grimm H, Jennings M. Ethical implications of using the minipig in regulatory toxicology studies. J Pharmacol Toxicol Methods 2010; 62: 160-6.

Weller M, Müller B, Stieger K. Long-Term Porcine Retina Explants as an Alternative to In Vivo Experimentation. Transl Vis Sci Technol 2024; 13: 9.

Wijeyesinghe S, Chinen J. Gene therapy for inborn errors of immunity: current clinical progress. Ann Allergy Asthma Immunol 2025;

Wold WS, Toth K. Adenovirus vectors for gene therapy, vaccination and cancer gene therapy. Curr Gene Ther 2013; 13: 421-33.

Wolf E, Braun-Reichhart C, Streckel E, Renner S. Genetically engineered pig models for diabetes research. Transgenic Res 2014; 23: 27-38.

Xiao Y, Tang Z, Huang X, Chen W, Zhou J, Liu H, Liu C, Kong N, Tao W. Emerging mRNA technologies: delivery strategies and biomedical applications. Chem Soc Rev 2022; 51: 3828-45.

Xu W, Dong Y, Li Y, Hu Z, Paquet-Durand F, Jiao K. Organotypic Retinal Explant Cultures from Macaque Monkey. J Vis Exp 2022;

Yadav T, Kumar S, Mishra G, Saxena SK. Tracking the COVID-19 vaccines: The global landscape. Hum Vaccin Immunother 2023; 19: 2191577.

Yang W, Chen X, Li S, Li XJ. Genetically modified large animal models for investigating neurodegenerative diseases. Cell Biosci 2021; 11: 218.

Yoshimatsu H, Konno Y, Ishii K, Satsukawa M, Yamashita S. Usefulness of

minipigs for predicting human pharmacokinetics: Prediction of distribution volume and plasma clearance. Drug Metab Pharmacokinet 2016; 31: 73-81.

Zang J, Neuhauss SCF. Biochemistry and physiology of zebrafish photoreceptors. Pflugers Arch 2021; 473: 1569-85.

Zhang X, Sun Q, Sai L, Yu H. The value of ABR- and ASSR-based hearing estimation in young children with congenital monaural malformation (atresia). Acta Otolaryngol 2019; 139: 769-76.

Zheng Q, Wang T, Zhu X, Tian X, Zhong C, Chang G, Ran G, Xie Y, Zhao B, Zhu L, Ling C. Low endotoxin E. coli strain-derived plasmids reduce rAAV vector-mediated immune responses both in vitro and in vivo. Mol Ther Methods Clin Dev 2021; 22: 293-303.

IX. Index of figures 137

IX. INDEX OF FIGURES

Figure 1: CRISPR-Cas variants for GE. Adapted from (UDDIN et al., 2020).	
Created with BioRender	9
Figure 2: Anatomy of the Retina	17
Figure 3: Key Aspects of Gene Editing for the Treatment of IRDs	22
Figure 4 : DSB-HDR Gene Repair Approach	42
Figure 5 : Adenosine Base Editing in USH1C Porcine Kidney Cells	44
Figure 6: Prime Editing Using PE3 with Different asgRNA and pegRNA	45
Figure 7: Prime Editing Using PEMax	46
Figure 8: Prime Editing Using TwinPE	47
Figure 9: Next generation sequencing (NGS) analysis of TwinPE set 2	48
Figure 10: Summary of GE Approaches in vitro	48
Figure 11: VLP testing in USH1C PKC	50
Figure 12: Efficiency after VLP-mediated Disruption of the B2M locus	51
Figure 13: GE Efficiency at the USH1C Locus Using Delivery Vector X	52
Figure 14: DVX-mediated Delivery of pegRNA and Intact Cas9	53
Figure 15: Postnatal Management for USH1C Piglets	55
Figure 16: Network of Collaborations and Translational Studies	57
Figure 17: ERG Measurements of USH1C vs. WT animals	58
Figure 18: ABR Tone Burst, ABR Click and ASSR Tests in USH1C vs. WT and	imals
	59
Figure 19: DPOAE Measurements of USH1C and WT animals	60
Figure 20 : Sampling protocol of pilot in vivo experiment	61
Figure 21: Fundus Image and OCT of the Retina – 1 Week after AdV5 Injection	on 63
Figure 22: IF Images of the Retina – 1 Week after HD-AdV5 Injection	64
Figure 23: Distribution of GFP Signal at the HD-AdV5-TwinPE-GFP Injection	оп
Site	65
Figure 24: Further IF Images of the Retina – 1 week after AdV5-TwinPE-GF.	P
injection	66
Figure 25: Quantitative Assessment of AdV5 Injection Sites	67
Figure 26: Fundus and IF Images of DVX Treated Retina	68
Figure 27: Cell Cycle Assessment in PKC Under Distinct Culture Conditions	70
Figure 28: GE Efficiency of DSB-HDR After Cell Cycle Arrest Assays	71

IX. Index of figures 138

Figure 29: Transfection Rates in PKC under Different Culture Conditions 72	2
Figure 30: GE Efficiencies under Different Culture Conditions	3
Figure 31: RE Integrity After 7 Days in Culture	5
Figure 32: Transcriptional Assessment of REs	6
Figure 33: Live Fluorescence Imaging of RE after AdV5-GFP treatment	7
Figure 34: qPCR after AdV5 Application on RE	8
Figure 35: Fluorescence Microscopy Image of Dissociated RE after AdV5-GFP	
Treatment	9
Figure 36: Flow cytometry analysis of dissociated AdV5-treated REs	9
Figure 37: Initial Quantitative 3D analysis of Vector Transduction in RE 80	0
Figure 38: Fluorescence Live Imaging and Flow Cytometry Analysis of VLP	
Transfection in REs	1

X. Index of tables

X. INDEX OF TABLES

Table 1: Most Common IRDs	3
Table 2: Plasmids	27
Table 3: Summary of gRNAs sequences	27
Table 4: ssODN Sequence	28
Table 5: Summary of Primer Sequences	28
Table 6: Primary antibodies	29
Table 7: Secondary antibodies	30
Table 8: Standard medium composition (15% FCS)	31
Table 9: PCR protocol upon sanger sequencing	34
Table 10 : PCR protocol upon NGS sequencing	34
Table 11: Transport Medium Composition	38
Table 12: Neurobasal Culture Medium for RE (5% Anti-anti)	38
Table 13: Summary of all USH1C Litters between April 2022-March 2025	56
Table 14: Injection Protocol of Pilot in vivo Experiment	61

X. Index of tables

XI. ACKNOWLEDGMENTS

I would like to express my gratitude to Prof. Eckhard Wolf for the opportunity to absolve my thesis at the Chair for Molecular Animal Breeding and Biotechnology, LMU Munich, thus allowing me to discover a passion for science through all ambitious projects taking place at the institute.

I would also like to thank my mentor, Prof. Dr. Nikolai Klymiuk, who supported my growth in the research field by encouraging independent work and the pursuit of great collaborations and ambitious undertakings early on in my scientific career.

I am especially grateful to my Postdoc and lab partner, Dr. Josep Miquel Cambra Bort for his support and great collaboration in scientific endeavors, animal management, as well for the emotional support.

Many thanks to Dr. Petra Runa-Vochozkova and Dr. Hannah Auch for teaching me all I needed to start my scientific journey. Hannah, thank you for your patience and great professionalism. Petra, I always appreciate your insights and our conversations, you are a great scientist, who I look up to, it is always a pleasure to work with you.

To all my fellow doctoral students, thank you for creating an atmosphere of support and mutual aid, especially appreciated on frustrating days! This also goes to the further members of the CiMM, Barbara, Mayuko, Tuna, who I really enjoyed working with these last years.

Merci aux membres de ma famille pour leur confiance, leur soutien et leurs encouragements à distance sans qui ces dernières années n'auraient pas eu la même signification. En contre-partie, je m'excuse d'avoir pris l'accent allemand. Merci Mo pour ton soutien direct toutes ces années.

My thanks also go to my friends in Munich and everywhere else for always reminding me to have fun and enjoy my time here.

Finally, I would like to thank the SPP2127 consortium for its support in my scientific journey and all my collaboration partners for the great work!